

# Designing Service Systems from Textual Evidence

Ruicheng Ao\* Hongyu Chen\* Siyang Gao† Hanwei Li‡ David Simchi-Levi\*

## Abstract

Designing service systems requires selecting among alternative configurations—choosing the best chatbot variant, the optimal routing policy, or the most effective quality control procedure. In many service systems, the primary evidence of performance quality is textual—customer support transcripts, complaint narratives, compliance review reports—rather than the scalar measurements assumed by classical optimization methods. Large language models (LLMs) can read such textual evidence and produce standardized quality scores, but these automated judges exhibit systematic biases that vary across alternatives and evaluation instances. Human expert review remains accurate but costly. We study how to identify the best service configuration with high confidence while minimizing expensive human audits, given that automated evaluation is cheap but biased. We formalize this as a sequential decision problem where a biased proxy score is observed for every evaluation, and a verified outcome can be acquired selectively at additional cost. We prove that LLM-only selection fails under arm-dependent bias, and that naive selective-audit estimators can be asymptotically biased. We develop an estimator combining proxy scores with inverse-propensity-weighted residuals and construct anytime-valid confidence sequences. Our algorithm, PP-LUCB, jointly decides which alternatives to evaluate and whether to request human audits, concentrating reviews where the LLM judge is least reliable. We prove correctness and establish instance-dependent cost bounds showing near-optimal efficiency. On a customer support ticket classification task, our algorithm correctly identifies the best model in 40/40 trials while achieving 90% audit cost reduction.

**Keywords:** service system design, LLM-as-a-judge, best-arm identification, human-AI collaboration, prediction-powered inference, selective auditing

## 1 Introduction

In many service operations applications, managers often face a fundamental design problem of choosing among alternative system designs to optimize service quality and customer experience. Applications include call center routing and staffing, customer-support escalation policies, content-moderation review workflows, healthcare triage protocols, and compliance screening rules [Gans et al., 2003, Aksin et al., 2007, Topol, 2019, Bates and Gawande, 2003]. In each case, the manager must compare competing system configurations under uncertainty and choose the one that delivers the best service in practice.

Existing work on learning-based service system design and performance optimization typically assumes access to random performance samples that are available as computable scalars. In bandit-based and Bayesian optimization methods [Bubeck and Cesa-Bianchi, 2012, Frazier, 2018], one

---

\*Institute for Data, Systems, and Society, Massachusetts Institute of Technology. {aorc, chenhy, dslevi}@mit.edu

†School of Data Science, City University of Hong Kong. siyangao@cityu.edu.hk

‡Department of Decision Analytics and Operations, City University of Hong Kong. hanweili@cityu.edu.hk

iteratively evaluates configurations on the real system and collects scalar-valued samples, while in ranking and selection and search-based simulation optimization methods [Kim and Nelson, 2001, Chen et al., 2000, Fu, 2002], one first builds a simulation model and then collects scalar-valued samples from the simulator for different configurations. These methods are effective and have been widely studied, but their methodological foundations are built on performance samples that can be directly aggregated, compared, and optimized.

However, in many real service systems, the primary evidence of performance is not a readily computable scalar. Instead, it appears as textual trajectories, such as ticket descriptions and resolution logs, agent-customer transcripts, customer complaints, compliance review reports, or medical encounter notes. These records faithfully reflect what the system did and contain important information for evaluating the system performance. However, since they are unstructured text, they are difficult to incorporate into standard design and optimization algorithms. In practice, one can ask human experts to review and compare these textual trajectories, but this process is often highly inefficient. For example, a call center supervisor may be able to review only a few dozen calls per day out of the thousands the center handles, and a content moderation team may assess a few hundred posts out of the millions that may be generated over a comparable period. When a firm must evaluate hundreds of system configurations or more, possibly under a short time horizon, relying on human review of textual trajectories alone quickly becomes infeasible. As a result, service systems whose performance evidence is predominantly textual often cannot be effectively designed at large scale.

In the meantime, the wide adoption of large language models (LLMs) offers a potential solution to this gap. As automated readers of natural language, LLMs can process text that describes service system performance and convert it into standardized scores. That is, they can serve as an *LLM-as-a-judge* that maps a text-based performance evaluation instance into a proxy scalar score. This mapping makes it possible to conduct service system design in settings where system performance is documented in language.

In this research, we study this setting. The manager must choose among a finite set of service configurations when the available performance samples are textual trajectories. Here, a configuration can include service operations design choices, such as staffing rules, queue discipline and priority weights, routing and transfer logic, etc. At the same time, since the system performance evaluation involves LLM-based scoring, a configuration can also include LLM-related choices, such as prompt templates, reasoning-depth settings, tool access, and the underlying language model.

Although it is conceptually straightforward to use an LLM judge to convert text trajectories into scores and apply standard design algorithms to compare configurations and identify the best one, the use of LLMs raises new and nontrivial questions.

First, we cannot rely on the LLM judge alone. LLM judges make evaluation cheap and scalable, but their scores can exhibit systematic biases that vary across configurations and evaluation instances [Wang et al., 2024, Stureborg et al., 2024, Panickssery et al., 2024]. A judge scoring customer service quality may favor verbose responses over concise ones, irrespective of correctness. A compliance-oriented judge may systematically reward conservative phrasing. More importantly, these biases can be configuration dependent. The judge might over-rate certain routing behaviors (e.g., faster handoffs) even when they increase downstream workload, or under-rate concise triage notes that are clinically correct but stylistically atypical. When such biases differ across the configurations being compared, simply collecting more proxy scores does not resolve the problem, and can even amplify confidence in the wrong choice. It can be proved that the proxy scores alone is not sufficient to distinguish between competing configurations, so that even with arbitrarily many LLM judge evaluations, a proxy-only procedure cannot be guaranteed to identify the true best configuration (Theorem 3.5, Part 1). To handle it, we still adopt human expert review, but use it

in a selective-audit manner to address the issue described above. We treat audited expert outcomes as the verified outcome of interest, obtain a proxy score for every evaluated text trajectory, and selectively acquire human audits only for the scored cases that are necessary for valid correction and reliable selection.

Second, even with access to human audits, we cannot use them carelessly. Under selective human audits, audited outcomes are not a random sample of all proxy scores, but are selected precisely from scores that look uncertain or otherwise salient. As a result, naive estimators that simply average audited outcomes, or that audit when the LLM is uncertain and then treat those audited outcomes as representative, can remain biased, even with infinitely many human audits, because the audit decision depends on samples that are predictive of the outcome ([Theorem 3.5](#), Part 2). Therefore, the design challenge is not merely to allocate a fixed audit budget, but to develop principled rules that decide when to request human audits and how to combine audited and unaudited evaluations so that inference remains valid. Our approach addresses this by correcting selective auditing via an inverse propensity weighting (IPW) estimator that remains unbiased under adaptive audit decisions, and using these corrected estimates to drive a selection algorithm.

We formulate this service system design problem under the fixed-confidence best arm identification (BAI) [[Even-Dar et al., 2006](#), [Kaufmann et al., 2016](#)] framework with  $K$  service configurations (arms) under comparison<sup>1</sup>. Each time we evaluate an arm on a text-based instance, we observe a proxy score  $F \in [0, 1]$  at low cost (e.g., \$0.01 per API call), which summarizes the textual trajectory into a scalar signal but may be biased in ways that depend on both the configuration and the instance. We may additionally request a human audit  $Y \in [0, 1]$  at higher cost (e.g., \$0.20 per review), which we treat as an unbiased sample of the verified outcome. Our goal is to identify the configuration with the best expected audited outcome with high confidence, while keeping the total cost small. To do so, we treat proxy scores as an always-available signal and use selective human audits to learn (and continuously monitor) how the proxy deviates from the verified outcome. The resulting procedure is designed to remain valid even when the proxy is systematically wrong for some configurations or for some segments of instances, and it aims to use audits only where they are most informative for the final selection decision.

Such a procedure design can significantly reduce the proportion of interactions that require human audit. At the same time, it raises the question of an audit policy, in which the system should decide whether to request a human audit after observing the textual instance and the proxy score. This observe-then-escalate structure is standard in service operations, but it creates a fundamental statistical difficulty, where audited outcomes form a selected subset rather than a simple random sample of all evaluations, because the system audits precisely the cases it finds uncertain. If one ignores this selection effect, the estimated quality of a configuration can be distorted, and the system may stop early with high confidence in the wrong choice. Our design addresses this by (i) treating auditing as a controlled source of missing outcomes with known probabilities, so that audited and unaudited scores can be combined in a way that remains valid under adaptive decisions, and (ii) steering audits toward configurations where the judge is least reliable and where the decision is still ambiguous. This the system to run many low-cost LLM judge evaluations, spend audits only when they can change the decision, and stop once the evidence is strong enough to separate the leading configuration from the rest.

Our contributions are summarized as follows.

First, we study service system design using textual evidence and formulate the problem as fixed-confidence BAI with biased proxy scores and limited human audits. We adopt a simple decompo-

---

<sup>1</sup>Hereafter, we use the terms “arm” and “configuration” interchangeably, and primarily use “arm” when presenting the BAI formulation and algorithms

sition that expresses the mean of a configuration as the proxy score plus a residual gap between the judge and the verified outcome and develop a prediction-powered estimator that combines the proxy mean with an IPW residual correction, so the resulting mean estimates of the configurations remain unbiased. We then construct anytime-valid confidence sequences for configuration means that are valid under adaptive sampling, adaptive auditing, and optional stopping, which enable the selection algorithm to stop as soon as the evidence separates the best configuration.

Second, we propose a fixed-confidence BAI algorithm called PP-LUCB (Prediction-Powered Lower and Upper Confidence Bound), to jointly decide which configurations to evaluate and when to request human audits in each iteration. The method uses LUCB-style comparisons [Kalyanakrishnan et al., 2012, Jamieson et al., 2014] together with an auditing rule inspired by Neyman allocation [Neyman, 1934] that concentrates audits on configuration and instance regions where the LLM judge is least reliable. This directly targets the dominant source of uncertainty in the debiased mean. We prove  $\delta$ -correctness of PP-LUCB and establish instance-dependent upper bounds on cost that suggest the near optimal efficiency of PP-LUCB and quantify how the informativeness of the proxy, the uncertainty in the debiasing correction, and relative measurement costs govern total evaluation cost. In addition, we develop a tracking variant, PP-Track-and-Audit, as a theoretical complement to PP-LUCB. The procedure adaptively targets the instance-dependent cost lower bound by learning how to allocate evaluations and audits across arms, and it achieves asymptotic optimality as  $\delta \rightarrow 0$ .

Third, in practice, human experts are not continuously on standby in the way an LLM judge is, so audit feedback typically arrives with delays. In view of this, we extend PP-LUCB to delayed audit feedback and show that anytime-valid inference can be preserved by working with an appropriate returned-outcome filtration, using confidence sequences that remain valid despite the pending audits. We further prove that  $\delta$ -correct stopping of PP-LUCB remains valid under delays. We also quantify how delays affect decision completion time, showing that the monetary cost is unaffected while the time to decision increases by at most the maximum audit delay.

Last, we evaluate our framework on synthetic examples with controlled bias structures and real-world service system design problems using live LLM APIs. They cover both simple model selection and composite configurations that combine routing policies, prompting, and model choice. The experiments corroborate the theoretical findings and demonstrate the empirical performance of PP-LUCB. In synthetic BAI instances, the confidence sequences achieve the desired time-uniform coverage, and Neyman-style auditing reduces total cost by about 48-50% relative to uniform auditing. With delayed audit feedback, PP-LUCB still identifies the best arm consistently and incurs only a small increase in stopping time. In real service case studies, PP-LUCB selects the best cost-adjusted support-ticket configuration while reducing audit cost by about 90%, and in the queue-design study it achieves high design-class accuracy.

A preliminary conference version of this work appeared as Ao et al. [2026a]. That paper introduced the BAI framework with biased proxies, the IPW estimator with confidence sequences, and the PP-LUCB algorithm with Neyman allocation, validated in synthetic environments. The present paper extends the conference version in scope, theory, and experiments. We reframe the problem for service system design, where each arm represents a full service configuration rather than a single model choice, and we use this perspective to clarify how judge bias and selective audits arise in the observe-then-escalate framework. On the theory side, we derive instance-dependent upper bounds and information-theoretic lower bounds on cost and design an asymptotically optimal tracking variant (PP-Track-and-Audit). We also develop a complete treatment of delayed audit feedback and prove that anytime-valid inference and  $\delta$ -correct stopping remain valid when audit outcomes return with delay. On the experiment side, we add synthetic tests to demonstrate the theoretical results and to evaluate PP-LUCB in a broader range of settings and performance dimensions. We also

include real-world case studies using live LLM APIs, including a customer support classification task and a queue-based service design task with composite, multi-layer configurations, and provide guidelines for deploying LLM-assisted evaluation systems.

## 2 Related Literature

Our work connects service system design, AI-assisted decision making, and statistical learning. We position our contributions relative to four streams of research.

**Service system design and quality evaluation.** Service system design is a central topic in operations management, covering dynamic pricing [Gallego and Van Ryzin, 1994, Besbes and Zeevi, 2009, Ao et al., 2025], staffing optimization [Gans et al., 2003, Ibrahim et al., 2016], and routing and scheduling [Aksin et al., 2007], etc. A critical component of design is quality evaluation. The operations literature has studied quality control systems that balance inspection costs against quality assurance [Juran and Gryna, 1988, Taguchi, 1986]. In call center operations, quality monitoring programs sample a small fraction of calls for supervisor review [Gans et al., 2003, Aksin et al., 2007]; in healthcare, selective case review balances thoroughness against resource constraints [Bates and Gawande, 2003]. Our work adds to this line of literature by studying a new and important setting in which the primary evidence of performance is textual, rather than directly observed as computable scalars.

**Best arm identification and ranking and selection.** BAI is a pure exploration bandit problem that identifies the arm with the best mean via samples [Even-Dar et al., 2006, Bubeck et al., 2011]. Closely related ranking and selection (R&S) methods in statistics and simulation pursue the same goal, but typically collect samples from simulation models rather than real systems [Chen et al., 2000, Gao et al., 2017]. Two standard BAI settings have been widely studied. In the fixed-budget setting, the learner is given a sampling budget and aims to minimize the misidentification probability at the end of the budget, while in the fixed-confidence setting, the learner aims to identify the best arm with probability at least  $1 - \delta$  while minimizing the number of samples. Multi-fidelity bandits extend these ideas by allowing cheap approximations to an expensive target, often under assumptions such as unbiasedness, known bias, or bounded deviations across fidelities [Kandasamy et al., 2016, 2017, Sen et al., 2018, Lattimore and Szepesvári, 2020, Ji et al., 2025]. In this research, we adopt the fixed-confidence setting and use LUCB-style comparisons together with a confidence-bound separation stopping rule to focus sampling on top arms [Jamieson et al., 2014, Kalyanakrishnan et al., 2012, Garivier and Kaufmann, 2016, Kaufmann et al., 2016], but differs from them in that the proxy score can have unknown, arm- and instance-dependent bias, and the high-fidelity outcome is observed only through an adaptive auditing decision after observing the instance and proxy score. In particular, this research is fundamentally different from multi-fidelity (bi-fidelity) BAI in that it always observes the low-fidelity proxy and only decides whether to request a high-fidelity human audit, and does not assume the proxy bias is known or controlled. This calls for new estimators and time-uniform inference.

**Prediction-powered inference.** Prediction-powered inference (PPI) combines a small verified set with model predictions to form valid confidence intervals [Angelopoulos et al., 2023a,b, Zrnic and Candès, 2024]. Recent work studies how to collect verified outcomes in an adaptive way within PPI [Zrnic and Candès, 2024], and how to jointly optimize sampling and measurement probabilities [Chen et al., 2024, Ao et al., 2026b]. Our approach borrows these ideas for the BAI setting by

combining the proxies with an IPW residual correction, which treats selective audits as Missing-at-Random missing outcomes and yields unbiased estimation despite that audit decisions depend on observables [Robins et al., 1994, Chernozhukov et al., 2018]. A key additional requirement in our problem is anytime-valid uncertainty quantification under adaptive sampling and optional stopping, which we address using confidence sequences and time-uniform concentration tools [Lai, 1976, Howard et al., 2021, Kaufmann and Koolen, 2021]. This combination lets us both correct selection bias from selective audits and stop early without breaking coverage. Concurrent work by Landesberg and Narayan [2025] studies a related offline setting in which a calibrated surrogate is combined with a small oracle slice for valid ranking under deployment shift.

**AI-assisted decision making and LLM-as-a-judge.** A growing literature studies how AI systems support human decisions, in domains including healthcare, lending, and customer service [Topol, 2019, Rajkomar et al., 2019, Fuster et al., 2022, Kleinberg et al., 2018, Huang et al., 2022]. In addition, LLM-as-a-judge has emerged as a scalable alternative to human evaluation for language systems [Zheng et al., 2023], but empirical studies document systematic issues such as position bias, self-preference, sensitivity to prompting, and drift over time [Wang et al., 2024, Panickssery et al., 2024, Stureborg et al., 2024, Baek et al., 2026]. More broadly, LLMs are increasingly applied to operations research tasks such as optimization formulation and solver interaction [Ao et al., 2026d,c, Liang et al., 2026]. Our work connects these themes in service operations by turning LLM-based evaluation into a sequential design problem and providing a statistically grounded way to use limited human audit for confident configuration selection.

The remainder of the paper is summarized as follows. Section 3 formulates the problem and identifies failure modes using existing methods. Sections 4 and 5 develop the IPW estimator and PP-LUCB algorithm and establish their validity. Section 6 derives information-theoretic lower bounds and demonstrates that PP-LUCB achieves near-optimal cost scaling. Section 7 extends the framework to delayed audit feedback. Section 8 evaluates the proposed method through synthetic examples and real service system case studies. Section 9 concludes this paper and discusses some managerial implications.

### 3 Model and Setup

Consider evaluating  $K$  arms, indexed by  $k \in [K] := \{1, \dots, K\}$ . At each time step, a *performance evaluation instance*  $X \in \mathcal{X}$  is drawn from a distribution  $\mathcal{D}$ . Each instance contains a textual trajectory that provides the relevant information for evaluating system performance, potentially accompanied by structured metadata (task type, language, risk tier). We refer to  $X$  simply as an *instance* hereafter. For every arm  $k$  and instance  $X = x$ , there is a potentially available *human audit outcome*  $Y(k, x) \in [0, 1]$ , which is expensive but is the objective we ultimately care about, and an always-available *proxy score*  $F(k, x) \in [0, 1]$ , which is cheap and observed at every evaluation but can be biased.

We allow judge bias to be arm- and instance-dependent via:

$$\mathbb{E}[F(k, X) \mid X = x] = \mathbb{E}[Y(k, X) \mid X = x] + b_k(x), \tag{1}$$

where  $b_k(x)$  is an unknown bias function that may vary among arms and instances. Define  $\theta_k := \mathbb{E}_{X \sim \mathcal{D}} [Y(k, X)]$  as the expected audited outcome for arm  $k$ , and let  $k^* \in \arg \max_{k \in [K]} \theta_k$  be the arm that achieves the maximal value. Our goal is to identify  $k^*$  with high confidence while keeping the total evaluation cost small.

In rounds  $t = 1, 2, \dots$ , the decision-maker selects arms and observes outcomes as follows:

1. Select an arm  $k_t \in [K]$  based on historical observations;
2. Draw an instance  $X_t \sim \mathcal{D}$  and observe the proxy score  $F_t := F(k_t, X_t)$  at cost  $c_F > 0$ ;
3. Decide whether to request a human audit:  $A_t \in \{0, 1\}$  with probability  $\pi_t$ , where if  $A_t = 1$ , we observe  $Y_t := Y(k_t, X_t)$  at additional cost  $c_Y > 0$ .

The audit decision may depend on all observable information available at the time of the decision. Accordingly, the auditing probability  $\pi_t$  can depend on the full history and the current instance and proxy score:

$$\pi_t := \mathbb{P}(A_t = 1 \mid \mathcal{F}_{t-1}, k_t, X_t, F_t), \quad (2)$$

where  $\mathcal{F}_t := \sigma(\{X_i, F_i, A_i, Y_i, k_i\}_{i=1}^t)$  is the history up to time  $t$  (with  $Y_i$  observed only when  $A_i = 1$ ). Note that the auditing decision cannot depend on the unobserved  $Y_t$ .

For a selection algorithm, a (random) stopping time  $\tau$  and its selected arm  $\hat{k}$  are called  $\delta$ -correct if they satisfy

$$\mathbb{P}(\hat{k} = k^*) \geq 1 - \delta. \quad (3)$$

We will design a selection algorithm that stops in finite time with probability one and outputs a  $\delta$ -correct arm with minimal cost, where the cost is the cumulative cost across time:

$$\text{Cost}(\tau) := c_F \cdot \tau + c_Y \cdot \sum_{t=1}^{\tau} A_t. \quad (4)$$

We make the following technical assumptions throughout the paper. They capture basic regularity of the outcomes and operational requirements of system design process.

**Assumption 3.1.** For all  $k, x$ ,  $Y(k, x) \in [0, 1]$  and  $F(k, x) \in [0, 1]$  almost surely.

**Assumption 3.2.** For each round  $t$ , conditional on the history  $\mathcal{F}_{t-1}$  and current observables  $(k_t, X_t, F_t)$ , the audit decision  $A_t$  is independent of the potential outcome  $Y(k_t, X_t)$ .

**Assumption 3.3.** There exists  $\pi_{\min} \in (0, 1]$  such that  $\pi_t \geq \pi_{\min}$  whenever an arm-instance pair is eligible for auditing.

[Assumption 3.1](#) is a reasonable assumption for system scoring and can be easily realized by requiring the LLM judge and human expert to restrict their evaluations to the interval  $[0, 1]$ , or by normalizing their scores from other ranges to  $[0, 1]$ . [Assumption 3.2](#) formalizes a real constraint that the system decides whether to request a human audit based only on what is observed at that point (the instance and the proxy score), not on the unobserved audit outcome. This is satisfied in our observe-then-escalate framework where auditing is triggered before any human review is performed. [Assumption 3.3](#) requires a minimum audit probability, i.e., no segment (any subset of instances defined by observables such as metadata in  $X$  or the proxy score  $F$ ) is never audited. In practice, this can be implemented in the selection algorithm as a small basic audit rate (and it makes sure the proxy-to-audit residual can be learned for all relevant cases).

With these assumptions, we next formalize why relying on proxy scores alone can fail under arm-dependent bias and naively using selectively audited outcomes can still lead to biased conclusions.

The true mean of each arm decomposes as

$$\theta_k = \mathbb{E}[Y \mid k] = \mathbb{E}[F \mid k] + \mathbb{E}[Y - F \mid k]. \quad (5)$$

The first term is observable from proxy scores alone, and the second term (the residual mean) requires human audits to estimate. Correct selection of the best arm requires learning both components, and we show that selecting the best arm is impossible given only the proxy scores.

We define an algorithm to be proxy-only if it does not audit at all.

**Definition 3.4** (Proxy-only algorithms). An algorithm is *proxy-only* if it never audits, i.e.,  $A_t \equiv 0$ , and its decision  $\widehat{k}$  depends only on  $\{(k_t, X_t, F_t)\}_{t \leq \tau}$ .

**Theorem 3.5.** Under [Assumption 3.1](#), consider the model class where instances are drawn i.i.d.  $X \sim \mathcal{D}$ , and for each arm  $k$  the joint distribution of  $(Y(k, X), F(k, X))$  is otherwise unrestricted (allowing arm- and instance-dependent bias).

1. For any proxy-only algorithm producing a selected arm  $\widehat{k}$  after any (possibly random) number of rounds, there exist two instances  $\mathcal{I}$  and  $\mathcal{I}'$  in the model class such that the distribution of all observations under  $\mathcal{I}$  and  $\mathcal{I}'$  is identical, but the best arm is different. Consequently, for at least one instance,

$$\mathbb{P}(\widehat{k} \neq k^*) \geq \frac{1}{2}.$$

2. Fix any algorithm that uses selective auditing with audit decisions allowed to depend on  $(X_t, F_t)$ , and that estimates  $\theta_k$  using a naive selective-audit estimator for at least one arm. Then there exists an instance in the model class and an audit policy (depending on  $F$ ) such that, even as rounds and audits go to infinity, the estimator converges to an incorrect limit for that arm, inducing a non-vanishing misidentification probability:

$$\liminf_{n \rightarrow \infty} \mathbb{P}(\widehat{k}_n \neq k^*) > 0.$$

[Theorem 3.5](#) establishes two key limitations that motivate our approach. Part 1 shows that correctly identifying the best arm can be impossible using only the (possibly biased) proxy scores, i.e., human audits are essential for reliable identification when bias differs among arms. Part 2 shows that auditing alone is not enough. If audits are triggered selectively based on observed scores, then simple estimators that ignore the audit-selection mechanism can remain biased, even with many audits. This motivates the IPW correction developed in the next section.

## 4 Prediction-Powered Estimation

We develop an estimator that combines the always-available proxy score with a correction term learned from selectively audited outcomes, and construct an anytime-valid confidence sequence that supports valid stopping.

### 4.1 IPW Residual Estimator

Let  $N_k(t) := \sum_{s \leq t} \mathbf{1}\{k_s = k\}$  be the number of times an arm  $k$  is pulled before time  $t$ . The key identity [\(5\)](#) suggests estimating  $\theta_k$  as the sum of the proxy mean and the residual mean. Thus, we employ the inverse propensity weighting (IPW) estimator to correct for selective auditing. We define the estimators for  $\mathbb{E}[F | k]$ ,  $\mathbb{E}[Y - F | k]$  and  $\theta_k$  as follows

$$\widehat{\mu}_{F,k}(t) := \frac{1}{N_k(t)} \sum_{s \leq t: k_s = k} F_s, \tag{6}$$

$$\widehat{\mu}_{R,k}(t) := \frac{1}{N_k(t)} \sum_{s \leq t: k_s = k} \frac{A_s}{\pi_s} (Y_s - F_s), \tag{7}$$

$$\widehat{\theta}_k(t) := \widehat{\mu}_{F,k}(t) + \widehat{\mu}_{R,k}(t). \tag{8}$$

Here, since we observe the proxy  $F$  every time we pull one arm, its mean is estimated via a simple average  $\widehat{\mu}_{F,k}(t)$ . The residual part captures the systematic gap between the proxy score and

the verified outcome. Since  $Y$  is observed only when we request an audit, we estimate the residual mean via an inverse-propensity adjustment that re-weights audited cases by  $1/\pi_s$ . This is the standard correction used in quality monitoring and program evaluation when inspection decisions are selective but their probabilities are known and logged.

Note that the estimators remain valid despite being formed from adaptively collected samples. Intuitively, audits are requested based only on observable information (instance and proxy score), so inverse-propensity weighting corrects the selection effect and generates an unbiased estimate of the residual mean. The main difficulty is valid inference (time-uniform uncertainty quantification) rather than point estimation, because classical fixed-sample concentration bounds and confidence intervals are generally not valid under adaptive sampling and optional stopping. Therefore, to facilitate the development of valid stopping rules, we need to construct anytime-valid confidence sequences that hold simultaneously over time.

## 4.2 Anytime-Valid Confidence Sequences

Let  $\{\mathcal{F}_t\}_{t \geq 0}$  be the natural filtration of the process, where  $\mathcal{F}_t$  contains all observed quantities up to time  $t$ , including  $(k_s, X_s, F_s, A_s, Y_s, \pi_s)$  for  $s \leq t$ , with  $Y_s$  missing when  $A_s = 0$ . Arm choices  $k_{t+1}$  and audit probabilities  $\pi_{t+1}$  are allowed to be  $\mathcal{F}_t$ -measurable. We construct anytime-valid confidence sequences (CS) separately for the proxy mean  $\mu_{F,k} := \mathbb{E}[F \mid k]$  and the residual mean  $\mu_{R,k} := \mathbb{E}[Y - F \mid k]$ , and then combine them for  $\theta_k = \mu_{F,k} + \mu_{R,k}$ .

We use the stitched boundary of Howard et al. [2021]:

$$\psi(v; \alpha) := 1.7 \sqrt{v \left( \log \log(2v) + 0.72 \log \frac{5.2}{\alpha} \right)}. \quad (9)$$

This boundary yields time-uniform control for martingales with a variance proxy  $v$ , which is the key technical requirement for valid stopping. We allocate failure probability  $\delta_k := \delta/K$  to each arm and split it evenly between proxy and residual CS.

**Proposition 4.1.** *Under Assumptions 3.1 to 3.3, fix an arm  $k$  and define the centered sum  $S_{F,k}(t) := \sum_{s \leq t: k_s = k} (F_s - \mu_{F,k})$ . Since  $F_s \in [0, 1]$  and  $X_s$  are drawn i.i.d. from  $\mathcal{D}$ , the terms  $(F_s - \mu_{F,k})$  form a bounded martingale-difference sequence along pulls of arm  $k$ . A valid variance proxy is  $V_{F,k}(t) = N_k(t)/4$ . Define the confidence half-width*

$$w_{F,k}(t) := \frac{\psi(V_{F,k}(t); \delta_k/2)}{N_k(t)} = \frac{\psi(N_k(t)/4; \delta_k/2)}{N_k(t)}.$$

Then, with probability at least  $1 - \delta/2$ , simultaneously for all  $t \geq 1$  and all  $k \in [K]$ ,

$$\mu_{F,k} \in [\hat{\mu}_{F,k}(t) \pm w_{F,k}(t)].$$

We now turn to the residual mean, which is identified from selectively audited outcomes. Define the raw residual  $R_t := Y_t - F_t$  and the IPW increment

$$Z_t := \frac{A_t}{\pi_t} R_t.$$

Under Assumption 3.2, the audit decision depends only on observables  $(\mathcal{F}_{t-1}, k_t, X_t, F_t)$  and not on the unobserved  $Y_t$ , so IPW corrects the selection induced by auditing:

$$\mathbb{E}[Z_t \mid \mathcal{F}_{t-1}, k_t, X_t, F_t] = \mathbb{E}[R_t \mid \mathcal{F}_{t-1}, k_t, X_t, F_t].$$

Therefore the centered sequence  $\mathbf{1}\{k_t = k\} (Z_t - \mu_{R,k})$  is a martingale difference sequence. This is the main reason we can combine proxy scores and selective audits without asymptotic bias.

Since  $R_t = Y_t - F_t \in [-1, 1]$  and  $\pi_t \geq \pi_{\min}$ ,

$$Z_t = \frac{A_t}{\pi_t} R_t \in \left[ -\frac{1}{\pi_{\min}}, \frac{1}{\pi_{\min}} \right].$$

Moreover,  $\mu_{R,k} = \mathbb{E}[Y - F \mid k] \in [-1, 1] \subseteq \left[ -\frac{1}{\pi_{\min}}, \frac{1}{\pi_{\min}} \right]$ . Therefore the centered increment  $Z_t - \mu_{R,k}$  is supported on an interval of length

$$\left( \frac{1}{\pi_{\min}} - \left( -\frac{1}{\pi_{\min}} \right) \right) = \frac{2}{\pi_{\min}} =: M.$$

By Hoeffding's lemma, this implies that  $Z_t - \mu_{R,k}$  is conditionally sub-Gaussian with variance proxy  $M^2/4 = 1/\pi_{\min}^2$ , i.e.,

$$\log \mathbb{E}[\exp(\lambda(Z_t - \mu_{R,k})) \mid \mathcal{F}_{t-1}] \leq \frac{\lambda^2}{2} \cdot \frac{M^2}{4}.$$

We therefore apply the same stitched boundary as for the proxy sequence, with a deterministic variance process.

**Proposition 4.2.** *Under Assumptions 3.1 to 3.3, let  $\hat{\mu}_{R,k}(t) := \frac{1}{N_k(t)} \sum_{s \leq t: k_s = k} Z_s$  and  $S_{R,k}(t) = N_k(t)(\hat{\mu}_{R,k}(t) - \mu_{R,k})$ . The centered increment  $Z_t - \mu_{R,k}$  is supported on an interval of length  $M := 2/\pi_{\min}$ , so the variance process  $V_{R,k}(t) = N_k(t) \cdot M^2/4$  is a valid sub-Gaussian envelope. Define*

$$w_{R,k}(t) := \frac{\psi(V_{R,k}(t); \delta_k/2)}{N_k(t)} = \frac{\psi(N_k(t) \cdot M^2/4; \delta_k/2)}{N_k(t)}.$$

Then with probability at least  $1 - \delta/2$ , simultaneously for all  $t \geq 1$  and all  $k \in [K]$ ,

$$\mu_{R,k} \in [\hat{\mu}_{R,k}(t) \pm w_{R,k}(t)].$$

Combining the proxy and residual CS produces an anytime-valid CS for the true mean  $\theta_k$ . Define

$$\begin{aligned} L_k(t) &:= \hat{\theta}_k(t) - w_{F,k}(t) - w_{R,k}(t), \\ U_k(t) &:= \hat{\theta}_k(t) + w_{F,k}(t) + w_{R,k}(t). \end{aligned} \tag{10}$$

**Theorem 4.3.** *Under Assumptions 3.1 to 3.3, allocate  $\delta_k = \delta/K$  to each arm. Using Propositions 4.1 and 4.2 and a union bound, we have*

$$\mathbb{P}\left(\forall t \geq 1, \forall k \in [K] : \theta_k \in [L_k(t), U_k(t)]\right) \geq 1 - \delta.$$

**Theorem 4.3** plays two roles in our setting. First, it supports valid early stopping, allowing the system to stop as soon as the best arm is separated from the rest. Second, it supports adaptive auditing and sampling, because both the choice of which arm to pull next and the decision of whether to request a human audit may depend on the full history and the current proxy score, and the confidence sequences remain valid under these adaptive choices.

---

**Algorithm 1** PP-LUCB with Residual-Uncertainty-Guided Auditing

---

**Require:** Arms  $[K]$ , confidence  $\delta$ , costs  $(c_F, c_Y)$ ,  $\pi_{\min} > 0$

**Require:** Target audit rate  $\rho \in [\pi_{\min}, 1]$

**Require:** Initial variance estimator  $\hat{s}_k$

```
1: Initialize: sample each arm; audit with prob.  $\pi_{\min}$ ; set  $t \leftarrow 0$ .
2: loop
3:   Update  $\hat{\theta}_k(t)$  and CS  $[L_k(t), U_k(t)]$  via (10).
4:    $\hat{k}_t \leftarrow \arg \max_k \hat{\theta}_k(t)$ ;  $c_t \leftarrow \arg \max_{k \neq \hat{k}_t} U_k(t)$ .
5:   if  $L_{\hat{k}_t}(t) > \max_{k \neq \hat{k}_t} U_k(t)$  then
6:     return  $\hat{k} = \hat{k}_t$ 
7:   end if
8:   for  $k \in \{\hat{k}_t, c_t\}$  do
9:      $t \leftarrow t + 1$ . { $t$  counts individual arm pulls}
10:    Draw  $X_t \sim \mathcal{D}$ ; observe  $F_t \leftarrow F(k, X_t)$ ; pay  $c_F$ .
11:    Compute score  $\hat{s}_k(X_t, F_t)$ .
12:    Set  $\pi_t \leftarrow \text{clip}(\lambda_t \hat{s}_k(X_t, F_t), \pi_{\min}, 1)$ .
13:    Draw  $A_t \sim \text{Bern}(\pi_t)$ ; if  $A_t = 1$ , observe  $Y_t$ , pay  $c_Y$ .
14:    Update  $\hat{s}_k$  from audited samples.
15:   end for
16: end loop
```

---

## 5 Selection Algorithm

We now present an algorithm for optimal sampling and auditing. The algorithm has two components. The outer loop operates like an LUCB algorithm, pulling both the arm with the highest estimated value and the arm with the highest upper confidence bound among the rest. The inner loop decides the auditing probability of the two pulled arms, with auditing probability proportional to the variance of the residual, which is related to Neyman allocation in causal inference. The full algorithm is provided in Algorithm 1.

**Outer loop.** The outer loop selects which arms to pull and decides when to stop. Here,  $t$  indexes individual arm pulls rather than rounds, because each round pulls two arms (leader and challenger), so  $t$  increments twice per round. After  $t$  pulls, we compute the estimator  $\hat{\theta}_k(t)$  and its confidence sequence  $[L_k(t), U_k(t)]$ . Let the leader  $\hat{k}_t \in \arg \max_k \hat{\theta}_k(t)$  be the estimated best arm, and the arm  $c_t \in \arg \max_{k \neq \hat{k}_t} U_k(t)$  be the challenger with the highest upper confidence bound among the remaining arms. Each round evaluates both  $\hat{k}_t$  and  $c_t$ . We stop at the first time  $t$  such that:

$$L_{\hat{k}_t}(t) > \max_{k \neq \hat{k}_t} U_k(t), \quad (11)$$

and output the selected arm  $\hat{k} = \hat{k}_t$ . Since  $[L_k(t), U_k(t)]$  is anytime-valid, the stopping rule (11) is valid without requiring a fixed horizon (formalized in Theorem 5.1 below).

**Inner loop.** The inner loop sets the auditing probability after observing the proxy score. Auditing affects uncertainty through estimating  $\mu_{R,k} = \mathbb{E}[Y - F \mid k]$ . Under IPW, the leading variance contribution is governed by

$$v_k^{(R)}(\pi) := \mathbb{E} \left[ \frac{(R_k(X, F))^2}{\pi(k, X, F)} \mid k \right], \quad (12)$$

where  $R_k(X, F) = \mathbb{E}[Y - F \mid X, k]$  is the residual that remains to be corrected by auditing.

We first show that under any auditing policy satisfying [Assumptions 3.2](#) and [3.3](#), our algorithm is  $\delta$ -correct if we use the proposed confidence sequence.

**Theorem 5.1.** *Consider [Algorithm 1](#) with stopping rule [\(11\)](#). If the confidence sequences satisfy simultaneous coverage as in [Theorem 4.3](#), and the auditing policy satisfies [Assumptions 3.2](#) and [3.3](#), then the algorithm is  $\delta$ -correct:*

$$\mathbb{P}(\widehat{k} = k^*) \geq 1 - \delta.$$

[Theorem 5.1](#) guarantees  $\delta$ -correctness for any valid auditing policy. To further improve the efficiency of [Algorithm 1](#), we develop the optimal auditing policy. This requires structure on how the conditional variability of the proxy–audit residual varies across instances. Specifically, we focus on the conditional second moment of the residual

$$g_k(x, f) := \mathbb{E}[(Y - F)^2 \mid k, X = x, F = f],$$

and assume it is bounded away from 0 and infinity.

**Assumption 5.2.** There exist constants  $0 < g_{\min} \leq g_{\max} < \infty$  such that  $g_k(x, f) \in [g_{\min}, g_{\max}]$  for all  $(k, x, f)$ .

Since  $g_k(x, f)$  is large in regions where the proxy-to-audit residual is more variable, [Assumption 5.2](#) captures instance-dependent heterogeneity in proxy reliability. In practice, one can discretize the  $(x, f)$  space into risk tiers and estimate  $g_k$  from audited samples. This assumption is a mild regularity condition for our auditing design because it rules out degenerate cases where the proxy is either perfectly accurate on a nontrivial region (so no auditing is needed there) or arbitrarily noisy (so no finite audit rate can control the IPW variance), and it ensures that the Neyman-style allocation is well-defined and stable. The following theorem shows that optimal auditing concentrates on regions with high values of function  $g$ .

**Theorem 5.3.** *Assume [Assumptions 3.1](#) to [3.3](#) and [5.2](#). Fix an arm  $k$  and consider an audit policy  $A \sim \text{Bernoulli}(\pi(X, F))$  with  $\pi \in [\pi_{\min}, 1]$  satisfying an average audit-rate constraint  $\mathbb{E}[\pi(X, F)] = \rho$ . Among all audit policies meeting the constraint, the asymptotic variance of the IPW estimator is minimized by*

$$\pi_k^*(x, f) \propto \sqrt{g_k(x, f)}. \tag{13}$$

Moreover, if  $g_k(X, F)$  is highly heterogeneous across segments, any uniform-audit policy  $\pi \equiv \rho$  can be arbitrarily less efficient than  $\pi^*$ .

[Theorem 5.3](#) formalizes an intuitive audit policy that if the proxy is unreliable in certain regions (high  $g_k(x, f)$ ), then audits should be concentrated there, rather than being spread evenly to mimic routine quality monitoring.

In practice, we implement a clipped, budget-normalized Neyman-shaped auditing rule:

$$\pi_t = \text{clip} \left( \lambda_t \cdot \widehat{s}_{k_t}(X_t, F_t), \pi_{\min}, 1 \right), \tag{14}$$

where  $\widehat{s}_k(x, f)$  is an online estimate of  $\sqrt{g_k(x, f)}$  learned from past audited residuals  $R = Y - F$  (e.g., by stratifying the observable pair  $(x, f)$  into finitely many bins and using within-bin sample second moments). The normalization coefficient  $\lambda_t$  is chosen by a one-dimensional calibration so that the empirical average audit probability among eligible pulls matches the target audit rate, i.e.,  $\frac{1}{m} \sum_{i \in \mathcal{W}_t} \pi_i \approx \rho$  over a recent window (or cumulatively up to time  $t$ ), with clipping ensuring  $\pi_t \in [\pi_{\min}, 1]$ .

## 6 Cost Analysis

This section translates the estimation and stopping guarantees of PP-LUCB into a bound on monetary cost. The goal is to study the main terms that govern evaluation cost in practice, and to place our procedure relative to a fundamental lower bound.

We first provide an instance-dependent bound that separates the cost contribution of always-observed proxy scores and selectively audited residual corrections.

**Theorem 6.1.** *Let  $\bar{\rho} := \mathbb{E}[\frac{1}{\tau} \sum_{t=1}^{\tau} A_t] \in [0, 1]$  denote the expected fraction of pulls that are audited up to the stopping time  $\tau$ . Under [Assumptions 3.1 to 3.3](#), the expected monetary cost of PP-LUCB satisfies*

$$\mathbb{E}[\text{Cost}(\tau)] \lesssim \sum_{k \neq k^*} \frac{\log(K/\delta)}{\Delta_k^2} \left( \frac{1}{4} + \frac{1}{\pi_{\min}^2} \right) (c_F + c_Y \bar{\rho}), \quad (15)$$

up to universal constants and  $\log \log$  factors.

The bound in (15) highlights several practical implications.

First, the expected cost grows with  $\log(K/\delta)/\Delta_k^2$ , as in many fixed-confidence BAI studies that enforce simultaneous validity for the  $K$  arms. The extra  $\log K$  term arises from allocating the overall error probability  $\delta$  across arms (and across the proxy and residual confidence sequences) and applying a union bound to obtain time-uniform coverage. For fixed  $K$ ,  $\log(K/\delta) = \log(1/\delta) + O(1)$ , so the leading dependence on  $\delta$  matches the standard  $\log(1/\delta)$  scaling.

Second, (15) takes the form

$$(\text{effective uncertainty per pull}) \times (\text{effective cost per pull}),$$

where the effective per-pull cost is  $c_F + c_Y \bar{\rho}$  and the effective uncertainty factor is the sum of two variance envelopes,  $1/4$  for the always-observed proxy mean and  $1/\pi_{\min}^2$  for the IPW residual correction. Note that these two sources interact multiplicatively in the bound. If the residual correction is hard to learn (e.g., small  $\pi_{\min}$  leading to a large IPW range), then more total pulls are needed, which increases both proxy spending (incurred on every pull) and audit spending (incurred on an average  $\bar{\rho}$  fraction of pulls).

Third, the dependence on  $\pi_{\min}$  reflects a coverage trade-off. A smaller  $\pi_{\min}$  reduces the minimum audit coverage requirement, but it enlarges the worst-case IPW range and thus the residual uncertainty envelope  $1/\pi_{\min}^2$ , which can increase the total number of pulls needed to separate arms with high confidence. The bound is conservative in that it uses a worst-case range-based envelope for anytime-valid inference. In practice, variance-adaptive bounds and residual-guided auditing can substantially reduce the realized audit fraction  $\bar{\rho}$  (and often the time to decision).

With the result of [Theorem 6.1](#), a natural question is whether the dependence on  $\log(1/\delta)$  and  $\Delta^{-2}$  can be further improved. To address this, we lower-bound the cost of any  $\delta$ -correct algorithm.

**Assumption 6.2.** There exists a local alternative path  $\{\nu_h : h \in \mathbb{R}\}$  with  $\nu_0 = \nu$  such that, as  $h \rightarrow 0$ ,

$$\text{KL}(P_\nu \parallel P_{\nu_h}) = \frac{h^2}{2} \mathcal{I}(\nu; \pi) + o(h^2),$$

for some Fisher information  $\mathcal{I}(\nu; \pi) \in (0, \infty)$  that may depend on the audit policy  $\pi$ .

[Assumption 6.2](#) imposes a local asymptotic normality (LAN)-type regularity condition along the considered local alternative paths. Intuitively, the lower bound is driven by how quickly the data distribution changes when we slightly change the underlying means, and [Assumption 6.2](#) provides

a way to capture this via a quadratic approximation to the KL divergence. The assumption is mild because it holds for many common bounded models that can be used to represent the audited outcomes, including Bernoulli logistic regression, Beta regression, and truncated Gaussian families (see Appendix A for examples). Note that we apply this assumption only to state a concrete instance-dependent lower bound below that benchmarks what any procedure can achieve as  $\delta \rightarrow 0$  (because to derive a meaningful lower bound, one must restrict the otherwise nonparametric model class by imposing additional local regularity structure on the data distribution), not as a requirement for running PP-LUCB. Our main algorithmic guarantees rely only on boundedness and the audit design assumptions (Assumptions 3.1 to 3.3).

Define the set of alternative problem instances where the best arm is different from  $\nu$  as  $\text{Alt}(\nu) = \{\nu' : k^*(\nu') \neq k^*(\nu)\}$ .

**Theorem 6.3.** *Assume Assumptions 3.1 to 3.3 and 6.2. For any  $\delta$ -correct algorithm stopping with respect to  $\mathcal{F}_t$ , the expected total cost on instance  $\nu$  satisfies:*

$$\liminf_{\delta \rightarrow 0} \frac{\mathbb{E}_\nu[\text{Cost}(\tau)]}{\log(1/\delta)} \geq C^*(\nu), \quad (16)$$

where the characteristic cost  $C^*(\nu)$  is the solution to the inverse-information maximization problem:

$$C^*(\nu)^{-1} = \sup_{w \in \Delta_K, \pi} \inf_{\nu' \in \text{Alt}(\nu)} \frac{\sum_{k=1}^K w_k \mathbb{E}_\nu[I_k(\nu, \nu'; \pi_k) | k]}{c_F + c_Y \sum_{k=1}^K w_k \mathbb{E}_\nu[\pi_k(X, F) | k]}. \quad (17)$$

Here,  $\Delta_K$  is the probability simplex,  $w \in \Delta_K$  represents the arm sampling proportions,  $\pi = \{\pi_k\}_{k=1}^K$  denotes the arm-specific auditing policies  $\pi_k : \mathcal{X} \times [0, 1] \rightarrow [0, 1]$ , and  $I_k(\nu, \nu'; \pi_k)$  is the KL divergence between the data distributions under  $\nu$  and  $\nu'$  given arm  $k$  and audit policy  $\pi_k$ .

According to Theorem 6.3, to make a high-confidence arm selection decision at low cost, a procedure must allocate its evaluations across arms in an informative way ( $w$ ) and spend its audit budget where it produces the most information ( $\pi$ ), in order to balance information gain and cost. Under the structure of Assumption 3.2, the KL term admits a decomposition that matches the two information sources:

$$I_k(\nu, \nu'; \pi_k) = \underbrace{\text{KL}(P_F \| P'_F)}_{\text{proxy information}} + \mathbb{E}_{X, F} \left[ \pi_k(X, F) \cdot \underbrace{\text{KL}(P_{Y|X, F} \| P'_{Y|X, F})}_{\text{audit information}} \right], \quad (18)$$

where  $P_F$  denotes the marginal distribution of the proxy score, and  $P_{Y|X, F}$  the conditional distribution of the human audit given the instance and proxy score. This expression makes the audit trade-off explicit: larger  $\pi_k(X, F)$  increases information per evaluation but raises expected audit cost.

To make the lower bound more concrete, we provide the following example.

*Example 6.4* (Truncated normal illustration). For each arm  $k$ , suppose  $F_k \sim \text{TN}(\mu_{F,k}, \sigma_{F,k}^2, [0, 1])$  and the residual  $R_k = Y_k - F_k \sim \text{TN}(\mu_{R,k}, \sigma_{R,k}^2, [-1, 1])$  are conditionally independent. Under truncation, Fisher information increases by a factor  $\kappa_{F,k} \geq 1$  (and  $\kappa_{R,k} \geq 1$ , respectively), so that the effective variances become  $\sigma_{F,k}^2/\kappa_{F,k}$  and  $\sigma_{R,k}^2/\kappa_{R,k}$ . Any  $\delta$ -correct algorithm must incur expected cost at least

$$\mathbb{E}[\text{Cost}(\tau)] \geq \sum_{k \neq k^*} \frac{2 \log(1/\delta)}{\Delta_k^2} \left( \sqrt{c_F} \frac{\sigma_{F,k}}{\sqrt{\kappa_{F,k}}} + \sqrt{c_Y} \frac{\sigma_{R,k}}{\sqrt{\kappa_{R,k}}} \right)^2. \quad (19)$$

When truncation is mild,  $\kappa \rightarrow 1$  and we recover the standard Gaussian form. See Appendix E.2 for details. The squared-sum structure shows that no algorithm can avoid the cost of both information sources. Proxy observations alone are insufficient when  $\sigma_{R,k}^2 > 0$ , and relying solely on audits is wasteful when the proxy contains useful signal.

Comparing Theorem 6.1 with the lower bound in Theorem 6.3 (and its illustration in Example 6.4), for fixed  $K$ , both bounds share the leading scaling

$$\sum_{k \neq k^*} \frac{\log(1/\delta)}{\Delta_k^2} \times (\text{instance-dependent constant}),$$

up to universal constants and  $\log \log$  factors, so PP-LUCB is rate optimal in its dependence on  $\delta$  and the gap parameters  $\Delta_k$ . The two bounds differ in their instance-dependent prefactors. The upper bound in Theorem 6.1 features the product

$$\left(\frac{1}{4} + \frac{1}{\pi_{\min}^2}\right) (c_F + c_Y \bar{\rho}),$$

which can be interpreted as a conservative uncertainty envelope times an average per-pull cost. In contrast, the lower bound in Example 6.4 involves the squared-sum structure

$$\left(\sqrt{c_F} \frac{\sigma_{F,k}}{\sqrt{\kappa_{F,k}}} + \sqrt{c_Y} \frac{\sigma_{R,k}}{\sqrt{\kappa_{R,k}}}\right)^2,$$

which reflects the cost-optimal combination of the two information sources under a local asymptotic normal approximation.

*Remark 6.5.* For completeness, Appendix F.3 describes PP-TRACK-AND-AUDIT, a tracking variant of PP-LUCB that iteratively solves (17) (with unknown parameters replaced by their estimates) and allocates samples to track the implied target sampling proportions. Under Assumption 6.2, it achieves

$$\limsup_{\delta \rightarrow 0} \frac{\mathbb{E}_\nu[\text{Cost}(\tau_\delta)]}{C^*(\nu) \log(1/\delta)} \leq 1, \quad (20)$$

which matches the lower bound up to vanishing terms (Theorem F.2). We present this result as a theoretical complement showing that the lower bound in Theorem 6.3 is attainable within our framework.

## 7 Delayed Audit Feedback

Unlike automated scoring, human auditing is constrained by resources and typically occurs in batch or through a queue, so audit outcomes may not be available immediately after an audit is requested. We show that the anytime-valid inference and  $\delta$ -correct stopping remain valid when audit outcomes are delayed, and quantify how delays affect the completion time via high-probability bounds.

### 7.1 Delay Model

When an audit is requested at time  $t$  (i.e.,  $A_t = 1$ ), the outcome  $Y_t$  may not be observed immediately. Let  $D_t \in \{0, 1, 2, \dots\}$  denote the delay, so that  $Y_t$  becomes available at time  $t + D_t$ .

**Assumption 7.1.** Conditional on the information available when the audit is requested, the delay  $D_t$  is independent of the unobserved outcome  $Y_t$ :

$$D_t \perp\!\!\!\perp Y_t \mid \sigma(\mathcal{F}_{t-1}, k_t, X_t, F_t, A_t = 1, \pi_t).$$

**Assumption 7.1** states that how long an audit takes to return can depend on workload and on information visible at the time the audit is requested (such as the instance and the proxy score), but not on the audit outcome itself. This is consistent with real review processes in which the outcome is produced after the review is completed.

To formalize the available information, we work with a filtration that reveals audit outcomes only upon return.

**Definition 7.2.** For each round  $s$ , let  $A_s \in \{0, 1\}$  indicate whether an audit was requested. Define the *return indicator* at time  $t$ :

$$B_s(t) := \mathbf{1}\{A_s = 1, s + D_s \leq t\}.$$

Let  $\mathcal{G}_t$  be the  $\sigma$ -field generated by all proxy scores  $\{(A_s, X_s, F_s)\}_{s \leq t}$ , all audit outcomes  $\{Y_s : B_s(t) = 1\}$  that have returned by time  $t$ , and the algorithm's audit probabilities  $\{\pi_s\}_{s \leq t}$ .

The algorithm may continue pulling arms and requesting audits while waiting for past outcomes to return, and any stopping rule that depends on audited outcomes must be based on  $\mathcal{G}_t$ , because outcomes not yet returned cannot be used.

## 7.2 $\delta$ -Correct Stopping under Delays

Under delayed audit feedback, the IPW-weighted residual increments indexed by the audit request time (i.e.,  $Z_t := \frac{A_t}{\pi_t}(Y_t - F_t)$ ) satisfy the same martingale-difference property as in the no-delay setting (delays only affect when audited outcomes become observable). Below we formally establish the  $\mathcal{G}_t$ -measurable CS.

**Theorem 7.3.** *Assumptions 3.1 to 3.3. Suppose the audit probability  $\pi_s$  is measurable with respect to  $\sigma(\mathcal{G}_{s-1}, k_s, X_s, F_s)$ . Fix an arm  $k$ . Define the delayed residual estimator*

$$\widehat{\mu}_{R,k}^{\text{del}}(t) := \frac{1}{N_k(t)} \sum_{s \leq t: k_s = k} B_s(t) \frac{A_s}{\pi_s} (Y_s - F_s),$$

and the pending audit count  $P_k(t) := |\{s \leq t : k_s = k, A_s = 1, B_s(t) = 0\}|$ , which tracks audits requested but not yet returned. Then, with probability at least  $1 - \delta_k$ , simultaneously for all  $t \geq 1$ :

$$|\widehat{\mu}_{R,k}^{\text{del}}(t) - \mu_{R,k}| \leq w_{R,k}(N_k(t)) + \frac{P_k(t)}{\pi_{\min} N_k(t)} =: w_{R,k}^{\text{del}}(t),$$

where  $w_{R,k}(n) = \psi(nM^2/4; \delta_k/2)/n$  is the no-delay residual CS width from [Proposition 4.2](#) with  $M = 2/\pi_{\min}$ . Both  $\widehat{\mu}_{R,k}^{\text{del}}(t)$  and  $w_{R,k}^{\text{del}}(t)$  are  $\mathcal{G}_t$ -measurable. When  $D_s = 0$  for all  $s$ ,  $P_k(t) = 0$  and the bound reduces to  $w_{R,k}(N_k(t))$ .

**Theorem 7.3** implies that delayed audits do not invalidate our anytime-valid inference for  $\mu_{R,k} = \mathbb{E}[Y - F \mid k]$  (and thus for  $\theta_k$ ). The delayed CS width  $w_{R,k}^{\text{del}}(t)$  consists of the no-delay width  $w_{R,k}(N_k(t))$  plus an additive correction  $P_k(t)/(\pi_{\min} N_k(t))$  that accounts for pending audits. Under bounded delays  $D_s \leq D_{\max}$ , the pending count satisfies  $P_k(t) \leq D_{\max}$ , so this correction is  $O(D_{\max}/(\pi_{\min} N_k(t)))$  and vanishes at rate  $O(1/N_k)$ , faster than the main CS width  $O(1/\sqrt{N_k})$ . Note that the proof (in [Section G.1](#)) derives this result from the martingale defined at audit-request time (i.e., the IPW-weighted residual increment process indexed by  $t$ ) via a triangle inequality, without constructing a new martingale on the returned-outcome filtration.

In implementation, one updates the proxy mean immediately (as before) and updates the residual correction whenever an audit outcome returns. All audit probabilities  $\pi_s$  must still be logged at request time, because IPW uses  $A_s/\pi_s$  even if  $Y_s$  returns later.

We now show that the stopping rule remains valid under delayed feedback.

**Theorem 7.4.** *Assume the setting of Theorem 7.3. Suppose for each arm  $k$  we construct confidence sequences  $\text{CS}_k(t) = [\underline{\mu}_k(t), \bar{\mu}_k(t)]$  that are  $\mathcal{G}_t$ -measurable and satisfy simultaneous coverage with probability at least  $1 - \delta$ . Define the stopping time:*

$$\tau = \inf \left\{ t \geq 1 : \exists \hat{k}(t) \text{ s.t. } \underline{\mu}_{\hat{k}(t)}(t) > \max_{j \neq \hat{k}(t)} \bar{\mu}_j(t) \right\},$$

where  $\hat{k}(t) \in \arg \max_k \underline{\mu}_k(t)$ . Then  $\tau$  is a stopping time with respect to  $\{\mathcal{G}_t\}$ , and the algorithm is  $\delta$ -correct, i.e.,  $\mathbb{P}(\hat{k}(\tau) = k^*) \geq 1 - \delta$ .

Theorem 7.4 is not merely a restatement of the no-delay case. Delays affect what information is available at each time and therefore change the underlying filtration with respect to which the algorithm is allowed to adapt its future decisions and stop. This matters because our guarantees must remain valid under sample-dependent stopping. The pending audit correction  $P_k(t)/(\pi_{\min} N_k(t))$  in the CS width ensures that the confidence bounds remain valid even when some submitted audits have not yet returned. Treating pending audits as if their outcomes were already observed would lead to bounds that are not  $\mathcal{G}_t$ -measurable, and the  $\delta$ -correct stopping result would fail.

In addition, unlike standard delayed-feedback bandits where the entire reward is delayed [Joulani et al., 2013, Pike-Burke et al., 2018], here the proxy mean can be updated immediately on every pull, while only the residual correction is delayed. Thus, delays slow down the rate at which residual uncertainty reduces, but they do not prevent learning from the always-available proxy scores.

An immediate implication of Theorem 7.4 is that statistical validity can be separated from timing. Delays may postpone stopping because the residual correction  $\hat{\mu}_{R,k}^{\text{del}}(t)$  updates only upon returned outcomes, but they do not introduce additional selection bias beyond that induced by selective auditing. As a result, in service applications, audit queues and staffing affect return times and thus decision latency, but not the correctness of the selected system configuration.

### 7.3 Decision Completion Time Bounds

Monetary cost of the algorithm depends on the number of requested audits, not their return times. Thus, delays do not change  $\text{Cost}(\tau)$  for a given sequence of requested audits. They affect only the time at which the algorithm can stop. To quantify this effect, we provide a high-probability bound comparing the completion times of PP-LUCB with and without delays.

Here we suppose that our algorithm is run with a known finite budget  $T_{\max}$  on the time steps (arm pulls), so that the no-delay stopping time  $\tau_0$  satisfies  $\tau_0 \leq T_{\max}$  almost surely. This is natural in practice because real deployment is subject to finite operational constraints (time, staffing, compute, or monetary limits), and the algorithm can always be implemented to stop and output its current decision once the budget  $T_{\max}$  is exhausted. Let  $\tau_D$  denote the stopping time under delayed audit returns, both using the same realized sequence of pulls and audit requests  $\{(k_s, X_s, F_s, A_s, \pi_s)\}_{s \geq 1}$  and the same stopping rule applied to the information available at the current time. In the no-delay setting, every requested audit outcome is revealed immediately (i.e.,  $D_s \equiv 0$ ), and in the delayed setting, outcomes return after delays  $\{D_s\}_{s \geq 1}$ .

**Theorem 7.5.** *Assume Assumptions 3.1 to 3.3 and 7.1. Suppose there exists a tail envelope  $h : \mathbb{N} \rightarrow [0, 1]$  such that for every  $s \geq 1$  and every  $d \in \mathbb{N}$ ,  $\mathbb{P}(D_s > d \mid \sigma(\mathcal{G}_{s-1}, k_s, X_s, F_s, A_s = 1, \pi_s)) \leq h(d)$  almost surely. For  $q \in (0, 1]$ , define the quantile index  $d_q \triangleq \min\{d \in \mathbb{N} : h(d) \leq q\}$ . Given  $\eta \in (0, 1)$ , let  $d^* \triangleq d_{\eta/T_{\max}}$ . Then*

$$\mathbb{P}(\tau_D \leq \tau_0 + d^*) \geq 1 - \eta.$$

The key observation is that delays affect only when already-requested audit outcomes become available, not which audits are requested. In particular, once all audit outcomes requested up to the (hypothetical) no-delay stopping time  $\tau_0$  have returned, the delayed-feedback procedure has enough information to certify the same stopping condition, and therefore must have stopped by then. [Theorem 7.5](#) quantifies the additional waiting time needed for these outstanding outcomes to arrive.

Note that [Assumption 7.1](#) is not required for the validity results in [Theorems 7.3](#) and [7.4](#). These theorems start from the martingale of IPW-weighted residual increments at audit request time (using [Assumption 3.2](#)) and handle delayed outcomes via a pathwise decomposition into returned and pending audits. The effect of unreturned outcomes is controlled by the deterministic term  $P_k(t)/(\pi_{\min}N_k(t))$ , without any distributional restriction on  $\{D_t\}$ . However, [Theorem 7.5](#) bounds the additional decision latency, which requires probabilistic control of audit return times and thus requires [Assumption 7.1](#).

Two special cases can concretely illustrate the bound in [Theorem 7.5](#). If delays are bounded almost surely by  $D_{\max}$ , then  $h(d) = 0$  for all  $d \geq D_{\max}$ . Therefore,  $d^* \leq D_{\max}$  and [Theorem 7.5](#) leads to

$$\mathbb{P}(\tau_D \leq \tau_0 + D_{\max}) \geq 1 - \eta.$$

If delays satisfy an exponential tail  $h(d) \leq Ce^{-\beta d}$ , then  $d^* = d_{\eta/T_{\max}} \leq \frac{1}{\beta} \log\left(\frac{CT_{\max}}{\eta}\right)$ , and thus

$$\mathbb{P}\left(\tau_D \leq \tau_0 + \frac{1}{\beta} \log\left(\frac{CT_{\max}}{\eta}\right)\right) \geq 1 - \eta.$$

## 8 Numerical Experiments

We test PP-LUCB in settings where an LLM judge produces a proxy score for every instance and a verified outcome requires a costly audit. The experiments mainly evaluate the empirical performance of PP-LUCB with and without delays, as well as the performance of the audit policy. The experiments are conducted in both synthetic environments and service system case studies using live API calls. Additional robustness checks and comparisons of auditing policies are provided in [Section H](#).

### 8.1 Experimental Setup

The experiments use the following environments, cost model, and evaluation protocol.

**Synthetic environment.** We first use a synthetic environment to test the anytime-valid inference and cost scaling in a setting where the bias structure is fully controlled ([Section 8.2-8.3](#)). We use a fixed-confidence BAI problem with  $K = 4$  arms and human-audited outcomes  $Y \sim \text{Bernoulli}(\theta_k)$  with means  $\theta_k \in \{0.7, 0.6, 0.5, 0.4\}$ , so the gap between the best and the second best arm is  $\Delta = 0.1$ . Proxy scores are generated to resemble an LLM judge that is informative but systematically biased  $F = \text{clip}(Y + b + \epsilon, 0, 1)$ , where a shared bias term  $b = 0.1$  shifts proxy scores away from the audit outcomes and  $\epsilon \sim \mathcal{N}(0, 0.15^2)$  adds random proxy noise. Unless otherwise stated, we set  $\delta = 0.05$ , impose a maximum horizon  $T_{\max} = 20,000$  to avoid rare extremely long runs, and report averages over 20-30 independent trials.

**Real LLM environment.** We then use live API calls to test PP-LUCB under delayed audit feedback (Section 8.4), where the main question is not whether the arms are hard to distinguish but whether our inference and stopping rule remains valid under delay. We use  $K = 2$  arms, represented by DeepSeek-V3.2 (empirical accuracy  $\hat{\theta}_0 = 1.00$  on this benchmark) and gpt-5-nano ( $\hat{\theta}_1 \approx 0.07$ ) respectively, with gpt-4.1-mini serving as the judge. The large gap  $\Delta \approx 0.93$  lets the algorithm stop quickly and consistently, so that we can verify convergence and coverage under delay ( $T_{\max} = 300$ ,  $\delta = 0.10$ ). Section J provides more details on the prompts, datasets, and the per-trial setup. For the service system case studies (Section 8.5), we evaluate  $K = 3$  to  $K = 6$  candidate arms on MT-Bench and customer support classification tasks.

**Cost model and audit policies for comparison.** We set judge cost  $c_F = 1.0$  and audit cost  $c_Y = 20.0$ . This reflects a reasonable ratio between an LLM API call (e.g., \$0.01 per request) and a human expert review (e.g., \$0.20 per review). With this normalization, reported costs can be interpreted as equivalents of judge calls. We compare five audit allocation policies. Each policy specifies the audit probability  $\pi_t = \mathbb{P}(A_t = 1 \mid \mathcal{F}_{t-1}, k_t, X_t, F_t)$  and then clips it to satisfy the positivity constraint  $\pi_t \in [\pi_{\min}, 1]$ .

- **Uniform.** A constant audit rate,  $\pi_t \equiv \rho$  (typically  $\rho = 0.1$ ).
- **Price of Precision.** A cost ratio-based simple rule with  $\pi$  increasing in the estimated relative variability of the residual correction,  $\pi \propto (\hat{\sigma}_R/\hat{\sigma}_F)\sqrt{c_F/c_Y}$  (scaled to match the same average rate  $\rho$ ).
- **Uncertainty Weighted.** A heuristic that assigns higher  $\pi_t$  when the current selection decision is more uncertain.
- **Neyman.** The auditing rule motivated by Theorem 5.3, i.e.,  $\pi_t \propto \hat{s}_{k_t}(X_t, F_t)$  with  $\hat{s}_k \approx \sqrt{\hat{g}_k}$ .
- **Oracle.** The same Neyman form but using the true  $g_k(x, f)$  in synthetic experiments, serving as an upper-bound reference for audit allocation efficiency.

Unless otherwise stated, we keep the arm sampling rule fixed and vary only the auditing policy, so the comparisons reflect differences in how audits are allocated rather than differences in which arms are sampled.

**Evaluation protocol.** All experiments use Python 3.10 with NumPy 1.24 and SciPy 1.10. Seeds are set as  $42 + \text{trial\_id}$  for reproducibility. We report selection accuracy, total cost, realized audit rate, and confidence sequence coverage (the fraction of trials in which the true mean remains inside the reported confidence sequence for all times).

## 8.2 Statistical Validity

We first test the coverage of the confidence sequences used by PP-LUCB and the cost efficiency of the Neyman auditing rule.

Since PP-LUCB stops based on the confidence sequences, coverage must hold uniformly over time, i.e.,  $\mathbb{P}(\mu \in [L_t, U_t] \forall t) \geq 1 - \delta$ . We test this property by generating  $n_{\text{trials}} = 1000$  independent sequences of Bernoulli observations with true mean  $\mu = 0.5$ , updating the confidence sequence at every time step, and recording whether any violation occurs at any time. We repeat this for  $\delta \in \{0.01, 0.05, 0.1, 0.2\}$ .

Figure 1 reports empirical coverage as a function of the time horizon. All tested cases meet or exceed their nominal targets. Specifically,  $\delta = 0.01$  achieves 99.8% coverage (target 99%),  $\delta = 0.05$

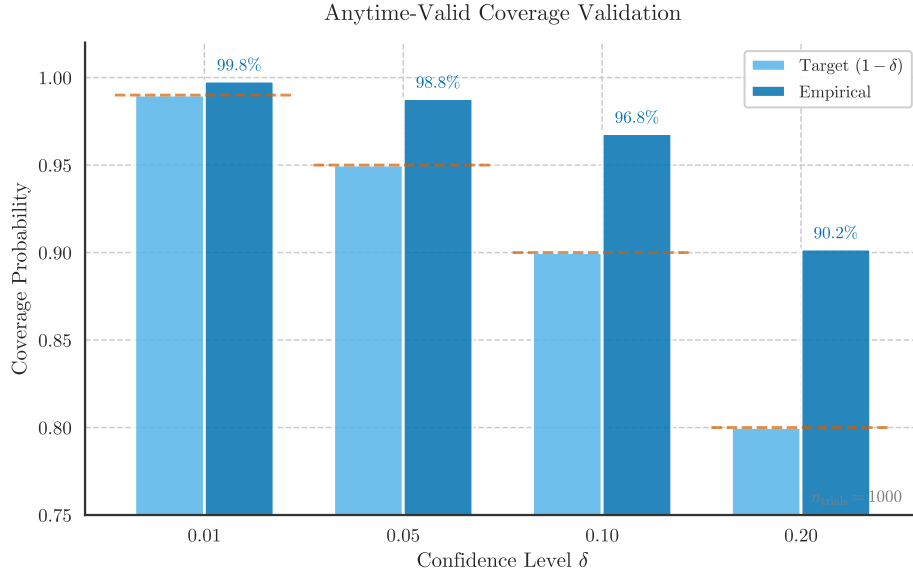


Figure 1: Empirical coverage of PP-LUCB. Error bars show 95% bootstrap confidence intervals over 1000 trials.

achieves 98.8% (target 95%),  $\delta = 0.1$  achieves 96.8% (target 90%), and  $\delta = 0.2$  achieves 90.2% (target 80%). The over-coverage is not surprising, because stitched boundaries are designed to be conservative so that validity is preserved under arbitrary stopping rules.

In addition to the  $\delta$ -correctness, the practical value of PP-LUCB hinges on whether it can make efficient use of audits, i.e., reduce audit usage without sacrificing this guarantee. We next compare the five audit allocation policies from Section 8.1 for three gap settings  $\Delta \in \{0.10, 0.15, 0.20\}$  and measure total cost (judge calls plus audits) and selection accuracy.

Figure 2 shows that Neyman allocation reduces cost by 48-50% relative to Uniform auditing while maintaining comparable identification accuracy. At  $\Delta = 0.1$ , for example, the average total cost drops from 1,552 under Uniform to 809 under Neyman, and similar reductions hold at larger gaps. The savings arise because audits concentrate where the proxy-to-audit residual  $Y - F$  is most variable, which is precisely where additional outcomes reduce uncertainty in the debiased mean most quickly. The remaining gap between Neyman and Oracle (about 20%) is caused by the estimation noise. Neyman relies on  $\hat{g}_k$ , which is noisy early on when few audits have been observed and stabilizes as the run proceeds.

Section H further compares four auditing policies (audit-only, proxy-only, fixed-rate, and adaptive (IPW-corrected)) under the same BAI instance. The proxy-only policy ends up with 0% correct identification under arm-dependent bias, confirming that selective auditing is necessary. The adaptive policy matches the fixed policy’s target confidence while reducing cost by about 10%.

### 8.3 Audit Allocation Patterns

Theorem 5.3 implies that, when proxy reliability varies across instance regions, an efficient auditing rule should spend a higher audit probability on the regions where the proxy-to-audit residual is more variable. This subsection provides a simple controlled experiment that makes this pattern visible and quantifies the resulting cost impact. We consider a synthetic environment in which, for each arm, instances fall into one of two observable segments of equal mass. The segments can be

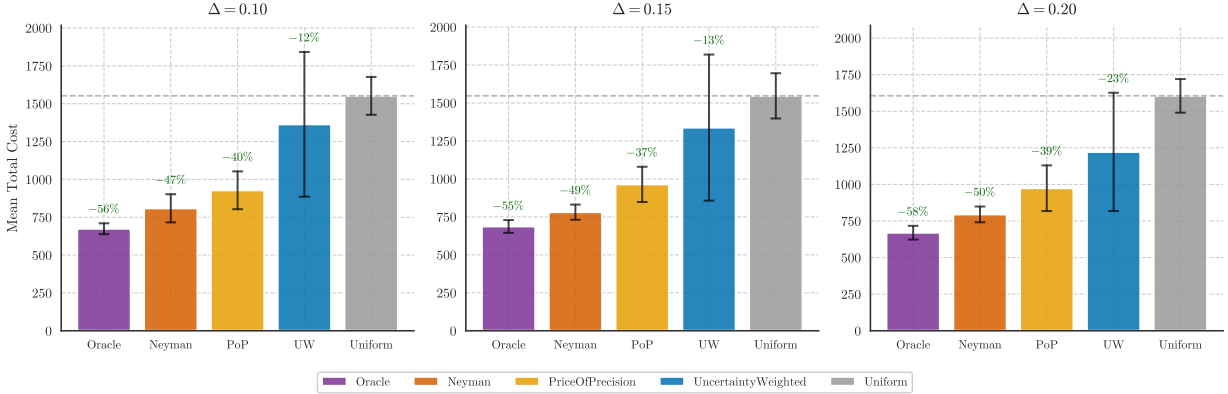


Figure 2: Performance of the five audit allocation policies. Error bars show standard deviations over 20 trials.

interpreted as coarse risk tiers or case types defined by observable metadata (e.g., language, issue category, or customer tier). We adopt a high-noise segment with residual variance  $\sigma_R^2 = 0.25$  (50% of samples) and a low-noise segment with  $\sigma_R^2 = 0.05$  (50% of samples). We keep the overall average audit rate fixed, and compare policies only in how they distribute audits between the two segments.

**Theorem 5.3** suggests an audit policy of  $\pi(x, f) \propto \sqrt{g_k(x, f)}$ . In this two-segment setting,  $g_k$  is constant within each segment, so the optimal policy audits the high-noise segment more often. The implied target ratio is

$$\frac{\pi_{\text{high}}}{\pi_{\text{low}}} = \sqrt{\frac{0.25}{0.05}} \approx 2.24.$$

In other words, when the residual is about five times more variable in one segment, the audit probability should be a little more than twice as large there (subject to clipping by  $\pi_{\min}$ ).

Figure 3 compares three auditing policies. *Uniform* ignores segment heterogeneity and uses a constant audit probability. *Discrete-Instance* treats the segment as a stratum and estimates segment-specific residual variances online and then applies a segment-level Neyman rule. *Oracle-Segment* uses the true segment variances, and is included as a reference for what is achievable when the heterogeneity structure is known. According to Figure 3, Oracle-Segment places substantially more audits on the high-noise segment, which is consistent with the ratio predicted above. It also achieves 21.2% cost savings relative to Uniform. Discrete-Instance moves the audits in the same direction but less aggressively in the early stage, because it must first learn the segment variances from audited outcomes. It achieves 7.8% cost savings relative to Uniform. These results suggest that targeted auditing is most beneficial when there is heterogeneity in segments. Even a coarse stratification with online variance estimation demonstrates a nontrivial improvement compared to uniform allocation.

## 8.4 Delayed Audit Feedback

We evaluate the performance of PP-LUCB when audited outcomes return with delay. We use the real LLM environment described in Section 8.1. In each trial, the algorithm observes a proxy score for every evaluated instance, requests audits according to the chosen audit policy, and then receives audited outcomes after random delays. The algorithm is allowed to continue pulling arms while audits are pending, but it can stop only when the stopping condition is certified using the returned-outcome filtration (as formalized in Section 7).

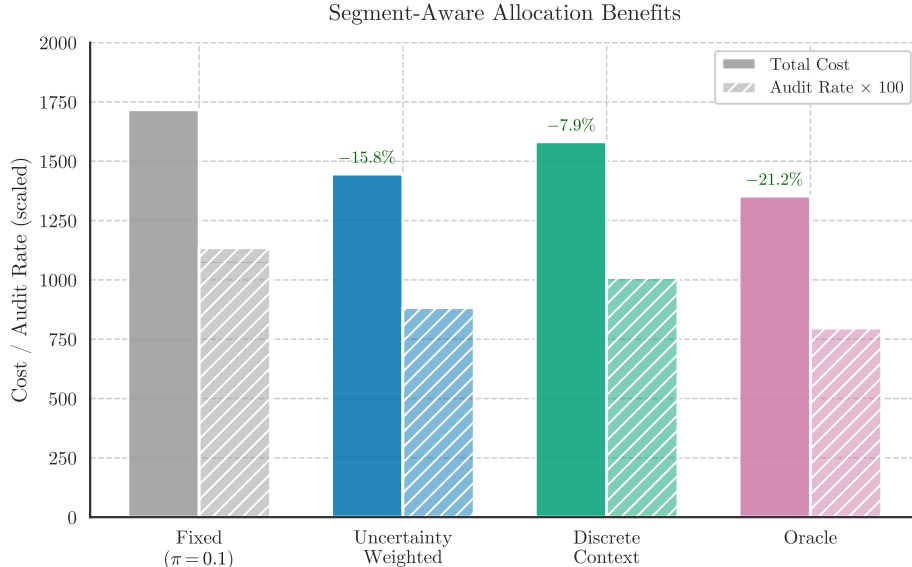


Figure 3: Audit allocation under segment heterogeneity. Oracle-Segment achieves 21.2% cost savings by concentrating audits on high-variance segments. Discrete-Instance learns segment statistics online, achieving 7.8% savings.

We consider three stylized delay distributions that reflect common audit processes: *Bounded* ( $D_{\max} = 10$ ) reflects a managed review SLA; *Geometric* ( $p = 0.3$ , mean  $\approx 2.3$ ) reflects a memoryless queue; and *Heavy-tailed* (Pareto with  $\alpha = 2.5$ , truncated at 50), represents long-tail backlogs. The goal is not to claim any particular distributional fit, but to assess the performance of PP-LUCB in a range of delay patterns that differ in tail behavior. Detailed numerical results are reported in [Section H.2](#).

Over 60 trials, PP-LUCB with delayed audit returns selects the best arm in every case. Empirical time-uniform coverage exceeds the nominal 90% target under every delay distribution. Specifically, No-Delay and Bounded achieve 100%, and Geometric and Heavy-tailed achieve 95%. This result is consistent with our confidence sequences being conservative and with the fact that delays mainly postpone when residual information becomes available, rather than changing its content. Delays have a limited effect on stopping time in this setting. In all three delay models, the median overhead relative to the no-delay baseline is 0-3 rounds, and 95% of trials fall within the high-probability completion-time bound.

## 8.5 Service System Case Studies

We apply PP-LUCB to three service system tasks where performance evidence is textual and naturally scored by an LLM judge. Each arm is a candidate service configuration, and each evaluation instance is a piece of textual evidence (a dialogue or support ticket) mapped to a proxy score  $F$ , with a verified outcome  $Y$  available only through audits. The three case studies gradually increase the complexity of the configurations. MT-Bench selects among language models, Support Tickets pairs a model with a prompt strategy, and Queue-Based Service Design combines a routing policy, a prompt, and a model into a composite configuration.

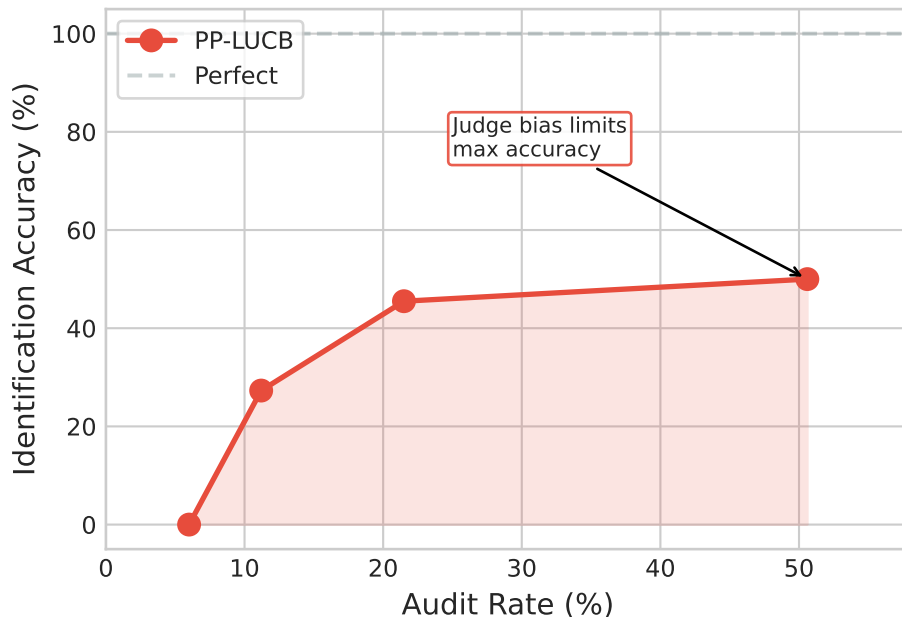


Figure 4: Audit-accuracy trade-off in MT-Bench ( $K = 6$  LLM models). Judge bias limits maximum accuracy, and increasing audit rate improves but does not perfect identification within the evaluation horizon.

### 8.5.1 MT-Bench

We first apply PP-LUCB to a standard LLM comparison task based on MT-Bench [Zheng et al., 2023], where each evaluation instance is a multi-turn dialogue. The arms correspond to  $K = 6$  models: `gpt-4`, `claude-v1`, `gpt-3.5-turbo`, `vicuna-13b-v1.2`, `alpaca-13b`, and `llama-13b`. For each instance, we obtain a proxy score  $F$  from an automated judge. Specifically, the judge (`gpt-5.2-chat`) returns a winner or tie in a pairwise comparison, which we encode as  $F \in \{0, 0.5, 1\}$ . Verified outcomes  $Y \in \{0, 0.5, 1\}$  are taken from human annotations for the same comparisons.

Over 40 trials, the algorithm achieves 32% accuracy in identifying `gpt-4` as the best model. Increasing the audit rate improves accuracy (Figure 4), but does not yield consistently correct identification within the range we tested. This performance is consistent with two features of our setting. First, MT-Bench comparisons aggregate multiple dimensions into a single pairwise outcome, and different dimensions may be weighted differently by the judge and by human annotators. Second, the top arms are close, and the resulting signal-to-noise ratio is modest at the sample sizes used in our evaluation horizon. Overall, this case highlights a practical limitation that, when the evaluation target is broad and the best arms are close, reliably separating them may require more evidence than the structured tasks below.

### 8.5.2 Support Tickets

We next consider a service operations setting in which each evaluation instance is a customer support ticket, which provides unstructured text describing a customer issue, interaction history, and available context. The service task is to assign each ticket one of five priority levels (`critical`, `high`, `medium`, `low`, `very_low`), which determines how tickets are queued, routed, and escalated.

Unlike the MT-Bench experiment where arms differ only in the underlying model, here each arm

pairs a model with a prompt strategy, forming a composite service configuration. Prompt engineering is a key design component in model selection. Recent work on prompt optimization [Zhou et al., 2023, Yang et al., 2024] can be viewed as a special case of our framework where the configuration space is the set of prompts.

We evaluate  $K = 3$  configurations (arms):

- **Arm 0** (`gpt-5-nano` + *Standard*): A concise prompt requesting only the priority label ( $\leq 20$  output tokens).
- **Arm 1** (`DeepSeek-V3.2` + *Verbose*): An open-source model with a detailed analysis prompt that assesses urgency, impact, and risk before classifying ( $\leq 200$  tokens).
- **Arm 2** (`gpt-5.2-chat` + *Chain-of-Thought*): The strongest model with a step-by-step reasoning prompt ( $\leq 300$  tokens).

In service operations, a cheap and accurate configuration is preferred to an expensive and marginally better one. We therefore use a cost-adjusted verified score

$$Y = \text{accuracy}(\hat{p}, p^*) - \lambda \cdot \frac{\text{response\_tokens}}{T_{\text{budget}}}, \tag{21}$$

where the accuracy term is an ordinal distance metric (1.0 for an exact match, 0.8 for a one-level error, and so on; see Section I.2),  $\lambda = 0.5$ , and  $T_{\text{budget}} = 300$ . The proxy score  $F \in [0, 1]$  is a judge rating (`gpt-5.2-chat`) of the predicted priority, normalized from a 0–100 scale.

Empirically, all three configurations achieve comparable classification accuracy (about 0.85) on this dataset, but they perform differently in their cost-adjusted scores due to output length. In particular, Arm 0 produces short responses that incur little cost penalty, while the verbose and chain-of-thought prompts generate longer outputs that reduce their cost-adjusted performance. The resulting estimated scores are  $\hat{\theta}_0 = 0.852$ ,  $\hat{\theta}_1 = 0.284$ , and  $\hat{\theta}_2 = 0.682$ , with a gap of  $\Delta^* \approx 0.17$  between the best and second best arms (see Section I.2 for full prompts and score details).

Over 40 independent trials at a 10% audit rate ( $\delta = 0.05$ ,  $T_{\text{max}} = 200$ ), the algorithm identifies Arm 0 (`gpt-5-nano` + *Standard*) as the best configuration in every trial. This is consistent with the relatively large gap  $\Delta^* \approx 0.17$ , which allows the anytime-valid confidence sequences to separate the leader from its challengers within the evaluation horizon.

### 8.5.3 Queue-Based Service Design

The previous experiment pairs a model with a prompt strategy. We now consider a service design task in which each arm represents a composite configuration that also includes a routing policy. The routing policy controls how incoming tickets are prioritized and processed before the LLM produces a classification. This setting is closer to many service operations applications, where performance is driven jointly by process design and the decision model.

Using the same customer support tickets, we form  $K = 6$  configurations by combining three design layers.

- **Layer 1 (Routing policy):** FIFO (first-in-first-out), Priority (urgency-weighted), or Adaptive (SLA-aware dynamic routing).
- **Layer 2 (Prompt strategy):** Standard (direct classification) or Chain-of-Thought (step-by-step reasoning).
- **Layer 3 (LLM model):** `gpt-5-nano` or `DeepSeek-V3.2`.

Table 1: Configurations for queue-based configuration combines routing policy (Layer 1), prompt strategy (Layer 2), and LLM model (Layer 3). Scores are computed from 200 expert-assessed samples per configuration.

Configuration	Routing	Prompt	Model	Acc.	SLA	$Y$
0	FIFO	Standard	gpt-5-nano	0.853	0.940	0.876
1	FIFO	CoT	gpt-5-nano	0.853	0.930	0.873
2	Priority	Standard	gpt-5-nano	0.853	0.995	<b>0.890</b>
3	Priority	CoT	gpt-5-nano	0.853	0.995	<b>0.890</b>
4	Priority	Standard	DeepSeek-V3.2	0.776	0.995	0.838
5	Adaptive	CoT	DeepSeek-V3.2	0.758	0.990	0.828

The verified outcome is a composite score  $Y = 0.5 \cdot \text{accuracy} + 0.3 \cdot \text{SLA compliance} + 0.2 \cdot \text{efficiency}$ . Accuracy measures correctness of the priority classification. SLA compliance captures whether response times meet priority-dependent deadlines. Efficiency penalizes unnecessary human escalation. The proxy score  $F$  is produced by a structured judge rubric that assesses classification quality, timeliness, and operational efficiency, and we normalize it to  $[0, 1]$ .

Table 1 lists the six configurations and their component-level scores, computed from 200 expert-assessed samples per configuration. The configurations fall into three performance tiers. Priority routing with `gpt-5-nano` (Configurations 2 and 3) achieves the highest composite score ( $Y = 0.890$ ). FIFO with `gpt-5-nano` is slightly lower ( $Y \approx 0.875$ ). The two `DeepSeek-V3.2` configurations are lower still ( $Y \approx 0.833$ ). The gap between the top two tiers is small ( $\Delta \approx 0.015$ ), while the gap to the lowest tier is larger ( $\Delta \approx 0.042$ ). A layer-by-layer decomposition (Figure 10) suggests that routing policy causes these differences. Priority routing improves SLA compliance relative to FIFO, while the prompt strategy has no measurable effect in this setting.

We run 100 trials per audit rate (6%, 11%, 20%, 50%) with  $\delta = 0.05$  and a fixed horizon  $T_{\max} = 500$ . Since Configurations 2 and 3 have identical composite scores, we report design-class accuracy, which is the fraction of trials that select any arm in the best design class (Priority routing with `gpt-5-nano`). We also report exact-arm accuracy for completeness.

Table 2 and Figure 5 summarize the results. The algorithm selects a `DeepSeek-V3.2` configuration in only 3 of 400 trials, so the evidence consistently separates the lowest tier from the top tier. Design-class accuracy rises from 75% at the lowest audit rate to 85% at 50%. This pattern is consistent with the role of auditing in our framework. When the gaps among strong designs are small, additional verified outcomes tighten the confidence sequences around the debiased means and improve the ability to distinguish the best design class within a fixed horizon.

The low exact-configuration accuracy (2-11%) reflects a different issue. Configurations 2 and 3 are tied in the verified objective, so there is no statistical signal that can separate them. Under a fixed budget, the procedure therefore focuses on separating the best class from clearly inferior alternatives rather than distinguishing between tied arms. These results illustrate that selective auditing can be most valuable in cases with small but practically meaningful gaps, where proxy scores are informative but human verification provides the additional discrimination needed for reliable identification.

## 9 Conclusions and Discussion

Designing service systems often requires choosing among competing service configurations when the main evidence of performance is textual. Compared with classic settings where system perfor-

Table 2: Identification results for queue-based service design ( $K = 6$  configurations, 100 trials per audit rate,  $T_{\max} = 500$ ). Design-class accuracy measures correct identification of the best design class (Priority + gpt-5-nano).

Audit Rate	Design-Class Acc.	Exact Acc.	Trials	Avg Steps
~6%	75%	11%	100	500
~11%	80%	5%	100	500
~20%	81%	3%	100	500
~50%	85%	2%	100	500

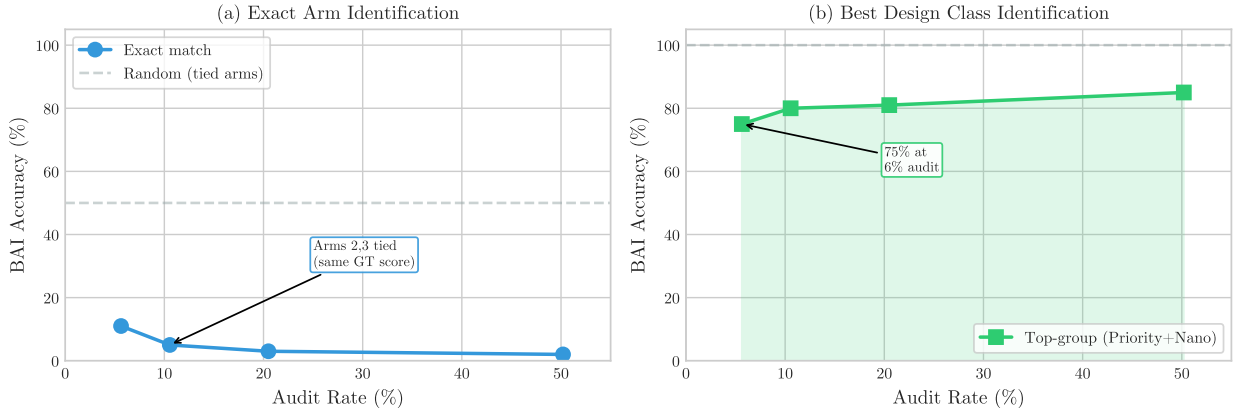


Figure 5: Identification accuracy for service configurations. (a) Exact configuration identification is limited by the tied Configurations 2 and 3. (b) Design-class accuracy (Priority + gpt-5-nano) rises from 75% to 85% as the audit rate increases from 6% to 50%.

mance is observed as readily computable scalar measurements, this text-based evidence has received relatively limited methodological attention in the service operations and learning-based design literature, in part because it is hard to aggregate and optimize. At the same time, as LLMs increasingly participate in service system operations and decisions, text becomes an even more central object of measurement, since many operational outcomes are recorded, explained, and assessed in language. LLMs can utilize such evaluations by turning text into standardized proxy scores for comparison and optimization. On the other hand, these LLM judges can be systematically biased in ways that vary across service configurations and across instances. Human review is more reliable but expensive and often delayed. To this end, this paper studies how to identify the best service configuration with fixed confidence while minimizing costly human audits.

Our main methodological contribution is a statistically valid way to combine always-available proxy scores with selectively acquired human audit outcomes in an observe-then-escalate framework. We develop a prediction-powered estimator that adds the proxy mean to an IPW correction based on audited residuals, and construct anytime-valid confidence sequences that remain valid under adaptive sampling, adaptive auditing, and optional stopping. Based on these tools, we propose PP-LUCB to jointly decide which service configurations to evaluate and when to request human audits in each iteration. We establish  $\delta$ -correctness and cost upper bounds for PP-LUCB. We also derive an information-theoretic lower bound that serves as a benchmark for the best achievable asymptotic cost for our problem, and present an asymptotically optimal tracking variant that matches this lower bound as  $\delta \rightarrow 0$  (up to vanishing terms). Last, we extend our framework to more realistic delayed audit feedback and show that statistical validity is preserved when outcomes

are returned with delays.

In synthetic environments and service case studies, the proposed approach can substantially reduce audit usage when the proxy contains useful information, while remaining valid under proxy bias. At the same time, when proxy bias is strong enough to change the ranking of service configurations, proxy-only evaluation can become unreliable. In such cases, the selective-audit residuals provide a direct diagnostic signal of judge bias and indicate where additional human review is needed.

From a managerial perspective, our results suggest some practical recommendations for LLM-assisted service systems.

First, managers should record the audit probability as part of the data record. Once audits are triggered after observing the instance and proxy score, the audit probability  $\pi_t$  should be logged together with  $(k_t, X_t, F_t, A_t, Y_t)$ . This matters because audited outcomes are a selected subset, so the selection rule must be visible in the data in order for inverse propensity weighting to correct it. In practice, this means the audit policy should be implemented in a reproducible way, and changes to the policy should be tracked, so that the same  $\pi_t$  can be reconstructed later when results are reviewed or audited.

Second, managers should keep a minimum audit rate within each segment. A small minimum audit probability (such as the  $\pi_{\min}$  in our setup) prevents segments from becoming never audited where the proxy-to-audit gap remains unknown. The key point is that a global average audit rate is not enough if some segments are effectively skipped. A practical approach is to define segments using observables available at decision time, such as task type, language, customer tier, or risk tier, and then apply the minimum audit rate within each segment. This stabilizes the learning problem by making residual information available throughout the system’s operating regions.

Third, managers can use the residual  $Y - F$  as a routine judge-audit discrepancy measure for the LLM judge. Segment-level summaries of the residual, including its mean and variance, provide an interpretable view of when the judge is helping and when it is misleading. More broadly,  $Y - F$  can be monitored as a key health metric, much like prediction error is tracked in forecasting and calibration error is tracked in measurement and risk scoring systems.

Last, audit delays are essentially a queueing constraint that can block stopping. With delayed audit returns, proxy scores update immediately, but uncertainty in the debiased mean shrinks only when audited outcomes return. Consequently, the stopping condition may not be met until enough outcomes have returned, even if many additional proxy scores are collected. This makes the audit delay distribution and audit queue management a key design choice when the decision period is short. In practice, managers should monitor the audit queue (backlog and delay) and adjust review capacity or prioritization when delays grow, especially for audits associated with the current leader and its closest challengers under the confidence bounds.

In this research, we treat audited outcomes as ground truth, but in practice, human audits can be noisy and may vary among reviewers. It is a promising future research direction to extend the framework to handle multiple reviewers and disagreements, which would better match how auditing works in reality. In addition, it would be useful to study how to model and correct for systematic auditor preferences (e.g., favoring certain writing styles or conservative decisions) that may induce structured deviations in human-audited outcomes.

## References

Zeynep Aksin, Mor Armony, and Vijay Mehrotra. The modern call center: A multi-disciplinary perspective on operations management research. *Production and Operations Management*, 16(6):

- 665–688, 2007.
- Anastasios N Angelopoulos, Stephen Bates, Clara Fannjiang, Michael I Jordan, and Tijana Zrnic. Prediction-powered inference. *Science*, 382(6671):669–674, 2023a.
- Anastasios N. Angelopoulos, John C. Duchi, and Tijana Zrnic. PPI++: Efficient prediction-powered inference, 2023b. arXiv preprint arXiv:2311.01453.
- Ruicheng Ao, Jiashuo Jiang, and David Simchi-Levi. Learning to price with resource constraints: From full information to machine-learned prices, 2025. arXiv preprint arXiv:2501.14155.
- Ruicheng Ao, Hongyu Chen, Siyang Gao, Hanwei Li, and David Simchi-Levi. Best arm identification with LLM judges and limited human audits. *arXiv preprint arXiv:2601.21471*, 2026a.
- Ruicheng Ao, Hongyu Chen, Haoyang Liu, David Simchi-Levi, and Will Wei Sun. PPI-SVRG: Unifying prediction-powered inference and variance reduction for semi-supervised optimization, 2026b. arXiv preprint arXiv:2601.21470.
- Ruicheng Ao, David Simchi-Levi, and Xinshang Wang. Optirepair: Closed-loop diagnosis and repair of supply chain optimization models with LLM agents. *arXiv preprint arXiv:2602.19439*, 2026c.
- Ruicheng Ao, David Simchi-Levi, and Xinshang Wang. Solver-in-the-loop: MDP-based benchmarks for self-correction and behavioral rationality in operations research, 2026d. arXiv preprint arXiv:2601.21008.
- Jackie Baek, Yunhan Chen, Ziyu Chi, and Will Ma. Evaluating LLM-persona generated distributions for decision-making. *arXiv preprint arXiv:2602.06357*, 2026.
- David W. Bates and Atul A. Gawande. Improving safety with information technology. *New England Journal of Medicine*, 348(25):2526–2534, 2003.
- Omar Besbes and Assaf Zeevi. Dynamic pricing without knowing the demand function: Risk bounds and near-optimal algorithms. *Operations Research*, 57(6):1407–1420, 2009.
- Sébastien Bubeck and Nicolò Cesa-Bianchi. Regret analysis of stochastic and nonstochastic multi-armed bandit problems. *Foundations and Trends in Machine Learning*, 5(1):1–122, 2012.
- Sébastien Bubeck, Rémi Munos, and Gilles Stoltz. Pure exploration in finitely armed and continuous armed bandits. *Theoretical Computer Science*, 412(19):1832–1852, 2011.
- C. H. Chen, J. Lin, E. Yücesan, and S. E. Chick. Simulation budget allocation for further enhancing the efficiency of ordinal optimization. *Discrete Event Dynamic Systems*, 10:251–270, 2000.
- Hongyu Chen, Ruicheng Ao, and David Simchi-Levi. Prediction-guided active experiments, 2024.
- Victor Chernozhukov, Denis Chetverikov, Mert Demirer, Esther Duflo, Christian Hansen, Whitney Newey, and James Robins. Double/debiased machine learning for treatment and structural parameters. *The Econometrics Journal*, 21(1):C1–C68, 2018. doi: 10.1111/ectj.12097.
- Eyal Even-Dar, Shie Mannor, and Yishay Mansour. Action elimination and stopping conditions for the multi-armed bandit and reinforcement learning problems. *Journal of Machine Learning Research*, 7:1079–1105, 2006.

- Peter I. Frazier. Bayesian optimization. In *INFORMS Tutorials in Operations Research*, pages 255–278. INFORMS, 2018. doi: 10.1287/educ.2018.0188.
- Michael C. Fu. Optimization for simulation: Theory vs. practice. *INFORMS Journal on Computing*, 14(3):192–215, 2002.
- Andreas Fuster, Paul Goldsmith-Pinkham, Tarun Ramadorai, and Ansgar Walther. Predictably unequal? the effects of machine learning on credit markets. *The Journal of Finance*, 77(1):5–47, 2022.
- Guillermo Gallego and Garrett Van Ryzin. Optimal dynamic pricing of inventories with stochastic demand over finite horizons. *Management Science*, 40(8):999–1020, 1994.
- Noah Gans, Ger Koole, and Avishai Mandelbaum. Telephone call centers: Tutorial, review, and research prospects. *Manufacturing & Service Operations Management*, 5(2):79–141, 2003.
- S. Gao, W. Chen, and L. Shi. A new budget allocation framework for the expected opportunity cost. *Operations Research*, 65:787–803, 2017.
- Aurélien Garivier and Emilie Kaufmann. Optimal best arm identification with fixed confidence. In *Proceedings of the 29th Conference on Learning Theory (COLT)*, 2016.
- Steven R Howard, Aaditya Ramdas, Jon McAuliffe, and Jasjeet Sekhon. Time-uniform, nonparametric, nonasymptotic confidence sequences. *The Annals of Statistics*, 49(2):1055–1080, 2021.
- He Huang, Anand Krishnaswamy, Andrey Kolobov, Bryan Koenig, and Anuj K. Shah. When to defer to a human? a cost-sensitive approach to combining human and machine classifiers. *Management Science*, 68(11):7867–7887, 2022.
- Rouba Ibrahim, Han Ye, Pierre L’Ecuyer, and Haipeng Shen. Forecasting call center arrivals: Fixed-effects, mixed-effects, and the holt-winters approach. *Manufacturing & Service Operations Management*, 18(1):137–153, 2016.
- Kevin G. Jamieson, Matthew Malloy, Robert D. Nowak, and Sébastien Bubeck. lil’UCB: An optimal exploration algorithm for multi-armed bandits. In *Proceedings of the 27th Conference on Learning Theory (COLT)*, pages 423–439, 2014.
- Wenlong Ji, Yihan Pan, Ruihao Zhu, and Lihua Lei. Multi-armed bandits with machine learning-generated surrogate rewards, 2025. arXiv preprint arXiv:2506.16658.
- Pooria Joulani, András Györfi, and Csaba Szepesvári. Online learning under delayed feedback. In *International Conference on Machine Learning*, pages 1453–1461. PMLR, 2013.
- Joseph M. Juran and Frank M. Gryna. *Juran’s Quality Control Handbook*. McGraw-Hill, 4th edition, 1988.
- Daniel Kahneman. *Thinking, Fast and Slow*. Farrar, Straus and Giroux, New York, 2011.
- Shivaram Kalyanakrishnan, Ambuj Tewari, Peter Auer, and Peter Stone. PAC subset selection in stochastic multi-armed bandits. In *Proceedings of the 29th International Conference on Machine Learning (ICML)*, 2012.

- Kirthevasan Kandasamy, Gautam Dasarathy, Junier Oliva, Jeff Schneider, and Barnabás Póczos. Gaussian process bandit optimisation with multi-fidelity evaluations. In *Advances in Neural Information Processing Systems (NeurIPS)*, 2016.
- Kirthevasan Kandasamy, Gautam Dasarathy, Jeff Schneider, and Barnabás Póczos. Multi-fidelity bayesian optimisation with continuous approximations. In *International Conference on Machine Learning (ICML)*, 2017.
- Emilie Kaufmann and Wouter M Koolen. Mixture martingales revisited with applications to sequential tests and confidence intervals. *Journal of Machine Learning Research*, 22(246):1–44, 2021.
- Emilie Kaufmann, Olivier Cappé, and Aurélien Garivier. On the complexity of best-arm identification in multi-armed bandit models. *The Journal of Machine Learning Research*, 17(1):1–42, 2016.
- Seong-Hee Kim and Barry L. Nelson. A fully sequential procedure for indifference-zone selection in simulation. *ACM Transactions on Modeling and Computer Simulation*, 11(3):251–273, 2001.
- Jon Kleinberg, Himabindu Lakkaraju, Jure Leskovec, Jens Ludwig, and Sendhil Mullainathan. Human decisions and machine predictions. *The Quarterly Journal of Economics*, 133(1):237–293, 2018.
- Tze Leung Lai. On confidence sequences. *The Annals of Statistics*, 4(2):265–280, 1976.
- Eddie Landesberg and Manjari Narayan. Causal judge evaluation: Calibrated surrogate metrics for LLM systems, 2025. arXiv preprint arXiv:2512.11150.
- Tor Lattimore and Csaba Szepesvári. *Bandit Algorithms*. Cambridge University Press, 2020.
- Kuo Liang, Yuhang Lu, Jianming Mao, Shuyi Sun, Chunwei Yang, Congcong Zeng, Xiao Jin, Hanzhang Qin, Ruihao Zhu, and Chung-Piaw Teo. Large-scale optimization model auto-formulation: Harnessing LLM flexibility via structured workflow, 2026. arXiv preprint arXiv:2601.09635.
- Jerzy Neyman. On the two different aspects of the representative method: The method of stratified sampling and the method of purposive selection. *Journal of the Royal Statistical Society*, 97(4): 558–625, 1934.
- Arjun Panickssery, Samuel Bowman, and Shi Feng. Llm evaluators recognize and favor their own generations. *Advances in Neural Information Processing Systems*, 37:68772–68802, 2024.
- Ciara Pike-Burke, Shipra Agrawal, Csaba Szepesvari, and Steffen Grunewalder. Bandits with delayed, aggregated anonymous feedback. In *International Conference on Machine Learning*, pages 4105–4113. PMLR, 2018.
- Alvin Rajkomar, Jeffrey Dean, and Isaac Kohane. Machine learning in medicine. *New England Journal of Medicine*, 380(14):1347–1358, 2019.
- James M Robins, Andrea Rotnitzky, and Lue Ping Zhao. Estimation of regression coefficients when some regressors are not always observed. *Journal of the American statistical Association*, 89(427): 846–866, 1994.

- Rajat Sen, Kirthevasan Kandasamy, and Sanjay Shakkottai. Multi-fidelity black-box optimization with hierarchical partitions. In *International Conference on Machine Learning (ICML)*, 2018.
- Rickard Stureborg, Dimitris Alikaniotis, and Yoshi Suhara. Large language models are inconsistent and biased evaluators, 2024. arXiv preprint arXiv:2405.01724.
- Genichi Taguchi. *Introduction to Quality Engineering: Designing Quality into Products and Processes*. Asian Productivity Organization, 1986.
- Eric J. Topol. High-performance medicine: the convergence of human and artificial intelligence. *Nature Medicine*, 25(1):44–56, 2019.
- Peiyi Wang, Lei Li, Liang Chen, Zefan Cai, Dawei Zhu, Binghuai Lin, Yunbo Cao, Lingpeng Kong, Qi Liu, Tianyu Liu, and Zhifang Sui. Large language models are not fair evaluators. In *Proceedings of the 62nd Annual Meeting of the Association for Computational Linguistics (ACL)*, 2024. doi: 10.18653/v1/2024.acl-long.511.
- Chengrun Yang, Xuezhi Wang, Yifeng Lu, Hanxiao Liu, Quoc V Le, Denny Zhou, and Xinyun Chen. Large language models as optimizers. *arXiv preprint arXiv:2309.03409*, 2024.
- Lianmin Zheng, Wei-Lin Chiang, Ying Sheng, Siyuan Zhuang, Zhanghao Wu, Yonghao Zhuang, Zi Lin, Zhuohan Li, Dacheng Li, Eric P Xing, Hao Zhang, Joseph E Gonzalez, and Ion Stoica. Judging LLM-as-a-judge with MT-Bench and chatbot arena. In *Advances in Neural Information Processing Systems*, volume 36, 2023.
- Yongchao Zhou, Andrei Ioan Muresanu, Zhiwei Han, Keiran Paster, Silviu Pitis, Harris Chan, and Jimmy Ba. Large language models are human-level prompt engineers. In *International Conference on Learning Representations*, 2023.
- Tijana Zrnic and Emmanuel Candes. Active statistical inference. In *International Conference on Machine Learning*, pages 62993–63010. PMLR, 2024.
- Tijana Zrnic and Emmanuel J Candès. Cross-prediction-powered inference. *Proceedings of the National Academy of Sciences*, 121(15):e2322083121, 2024.

## A Extended Examples

We provide three examples of common bounded models on  $[0, 1]$  for audit outcomes that satisfy the Local Asymptotic Normality (LAN) assumption ([Assumption 6.2](#)). In each example, the key point is that the model is quadratic mean differentiable (QMD) in the parameter governing the arm-dependent mean gap (possibly after conditioning on  $(X, F)$ ), which implies LAN under standard regularity conditions

*Example A.1* (Bernoulli logistic regression). Let  $Y \in \{0, 1\}$  and suppose that conditional on  $(k, X = x, F = f)$ ,

$$\mathbb{P}(Y = 1 \mid k, X = x, F = f) = \sigma(\beta_k^\top \phi(x, f)), \quad \sigma(u) := \frac{1}{1 + e^{-u}},$$

for a known feature map  $\phi : \mathcal{X} \times [0, 1] \rightarrow \mathbb{R}^d$  and arm parameter  $\beta_k \in \mathbb{R}^d$ . This model generates bounded outcomes automatically and is a regular exponential family in canonical form.

To see why LAN holds, note that the conditional log-likelihood for one observation is

$$\ell(\beta_k; y, x, f) = y \beta_k^\top \phi(x, f) - \log(1 + e^{\beta_k^\top \phi(x, f)}).$$

The score is

$$\nabla_{\beta_k} \ell(\beta_k; y, x, f) = \phi(x, f) (y - \sigma(\beta_k^\top \phi(x, f))),$$

and the (negative) Hessian is

$$-\nabla_{\beta_k}^2 \ell(\beta_k; y, x, f) = \phi(x, f) \phi(x, f)^\top \sigma(\eta) (1 - \sigma(\eta)), \quad \eta = \beta_k^\top \phi(x, f),$$

which is bounded and continuous in  $\beta_k$  for fixed  $(x, f)$ . Under standard moment and identifiability conditions such as  $\mathbb{E}[\|\phi(X, F)\|^2] < \infty$  and the Fisher information matrix

$$\mathcal{I}_k(\beta_k) := \mathbb{E} \left[ \phi(X, F) \phi(X, F)^\top \sigma(\eta) (1 - \sigma(\eta)) \mid k \right]$$

being finite and non-singular in a neighborhood of the true parameter, the model is QMD and therefore LAN holds. Concretely, for local alternatives  $\beta'_k = \beta_k + h/\sqrt{n}$ , the log-likelihood ratio admits the quadratic expansion

$$\log \frac{dP_{\beta'_k}^{(n)}}{dP_{\beta_k}^{(n)}} = h^\top \Delta_{n,k} - \frac{1}{2} h^\top \mathcal{I}_k(\beta_k) h + o_P(1),$$

where  $\Delta_{n,k}$  is asymptotically normal with covariance  $\mathcal{I}_k(\beta_k)$ . This is exactly the LAN structure used in [Assumption 6.2](#).

*Example A.2* (Beta regression). Let  $Y \in (0, 1)$  and suppose that conditional on  $(k, X = x, F = f)$ ,

$$Y \mid (k, X = x, F = f) \sim \text{Beta}(\alpha_k(x, f), \beta_k(x, f)).$$

A common parameterization is via a conditional mean  $m_k(x, f) \in (0, 1)$  and precision  $\varphi_k(x, f) > 0$ , with  $\alpha_k(x, f) = m_k(x, f)\varphi_k(x, f)$  and  $\beta_k(x, f) = (1 - m_k(x, f))\varphi_k(x, f)$ . For example, one may model  $m_k(x, f) = \sigma(\beta_k^\top \phi(x, f))$  and let  $\varphi_k(x, f)$  be either fixed or smoothly parameterized.

LAN holds for this model under standard regularity conditions for smooth parametric families dominated by Lebesgue measure on  $(0, 1)$ . The Beta density is

$$p(y; \alpha, \beta) = \frac{\Gamma(\alpha + \beta)}{\Gamma(\alpha)\Gamma(\beta)} y^{\alpha-1} (1 - y)^{\beta-1}, \quad y \in (0, 1),$$

which is smooth in  $(\alpha, \beta)$  on any compact subset bounded away from 0. If we assume there exist constants  $0 < a_{\min} \leq a_{\max}$  such that for all  $(k, x, f)$ ,

$$\alpha_k(x, f), \beta_k(x, f) \in [a_{\min}, a_{\max}],$$

then the log-density and its first two derivatives with respect to the underlying finite-dimensional parameter (e.g.,  $\beta_k$ ) are uniformly integrable. This ensures differentiability under the integral sign and a finite Fisher information matrix.

More explicitly, the score for the mean-parameter component can be written (by chain rule) as a product of  $\nabla_{\beta_k} m_k(x, f)$  and the derivative of the log-likelihood with respect to  $m$ , which involves the digamma function  $\psi_0(\cdot)$  evaluated at  $\alpha, \beta, \alpha + \beta$ . Under the condition of being bounded away from zero, these special functions remain bounded on the relevant parameter neighborhood, so the Fisher information  $\mathcal{I}_k(\beta_k)$  is finite. Together with a full-rank condition (identifiability), the model is QMD and therefore satisfies LAN. Along local alternatives  $\beta'_k = \beta_k + h/\sqrt{n}$ , the KL divergence admits the quadratic expansion in [Assumption 6.2](#) with  $\mathcal{I}(\nu; \pi)$  equal to the Fisher information contributed by proxy and audited components.

*Example A.3 (Truncated Gaussian).* Let  $Z \mid (k, X = x, F = f) \sim \mathcal{N}(\mu_k(x, f), \sigma_k^2)$  with  $\sigma_k$  bounded away from 0, and define the bounded outcome by clipping:

$$Y := \text{clip}(Z, 0, 1).$$

Equivalently,  $Y$  has a mixed distribution consisting of point masses at 0 and 1 capturing the events  $\{Z \leq 0\}$  and  $\{Z \geq 1\}$ , and a continuous density on  $(0, 1)$  equal to the Gaussian density of  $Z$  restricted to  $(0, 1)$ . This construction satisfies [Assumption 3.1](#) by definition.

Intuitively, the underlying Gaussian family is smooth in  $\mu$ , and clipping is a measurable transformation. As long as the resulting likelihood remains differentiable in quadratic mean with finite Fisher information, LAN follows.

One convenient way to formalize this is to work with a dominating measure  $m$  on  $[0, 1]$  that is the sum of Lebesgue measure on  $(0, 1)$  plus two endpoints  $\{0, 1\}$ . The likelihood  $p_\mu(y)$  with respect to  $m$  is

$$p_\mu(y) = \begin{cases} \Phi\left(\frac{0-\mu}{\sigma}\right), & y = 0, \\ \frac{1}{\sigma} \varphi\left(\frac{y-\mu}{\sigma}\right), & y \in (0, 1), \\ 1 - \Phi\left(\frac{1-\mu}{\sigma}\right), & y = 1, \end{cases}$$

where  $\varphi$  and  $\Phi$  are the standard normal pdf and cdf. All three pieces are smooth in  $\mu$ , with derivatives bounded by constants depending on  $\sigma$  and on how close  $\mu$  can get to extreme values. If we assume  $\sigma_k \geq \sigma_{\min} > 0$  and  $\mu_k(x, f)$  ranges over a bounded set (or more generally satisfies integrability conditions ensuring finite information after averaging over  $(X, F)$ ), then the Fisher information for  $\mu$  is finite (the continuous part contributes a term comparable to  $1/\sigma^2$  weighted by  $\mathbb{P}(0 < Z < 1)$ , and the endpoints contribute additional finite terms involving derivatives of  $\Phi$ ). Then the model is QMD with respect to  $\mu$ , which implies LAN.

Therefore, along local alternatives  $\mu'_k(x, f) = \mu_k(x, f) + h/\sqrt{n}$ , the KL divergence between the resulting clipped distributions satisfies the quadratic LAN expansion used in [Assumption 6.2](#), with an effective Fisher information that can be interpreted as the Gaussian information scaled by the truncation effects (and remains finite and positive under the conditions above).

Note that these examples not only make [Assumption 6.2](#) concrete, but also demonstrate that the boundedness assumption ([Assumption 3.1](#)) is compatible with [Assumption 6.2](#). All main results (including the instance-dependent lower bound ([Theorem 6.3](#)) and asymptotic optimality ([Theorem F.2](#))) hold under these bounded models without requiring specific distributional forms.

## B Proof of Theorem 3.5

### B.1 Proof of Part 1

Consider a setting with  $K = 2$  arms. We construct two problem instances where the marginal distribution of proxy scores  $F$  is identical for all arms, but the true means  $\theta$  (and thus the better arm) are different. All variables are bounded in  $[0, 1]$ . The main text allows the algorithm to observe  $(X_t, F_t)$  in each pull. The construction below remains valid by taking the instance distribution  $\mathcal{D}$  to be degenerate, e.g.,  $X \equiv x_0$  almost surely. Then  $X_t$  carries no information and the observable history reduces to  $\{(k_t, F_t)\}_{t \leq \tau}$  without loss of generality.

**Instance A (Arm 1 is better).** For Arm 1, let  $F \sim \text{Bernoulli}(0.5)$  with  $Y$  being deterministic given  $F$ :  $Y = 0.2$  if  $F = 0$ , and  $Y = 1.0$  if  $F = 1$ . The marginal mean is  $\theta_1 = 0.5(0.2) + 0.5(1.0) = 0.6$ , and the marginal distribution of  $F$  is  $\text{Bernoulli}(0.5)$ .

For Arm 2, let  $F \sim \text{Bernoulli}(0.5)$  with  $Y = 0$  if  $F = 0$ , and  $Y = 0.8$  if  $F = 1$ . The marginal mean is  $\theta_2 = 0.5(0.0) + 0.5(0.8) = 0.4$ , and the marginal distribution of  $F$  is again  $\text{Bernoulli}(0.5)$ .

Since  $\theta_1 = 0.6 > \theta_2 = 0.4$ , Arm 1 is the better arm ( $k^* = 1$ ).

**Instance B (Arm 2 is better).** We swap the arm distributions. Arm 1 uses the distribution of Arm 2 from Instance A ( $\theta_1 = 0.4$ ), and Arm 2 uses the distribution of Arm 1 from Instance A ( $\theta_2 = 0.6$ ). In both cases, the marginal distribution of  $F$  remains  $\text{Bernoulli}(0.5)$ . Since  $\theta_2 = 0.6 > \theta_1 = 0.4$ , Arm 2 is now better ( $k^* = 2$ ).

A proxy-only algorithm observes only the sequence of proxy scores  $(\{(k_t, F_t)\}_{t=1}^T)$ . In both instances, for any arm  $k$ , the marginal distribution of  $F_t$  is  $\text{Bernoulli}(0.5)$ . Since the algorithm does not observe  $Y_t$ , the probability distribution of the observed history is identical for Instance A and Instance B. Let  $\psi$  be the algorithm's decision rule mapping history to a selected arm, and let  $p = \mathbb{P}(\psi(\text{History}) = 1)$ . On Instance A, the error probability is  $\mathbb{P}(\text{Error}) = \mathbb{P}(\text{Select } 2) = 1 - p$ , and on Instance B,  $\mathbb{P}(\text{Error}) = \mathbb{P}(\text{Select } 1) = p$ . The maximum error probability is  $\max(1 - p, p) \geq 0.5$ . Thus, no proxy-only algorithm can achieve  $\delta$ -correctness for any  $\delta < 0.5$ .

### B.2 Proof of Part 2

Consider a naive estimator that estimates  $\theta_k$  by the simple average of audited outcomes, ignoring the selectivity of auditing:

$$\hat{\theta}_k^{\text{naive}} = \frac{\sum_{t=1}^n A_t Y_t}{\sum_{t=1}^n A_t}. \quad (22)$$

Let the audit policy depend on the proxy score while satisfying positivity ([Assumption 3.3](#)), i.e., for some small  $\pi_{\min} > 0$ ,

$$\pi(f) = \begin{cases} 1 & \text{if } f > 0.5, \\ \pi_{\min} & \text{otherwise.} \end{cases} \quad (23)$$

This policy satisfies  $\pi(f) \geq \pi_{\min}$  for all  $f$ , but concentrates audits in regions with high proxy scores. Consider an arm where  $F \sim \text{Uniform}[0, 1]$ .

**Instance A (Positive Correlation).** Let  $Y = F$ . The true mean is  $\theta = \mathbb{E}[F] = 0.5$ . Under the audit policy, the audit probability is  $\mathbb{P}(A = 1) = 0.5(1 + \pi_{\min})$ . The conditional expectation of  $Y$

given audit is:

$$\begin{aligned}\mathbb{E}[Y | A = 1] &= \frac{\mathbb{P}(F > 0.5) \cdot \mathbb{E}[Y | F > 0.5] + \pi_{\min} \cdot \mathbb{P}(F \leq 0.5) \cdot \mathbb{E}[Y | F \leq 0.5]}{\mathbb{P}(A = 1)} \\ &= \frac{0.5 \cdot 0.75 + \pi_{\min} \cdot 0.5 \cdot 0.25}{0.5(1 + \pi_{\min})} = \frac{0.75 + 0.25\pi_{\min}}{1 + \pi_{\min}}.\end{aligned}\quad (24)$$

By the law of large numbers,  $\hat{\theta}^{\text{naive}} \xrightarrow{a.s.} \frac{0.75 + 0.25\pi_{\min}}{1 + \pi_{\min}} \neq 0.5$  for any  $\pi_{\min} < 1$ . For small  $\pi_{\min}$ , the asymptotic bias is  $+0.25(1 - \pi_{\min})/(1 + \pi_{\min}) \rightarrow +0.25$  as  $\pi_{\min} \rightarrow 0$ .

**Instance B (Negative Correlation).** Let  $Y = 1 - F$ . The true mean is  $\theta = \mathbb{E}[1 - F] = 0.5$ . A similar calculation shows

$$\mathbb{E}[Y | A = 1] = \frac{0.5 \cdot 0.25 + \pi_{\min} \cdot 0.5 \cdot 0.75}{0.5(1 + \pi_{\min})} = \frac{0.25 + 0.75\pi_{\min}}{1 + \pi_{\min}}.\quad (25)$$

For small  $\pi_{\min}$ , the asymptotic bias is  $-0.25(1 - \pi_{\min})/(1 + \pi_{\min}) \rightarrow -0.25$  as  $\pi_{\min} \rightarrow 0$ .

We embed the above inconsistency into a  $K = 2$  best arm identification instance. For each arm  $k \in \{1, 2\}$ , let the proxy score satisfy  $F \sim \text{Uniform}[0, 1]$  on each pull. Consider the audit policy (23). Define the outcomes by

$$Y(1) := F, \quad Y(2) := \begin{cases} 1, & F \leq 0.5, \\ 1 - F, & F > 0.5. \end{cases}$$

Both outcomes lie in  $[0, 1]$  almost surely, so [Assumption 3.1](#) holds.

We have

$$\theta_1 = \mathbb{E}[Y(1)] = \mathbb{E}[F] = 0.5,$$

and

$$\begin{aligned}\theta_2 &= \mathbb{E}[Y(2)] = \mathbb{E}[1 \cdot \mathbb{1}\{F \leq 0.5\}] + \mathbb{E}[(1 - F) \cdot \mathbb{1}\{F > 0.5\}] \\ &= 0.5 \cdot 1 + 0.5 \cdot \mathbb{E}[1 - F | F > 0.5] = 0.5 + 0.5 \cdot (1 - 0.75) = 0.625.\end{aligned}\quad (26)$$

Then Arm 2 is better ( $k^* = 2$ ).

Consider the naive selective-audit estimator (22). The conditional mean among audited samples for Arm 1 is

$$m_1 := \mathbb{E}[Y(1) | A = 1] = \frac{0.75 + 0.25\pi_{\min}}{1 + \pi_{\min}} > 0.5.\quad (27)$$

For Arm 2,

$$\begin{aligned}m_2 := \mathbb{E}[Y(2) | A = 1] &= \frac{\mathbb{E}[Y(2) \mathbb{1}\{F > 0.5\}] + \pi_{\min} \mathbb{E}[Y(2) \mathbb{1}\{F \leq 0.5\}]}{\mathbb{P}(F > 0.5) + \pi_{\min} \mathbb{P}(F \leq 0.5)} \\ &= \frac{0.5 \cdot \mathbb{E}[1 - F | F > 0.5] + \pi_{\min} \cdot 0.5 \cdot 1}{0.5(1 + \pi_{\min})} = \frac{0.25 + \pi_{\min}}{1 + \pi_{\min}} < 0.5,\end{aligned}\quad (28)$$

where the last inequality uses  $\pi_{\min} < 1/2$ .

Moreover, for  $\pi_{\min} < 2/3$  (in particular for  $\pi_{\min} < 0.5$ ), we have  $m_1 > m_2$  since

$$m_1 - m_2 = \frac{(0.75 + 0.25\pi_{\min}) - (0.25 + \pi_{\min})}{1 + \pi_{\min}} = \frac{0.5 - 0.75\pi_{\min}}{1 + \pi_{\min}} > 0.$$

On any event where each arm is pulled infinitely often and receives infinitely many audits (which holds almost surely, e.g., under any strategy that continues sampling both arms while  $\pi_{\min} > 0$ ), the strong law of large numbers yields

$$\hat{\theta}_1^{\text{naive}}(n) \xrightarrow{a.s.} m_1, \quad \hat{\theta}_2^{\text{naive}}(n) \xrightarrow{a.s.} m_2, \quad m_1 > m_2,$$

while the true ordering is  $\theta_2 > \theta_1$ . Therefore, any procedure that uses the naive estimator (22) to rank will have a non-vanishing misidentification probability. In fact, it will eventually favor Arm 1 and thus misidentify the better Arm 2 with probability bounded away from 0 (and typically tending to 1).

## C Proofs of Coverage and $\delta$ -Correctness (Theorems 4.3 and 5.1)

We prove that our confidence sequences are anytime-valid and that PP-LUCB correctly identifies the best arm with probability at least  $1 - \delta$ .

The proof proceeds in four parts. We first review the polynomial stitched boundary method that establishes time-uniform concentration for sub-Gaussian martingales (Theorem C.1). For the proxy mean, we construct a sub-Gaussian martingale from the centered observations and apply the boundary function  $\psi$  to the known variance process (Proposition 4.1). For the residual mean, we show the IPW increments form a bounded martingale difference sequence and apply the same sub-Gaussian boundary with a deterministic worst-case variance process (Proposition 4.2). Last, we combine these via a union bound to prove  $\delta$ -correctness (Theorem 4.3).

### C.1 Martingale Concentration

Both our estimators (the proxy mean  $\hat{\mu}_{F,k}(t)$  and the IPW residual mean  $\hat{\mu}_{R,k}(t)$ ) are sums of adaptively collected observations. For the proxy, the adaptive arm selection creates dependencies. For the residual, the adaptive auditing policy introduces time-varying importance weights. Both cases require martingale concentration tools that handle these dependencies gracefully.

We use the boundary function from Howard et al. [2021]:

$$\psi(v; \alpha) := 1.7 \sqrt{v \left( \log \log(2v) + 0.72 \log \frac{5.2}{\alpha} \right)}. \quad (29)$$

This function derives from polynomial stitching with parameters  $\eta = 2$  and  $s = 1.4$ , which yields leading constant 1.7 and crossing probability at most  $\alpha$ .

Both our estimators involve bounded increments with known range. We apply the sub-Gaussian stitched boundary to each using a deterministic worst-case variance process.

**Theorem C.1** (Howard et al. [2021] Theorem 1). *Let  $(S_t)_{t \geq 1}$  be a sub-Gaussian martingale with variance process  $(V_t)_{t \geq 1}$  such that for all  $\lambda \in \mathbb{R}$ ,*

$$\log \mathbb{E}[\exp(\lambda(S_t - S_{t-1})) \mid \mathcal{F}_{t-1}] \leq \frac{\lambda^2}{2}(V_t - V_{t-1}).$$

*Then, for any  $\alpha \in (0, 1)$ :*

$$\mathbb{P}(\exists t \geq 1 : |S_t| \geq \psi(V_t; \alpha/2)) \leq \alpha.$$

*The factor  $\alpha/2$  leads to a two-sided interval with total error  $\alpha$ .*

For the proxy mean, since  $F \in [0, 1]$ , Hoeffding's lemma produces a conditional sub-Gaussian proxy  $1/4$ , so we may take  $V_{F,k}(n) = n/4$ . For the residual mean, the IPW increment  $Z_t = (A_t/\pi_t) R_t$  (where  $R_t = Y_t - F_t$  is the raw residual) lies in  $[-1/\pi_{\min}, 1/\pi_{\min}]$ , giving range  $M = 2/\pi_{\min}$  and variance proxy  $V_{R,k}(n) = n \cdot M^2/4$ . Both are deterministic and conservative and ensure validity without requiring knowledge of the unknown mean.

## C.2 Proof of Proposition 4.1

Fix arm  $k$ . The proxy observations  $F_s$  for arm  $k$  are collected adaptively, but because  $F_s$  is conditionally independent of past samples given the instance  $X_s$ , the centered observations form a sub-Gaussian martingale difference sequence.

Let  $t_i$  denote the time of the  $i$ -th pull of arm  $k$ , and define the centered increment  $Z_i := F_{t_i} - \mu_{F,k}$ . Since  $F \in [0, 1]$ , by Hoeffding's lemma we have for all  $\lambda \in \mathbb{R}$ ,

$$\log \mathbb{E} \left[ \exp(\lambda(F_{t_i} - \mu_{F,k})) \mid \mathcal{F}_{t_{i-1}}, k_{t_i} = k \right] \leq \frac{\lambda^2}{8}.$$

Equivalently, the centered increment  $Z_i$  is conditionally sub-Gaussian with variance proxy  $1/4$ . Thus a valid variance process is  $V_{F,k}(n) = n/4$ .

Define the martingale sum  $S_{F,k}(n) = \sum_{i=1}^n Z_i = n(\hat{\mu}_{F,k}(n) - \mu_{F,k})$ , with variance process  $V_{F,k}(n) = \sum_{i=1}^n \sigma^2 \leq n/4$ . Since  $\psi(v; \alpha)$  is increasing in  $v$ , using  $V_{F,k}(n) = n/4$  gives a valid bound. Applying [Theorem C.1](#) with error probability  $\delta_k$ , we have

$$\mathbb{P}(\exists n \geq 1 : |S_{F,k}(n)| \geq \psi(V_{F,k}(n); \delta_k/2)) \leq \delta_k.$$

Equivalently,  $|S_{F,k}(n)| \leq \psi(n/4; \delta_k/2)$  for all  $n$  with probability at least  $1 - \delta_k$ . Dividing by  $n$  gives

$$|\hat{\mu}_{F,k}(n) - \mu_{F,k}| \leq \frac{\psi(n/4; \delta_k/2)}{n} = w_{F,k}(n),$$

which holds uniformly over all  $n \geq 1$ . To obtain a joint guarantee over all  $K$  arms, we set  $\delta_k = \delta/(2K)$  per arm (so the boundary uses  $\delta_k/2 = \delta/(4K)$ ). A union bound over  $K$  arms gives total failure probability at most  $K \cdot \delta/(2K) = \delta/2$  for the proxy confidence sequences. The remaining  $\delta/2$  error budget is allocated to the residual confidence sequences.

## C.3 Proof of Proposition 4.2

Fix arm  $k$ . The IPW increments  $Z_{t_i} = (A_{t_i}/\pi_{t_i}) R_{t_i}$  involve random importance weights that depend on the adaptive audit policy. Despite this adaptivity, the centered increments form a bounded martingale difference sequence under [Assumption 3.2](#), and we apply the sub-Gaussian stitched boundary.

Let  $t_i$  denote the time of the  $i$ -th pull of arm  $k$ , and define the centered increment  $\xi_i = Z_{t_i} - \mu_{R,k}$ . The audit decision  $A_{t_i}$  is made based on the history  $\mathcal{F}_{t_{i-1}}$  and current observables  $(X_{t_i}, F_{t_i})$ . Under [Assumption 3.2](#), we have  $Y_{t_i} \perp A_{t_i} \mid \mathcal{F}_{t_{i-1}}, X_{t_i}, F_{t_i}$ . Thus, the conditional expectation of the IPW increment is:

$$\begin{aligned} \mathbb{E}[\xi_i \mid \mathcal{F}_{t_{i-1}}] &= \mathbb{E} \left[ \frac{A_{t_i}}{\pi_{t_i}} (Y_{t_i} - F_{t_i}) - \mu_{R,k} \mid \mathcal{F}_{t_{i-1}} \right] \\ &= \mathbb{E}_{(X,F)} \left[ \mathbb{E} \left[ \frac{A_{t_i}}{\pi_{t_i}} (Y_{t_i} - F_{t_i}) \mid \mathcal{F}_{t_{i-1}}, X_{t_i}, F_{t_i} \right] \right] - \mu_{R,k} \\ &= \mathbb{E}_{(X,F)} \left[ \frac{\mathbb{E}[A_{t_i} \mid \cdot]}{\pi_{t_i}} \mathbb{E}[(Y_{t_i} - F_{t_i}) \mid \cdot] \right] - \mu_{R,k} \\ &= \mathbb{E}_{(X,F)} [\mu_{R,k}(X_{t_i}, F_{t_i})] - \mu_{R,k} = 0. \end{aligned}$$

The third equality uses the conditional independence  $Y \perp A$  and the fact that  $\pi_{t_i} = \mathbb{E}[A_{t_i} \mid \mathcal{F}_{t_i-1}, X_{t_i}, F_{t_i}]$ .

Recall  $R_{t_i} = Y_{t_i} - F_{t_i} \in [-1, 1]$  and  $\pi_{t_i} \geq \pi_{\min}$ . Then

$$Z_{t_i} = \frac{A_{t_i}}{\pi_{t_i}} R_{t_i} \in \left[ -\frac{1}{\pi_{\min}}, \frac{1}{\pi_{\min}} \right].$$

Also,  $\mu_{R,k} = \mathbb{E}[Y - F \mid k] \in [-1, 1] \subseteq \left[ -\frac{1}{\pi_{\min}}, \frac{1}{\pi_{\min}} \right]$ . Therefore the centered increment  $\xi_i = Z_{t_i} - \mu_{R,k}$  is supported on an interval of length  $M = \frac{2}{\pi_{\min}}$ . By Hoeffding's lemma (conditionally on  $\mathcal{F}_{t_i-1}$ ), for all  $\lambda \in \mathbb{R}$ ,

$$\log \mathbb{E}[\exp(\lambda \xi_i) \mid \mathcal{F}_{t_i-1}] \leq \frac{\lambda^2 M^2}{8} = \frac{\lambda^2}{2} \cdot \frac{M^2}{4}.$$

Thus  $\xi_i$  is conditionally sub-Gaussian with variance proxy  $M^2/4$ , and a valid deterministic variance process is  $V_{R,k}(n) = n \cdot M^2/4$ .

Define the martingale sum  $S_{R,k}(n) = \sum_{i=1}^n \xi_i = n(\widehat{\mu}_{R,k}(n) - \mu_{R,k})$ . Applying [Theorem C.1](#) with variance process  $V_{R,k}(n) = n \cdot M^2/4$  and error probability  $\delta_k$ , we have

$$\mathbb{P}(\exists n \geq 1 : |S_{R,k}(n)| \geq \psi(n \cdot M^2/4; \delta_k/2)) \leq \delta_k.$$

Dividing by  $n$  gives

$$|\widehat{\mu}_{R,k}(n) - \mu_{R,k}| \leq \frac{\psi(n \cdot M^2/4; \delta_k/2)}{n} = w_{R,k}(n).$$

This bound holds uniformly over all  $n \geq 1$ . Setting  $\delta_k = \delta/(2K)$  per arm (so the boundary uses  $\delta_k/2 = \delta/(4K)$ ) and applying a union bound over  $K$  arms gives a total failure probability at most  $K \cdot \delta/(2K) = \delta/2$  for the residual confidence sequences.

#### C.4 Proof of [Theorems 4.3](#) and [5.1](#)

We prove the  $\delta$ -correctness in two parts. First, all confidence sequences hold simultaneously with high probability. Second, the stopping rule guarantees correct identification when this event occurs.

Define  $\mathcal{E}$  as the event that all confidence sequences hold for all arms and all times:

$$\mathcal{E} = \bigcap_{k=1}^K \bigcap_{t=1}^{\infty} \{\theta_k \in [L_k(t), U_k(t)]\}.$$

Each interval  $[L_k(t), U_k(t)]$  combines a proxy confidence sequence (width  $w_{F,k}(t)$ ) and a residual confidence sequence (width  $w_{R,k}(t)$ ). By [Propositions 4.1](#) and [4.2](#), each type of sequence (proxy and residual) has total failure probability at most  $\delta/2$  across all  $K$  arms. Thus, by a union bound,

$$\mathbb{P}(\mathcal{E}^c) \leq \frac{\delta}{2} + \frac{\delta}{2} = \delta,$$

and  $\mathbb{P}(\mathcal{E}) \geq 1 - \delta$ .

The algorithm stops at time  $\tau$  when the confidence sequences separate

$$L_{\widehat{k}_\tau}(\tau) > \max_{k \neq \widehat{k}_\tau} U_k(\tau),$$

where  $\widehat{k}_t \in \arg \max_{k \in [K]} \widehat{\theta}_k(t)$  is the leader arm used by [Algorithm 1](#), and it outputs  $\widehat{k} = \widehat{k}_\tau$ .

On the event  $\mathcal{E}$ , we have  $\theta_k \in [L_k(\tau), U_k(\tau)]$  for all  $k$ . Therefore, for any  $j \neq \widehat{k}_\tau$ ,

$$\theta_{\widehat{k}_\tau} \geq L_{\widehat{k}_\tau}(\tau) > U_j(\tau) \geq \theta_j.$$

Then  $\theta_{\widehat{k}_\tau} > \theta_j$  for all  $j \neq \widehat{k}_\tau$ , which implies  $\widehat{k}_\tau = k^*$ . Since  $\mathbb{P}(\mathcal{E}) \geq 1 - \delta$ , the algorithm is  $\delta$ -correct.

## D Proof of Optimal Auditing (Theorem 5.3)

We derive the auditing policy that minimizes the asymptotic variance of the IPW residual estimator under an average audit-rate constraint.

Fix arm  $k$ . On each pull of arm  $k$ , we observe an instance  $X_t$  and a proxy score  $F_t \in [0, 1]$ , and define the residual

$$R_t := Y_t - F_t \in [-1, 1].$$

An audit is requested with probability  $\pi_t$ , where

$$\pi_t = \pi_k(X_t, F_t) \in [\pi_{\min}, 1], \quad A_t \mid (\mathcal{F}_{t-1}, k_t = k, X_t, F_t) \sim \text{Bernoulli}(\pi_t).$$

The IPW residual increment used in the estimator is  $Z_t = \frac{A_t}{\pi_t} R_t$ . Define the conditional first and second moments of the residual given the observables at audit-decision time:

$$m_k(x, f) := \mathbb{E}[R_t \mid k_t = k, X_t = x, F_t = f], \quad g_k(x, f) := \mathbb{E}[R_t^2 \mid k_t = k, X_t = x, F_t = f].$$

Under [Assumption 3.2](#), conditional on the history and current observables  $(\mathcal{F}_{t-1}, k_t, X_t, F_t)$ , the audit decision  $A_t$  is independent of the potential outcome  $Y_t$ , and thus independent of  $R_t = Y_t - F_t$ . Therefore, conditioning on  $(k_t = k, X_t, F_t)$ ,

$$\mathbb{E}[Z_t \mid k_t = k, X_t, F_t] = \mathbb{E}\left[\frac{A_t}{\pi_t} R_t \mid k_t = k, X_t, F_t\right] = \mathbb{E}[R_t \mid k_t = k, X_t, F_t] = m_k(X_t, F_t),$$

and, using  $A_t^2 = A_t$  for Bernoulli variables,

$$\mathbb{E}[Z_t^2 \mid k_t = k, X_t, F_t] = \mathbb{E}\left[\frac{A_t^2}{\pi_t^2} R_t^2 \mid k_t = k, X_t, F_t\right] = \frac{1}{\pi_t} \mathbb{E}[R_t^2 \mid k_t = k, X_t, F_t] = \frac{g_k(X_t, F_t)}{\pi_t}.$$

Then the conditional variance is

$$\text{Var}(Z_t \mid k_t = k, X_t, F_t) = \frac{g_k(X_t, F_t)}{\pi_t} - m_k(X_t, F_t)^2.$$

Taking expectations, and noting that  $\mathbb{E}[Z_t \mid k_t = k] = \mathbb{E}[m_k(X_t, F_t) \mid k_t = k] = \mu_{R,k}$ , we obtain

$$\text{Var}(Z_t \mid k_t = k) = \mathbb{E}\left[\frac{g_k(X_t, F_t)}{\pi_k(X_t, F_t)} \mid k_t = k\right] - \mu_{R,k}^2.$$

Since  $-\mu_{R,k}^2$  does not depend on the audit policy, minimizing  $\text{Var}(Z_t \mid k_t = k)$  is equivalent to minimizing

$$J(\pi_k) := \mathbb{E}\left[\frac{g_k(X_t, F_t)}{\pi_k(X_t, F_t)} \mid k_t = k\right]$$

over measurable policies  $\pi_k : \mathcal{X} \times [0, 1] \rightarrow [\pi_{\min}, 1]$  that satisfy the average audit-rate constraint  $\mathbb{E}[\pi_k(X_t, F_t) \mid k_t = k] = \rho$ .

Consider the Lagrangian functional with multiplier  $\lambda \in \mathbb{R}$ :

$$\mathcal{L}(\pi_k, \lambda) = \mathbb{E}\left[\frac{g_k(X_t, F_t)}{\pi_k(X_t, F_t)} + \lambda \pi_k(X_t, F_t) \mid k_t = k\right] - \lambda \rho.$$

By linearity of expectation, minimizing  $\mathcal{L}$  over functions  $\pi_k(\cdot) \in [\pi_{\min}, 1]$  reduces to minimizing the integrand pointwise. Fix  $(x, f)$  and write  $g = g_k(x, f)$ . We seek

$$\min_{p \in [\pi_{\min}, 1]} \left\{ \frac{g}{p} + \lambda p \right\}.$$

For  $p > 0$ , the objective is convex since  $2g/p^3 \geq 0$ . The unconstrained minimizer satisfies

$$-\frac{g}{p^2} + \lambda = 0 \quad \implies \quad p^\circ(x, f) = \sqrt{\frac{g_k(x, f)}{\lambda}}.$$

Projecting onto the feasible interval  $[\pi_{\min}, 1]$  gives

$$\pi_k^*(x, f) = \text{clip}\left(\sqrt{\frac{g_k(x, f)}{\lambda}}, \pi_{\min}, 1\right).$$

The normalizing constant  $\lambda > 0$  is chosen so that the budget binds  $\mathbb{E}[\pi_k^*(X_t, F_t) \mid k_t = k] = \rho$ . In particular, before clipping,  $\pi_k^*(x, f) \propto \sqrt{g_k(x, f)}$ , which is exactly (13) in [Theorem 5.3](#).

Next, we give a simple two-segment construction showing that ignoring heterogeneity in  $g_k(x, f)$  can incur a large variance penalty.

Let the conditional second moment  $g_k(X_t, F_t)$  take two values:

$$g_k(X_t, F_t) = \begin{cases} G & \text{with probability } p, \\ \varepsilon & \text{with probability } 1 - p, \end{cases} \quad \text{where } G \gg \varepsilon > 0.$$

Consider the feasible clipped policy

$$\pi_{\text{seg}}(X_t, F_t) = \begin{cases} 1 & \text{on the } g = G \text{ segment,} \\ \pi_{\min} & \text{on the } g = \varepsilon \text{ segment,} \end{cases}$$

and choose  $p := \frac{\rho - \pi_{\min}}{1 - \pi_{\min}}$  so that  $\mathbb{E}[\pi_{\text{seg}}] = \rho$ . For sufficiently large  $G/\varepsilon$ ,  $\pi_{\text{seg}}$  is of the clipped Neyman form since it concentrates audits on the regions with high  $g$  values.

The objective under uniform auditing  $\pi_k \equiv \rho$  is

$$J(\pi_k \equiv \rho) = \mathbb{E}\left[\frac{g_k(X_t, F_t)}{\rho}\right] = \frac{pG + (1 - p)\varepsilon}{\rho}.$$

Under  $\pi_{\text{seg}}$ ,

$$J(\pi_{\text{seg}}) = \mathbb{E}\left[\frac{g_k(X_t, F_t)}{\pi_{\text{seg}}(X_t, F_t)}\right] = p\frac{G}{1} + (1 - p)\frac{\varepsilon}{\pi_{\min}} = pG + (1 - p)\frac{\varepsilon}{\pi_{\min}}.$$

Letting  $G \rightarrow \infty$  (with  $\rho, \pi_{\min}, \varepsilon$  fixed), we have

$$\frac{J(\pi_k \equiv \rho)}{J(\pi_{\text{seg}})} \longrightarrow \frac{1}{\rho}.$$

Thus, when  $\rho$  is small, a uniform audit policy can be worse than a policy guided by residual uncertainty (clipped Neyman) by a large factor (on the order of  $1/\rho$ ). This proves the stated inefficiency of uniform auditing under strong heterogeneity.

## E Proof of the Cost Upper Bound

This section proves the cost upper bound in [Theorem 6.1](#) under the same anytime-valid confidence sequences used in the main text. We also provide the derivation necessary for [Example 6.4](#).

## E.1 Proof of Cost Upper Bound (Theorem 6.1)

Let  $\tau$  be the stopping time and recall the monetary cost

$$\text{Cost}(\tau) := c_F \tau + c_Y \sum_{t=1}^{\tau} A_t.$$

Write  $k^* \in \arg \max_k \theta_k$  and define the gaps  $\Delta_k := \theta_{k^*} - \theta_k$  for  $k \neq k^*$ .

A convenient sufficient condition for the LUCB stopping rule is that, for every nonbest arm  $k \neq k^*$ , the confidence half-width satisfies

$$w_{F,k}(t) + w_{R,k}(t) \leq \frac{\Delta_k}{2},$$

where  $w_{F,k}(t)$  and  $w_{R,k}(t)$  are the proxy and residual half-widths defined in Propositions 4.1 and 4.2. On the event of simultaneous confidence sequence coverage, this implies  $U_k(t) \leq \theta_k + \Delta_k/2 \leq \theta_{k^*} - \Delta_k/2 \leq L_{k^*}(t)$ , so the best arm is separated from all challengers.

Fix arm  $k$  and let  $N_k(t)$  be its number of pulls up to time  $t$ . Under Assumptions 3.1 to 3.3, the stitched boundary  $\psi(\cdot; \cdot)$  in (9) gives, up to universal constants and log log factors,

$$w_{F,k}(t) = \frac{\psi(N_k(t)/4; \delta_k/2)}{N_k(t)} \lesssim \sqrt{\frac{\log(1/\delta_k)}{N_k(t)}} \cdot \frac{1}{2},$$

because the proxy uses the range-based variance proxy  $V_{F,k}(t) = N_k(t)/4$ .

For the residual, recall  $Z_t = (A_t/\pi_t)(Y_t - F_t)$ , and with  $\pi_t \geq \pi_{\min}$  we have  $Z_t \in [-1/\pi_{\min}, 1/\pi_{\min}]$ , i.e., range length  $M = 2/\pi_{\min}$ . Therefore the residual CS uses the deterministic envelope  $V_{R,k}(t) = N_k(t) \cdot M^2/4 = N_k(t)/\pi_{\min}^2$ , and

$$w_{R,k}(t) = \frac{\psi(N_k(t)/\pi_{\min}^2; \delta_k/2)}{N_k(t)} \lesssim \sqrt{\frac{\log(1/\delta_k)}{N_k(t)}} \cdot \frac{1}{\pi_{\min}}.$$

Combining the two bounds gives

$$w_{F,k}(t) + w_{R,k}(t) \lesssim \sqrt{\frac{\log(1/\delta_k)}{N_k(t)}} \left( \frac{1}{2} + \frac{1}{\pi_{\min}} \right).$$

Thus a sufficient condition for  $w_{F,k}(t) + w_{R,k}(t) \leq \Delta_k/2$  is

$$N_k(t) \gtrsim \frac{\log(1/\delta_k)}{\Delta_k^2} \left( \frac{1}{2} + \frac{1}{\pi_{\min}} \right)^2.$$

Using  $(a+b)^2 \leq 2(a^2 + b^2)$ , we can further simplify the factor as

$$\left( \frac{1}{2} + \frac{1}{\pi_{\min}} \right)^2 \leq 2 \left( \frac{1}{4} + \frac{1}{\pi_{\min}^2} \right),$$

so it suffices that

$$N_k(t) \gtrsim \frac{\log(1/\delta_k)}{\Delta_k^2} \left( \frac{1}{4} + \frac{1}{\pi_{\min}^2} \right), \quad k \neq k^*. \quad (30)$$

This establishes the advertised  $\log(1/\delta)/\Delta_k^2$  scaling, with the proxy and residual uncertainty contributions governed by the same range-based envelopes used in the anytime-valid CS.

On the simultaneous-coverage event from [Theorem 4.3](#), once every non-best arm  $k \neq k^*$  satisfies [\(30\)](#), its upper confidence bound cannot exceed the best arm's lower bound, so it cannot be selected as the LUCB challenger thereafter. Standard LUCB arguments then imply that the total number of pulls until stopping satisfies

$$\tau \lesssim \sum_{k \neq k^*} \frac{\log(1/\delta_k)}{\Delta_k^2} \left( \frac{1}{4} + \frac{1}{\pi_{\min}^2} \right),$$

up to universal constants and log log factors.

For the monetary cost, write

$$\mathbb{E}[\text{Cost}(\tau)] = c_F \mathbb{E}[\tau] + c_Y \mathbb{E} \left[ \sum_{t=1}^{\tau} A_t \right].$$

Introduce the (random) average audit fraction up to stopping,  $\hat{\rho}_\tau := \frac{1}{\tau} \sum_{t=1}^{\tau} A_t \in [0, 1]$ , and define its expectation  $\bar{\rho} := \mathbb{E}[\hat{\rho}_\tau]$ . Then

$$\mathbb{E}[\text{Cost}(\tau)] = \mathbb{E}[\tau] (c_F + c_Y \bar{\rho}).$$

Combining with the bound on  $\mathbb{E}[\tau]$  and using  $\delta_k = \delta/K$  lead to the stated scaling

$$\mathbb{E}[\text{Cost}(\tau)] \lesssim \sum_{k \neq k^*} \frac{\log(K/\delta)}{\Delta_k^2} \left( \frac{1}{4} + \frac{1}{\pi_{\min}^2} \right) (c_F + c_Y \bar{\rho}),$$

up to universal constants and log log factors.

## E.2 Derivation for [Example 6.4](#)

The following derivation illustrates the lower-bound cost structure under a truncated normal model satisfying [Assumption 3.1](#). Note that this illustration is not required for running PP-LUCB.

Consider a stylized model where  $F \sim \text{TN}(\mu_F, \sigma_F^2, [0, 1])$  and  $R = Y - F \sim \text{TN}(\mu_R, \sigma_R^2, [-1, 1])$  are conditionally independent, with total mean  $\mu = \mathbb{E}[F] + \mathbb{E}[R]$ . The observation at each round is  $(F, A, A \cdot R)$ , where  $A \sim \text{Bernoulli}(\pi)$ .

For a truncated normal  $\text{TN}(\mu, \sigma^2, [a, b])$  with  $\alpha = (a - \mu)/\sigma$ ,  $\beta = (b - \mu)/\sigma$ , the Fisher information for the mean parameter is  $\mathcal{I}_{\text{TN}} = \kappa/\sigma^2$ , where the correction factor is

$$\kappa = 1 + \frac{\alpha\phi(\alpha) - \beta\phi(\beta)}{\Phi(\beta) - \Phi(\alpha)} - \left( \frac{\phi(\alpha) - \phi(\beta)}{\Phi(\beta) - \Phi(\alpha)} \right)^2 \geq 1,$$

with  $\phi$  and  $\Phi$  the standard normal density and CDF. The factor  $\kappa \geq 1$  approaches 1 when truncation is mild. For instances differing by  $\Delta\mu_F$  and  $\Delta\mu_R$ , the LAN approximation gives

$$\text{KL}(\nu \parallel \nu') \approx \frac{\kappa_F (\Delta\mu_F)^2}{2\sigma_F^2} + \pi \cdot \frac{\kappa_R (\Delta\mu_R)^2}{2\sigma_R^2},$$

where  $\kappa_F, \kappa_R \geq 1$  are truncation correction factors.

Under the constraint  $\Delta\mu_F + \Delta\mu_R = \Delta$ , the least favorable split yields the effective variance

$$\sigma_{\text{eff}}^2(\pi) = \frac{\sigma_F^2}{\kappa_F} + \frac{\sigma_R^2}{\kappa_R \pi},$$

and the minimal KL scales as  $\Delta^2/(2\sigma_{\text{eff}}^2(\pi))$ . Minimizing

$$f(\pi) = \left( \frac{\sigma_F^2}{\kappa_F} + \frac{\sigma_R^2}{\kappa_R \pi} \right) (c_F + c_Y \pi),$$

we have

$$\pi^* = \sqrt{\frac{c_F}{c_Y}} \cdot \frac{\sigma_R/\sqrt{\kappa_R}}{\sigma_F/\sqrt{\kappa_F}},$$

clipped to  $[\pi_{\min}, 1]$  if needed. Substituting  $\pi^*$  gives

$$\mathbb{E}[\text{Cost}] \gtrsim \frac{2 \log(1/\delta)}{\Delta^2} \left( \sqrt{c_F} \frac{\sigma_F}{\sqrt{\kappa_F}} + \sqrt{c_Y} \frac{\sigma_R}{\sqrt{\kappa_R}} \right)^2.$$

## F Proofs for Instance-Dependent Lower Bound and Optimality

This section provides complete proofs for the information-theoretic lower bound ([Theorem 6.3](#)) and the asymptotic optimality of PP-Track-and-Audit ([Theorem F.2](#)).

### F.1 Proof of Instance-Dependent Lower Bound ([Theorem 6.3](#))

Fix the true instance  $\nu$  and an alternative  $\nu' \in \text{Alt}(\nu)$  such that  $k^*(\nu') \neq k^*(\nu)$ . Consider any  $\delta$ -correct algorithm with stopping time  $\tau$  (with respect to the natural filtration defined below) and finite expected cost.

Let the per-pull observation be  $O_t = (X_t, F_t, A_t, Y_t)$ , and the filtration  $\mathcal{F}_t = \sigma((k_s, O_s, \pi_s)_{s \leq t})$ . Here  $k_t$  is  $\mathcal{F}_{t-1}$ -measurable, and  $\pi_t = \mathbb{P}(A_t = 1 \mid \mathcal{F}_{t-1}, k_t, X_t, F_t)$  is measurable with respect to  $\sigma(\mathcal{F}_{t-1}, k_t, X_t, F_t)$ . By [Assumption 3.2](#),  $A_t$  cannot depend on the unobserved  $Y_t$  given  $(\mathcal{F}_{t-1}, k_t, X_t, F_t)$ .

Under [Assumption 3.2](#), conditional on  $(\mathcal{F}_{t-1}, k_t)$ , the conditional distribution of  $O_t$  factors as

$$P_\nu(O_t \mid \mathcal{F}_{t-1}, k_t) = P(X_t) P_\nu(F_t \mid X_t, k_t) P(A_t \mid \mathcal{F}_{t-1}, k_t, X_t, F_t) P_\nu(Y_t \mid X_t, F_t, k_t)^{A_t}.$$

The audit mechanism  $P(A_t \mid \cdot)$  is part of the algorithm, so it is identical under  $\nu$  and  $\nu'$ . Therefore the one-step log-likelihood ratio is

$$\begin{aligned} \ell_t(\nu, \nu') &:= \log \frac{dP_\nu(O_t \mid \mathcal{F}_{t-1}, k_t)}{dP_{\nu'}(O_t \mid \mathcal{F}_{t-1}, k_t)} \\ &= \log \underbrace{\frac{dP_\nu(F_t \mid X_t, k_t)}{dP_{\nu'}(F_t \mid X_t, k_t)}}_{=: \ell_t^{(F)}(\nu, \nu')} + A_t \log \underbrace{\frac{dP_\nu(Y_t \mid X_t, F_t, k_t)}{dP_{\nu'}(Y_t \mid X_t, F_t, k_t)}}_{=: \ell_t^{(Y|X,F)}(\nu, \nu')}. \end{aligned} \quad (31)$$

Let

$$L_\tau(\nu, \nu') := \sum_{t=1}^{\tau} \ell_t(\nu, \nu')$$

denote the cumulative log-likelihood ratio.

By the KL chain rule (see, e.g., [Kaufmann et al. \[2016\]](#)),

$$\mathbb{E}_\nu[L_\tau(\nu, \nu')] = \mathbb{E}_\nu \left[ \sum_{t=1}^{\tau} \text{KL} \left( P_\nu(O_t \mid \mathcal{F}_{t-1}, k_t) \parallel P_{\nu'}(O_t \mid \mathcal{F}_{t-1}, k_t) \right) \right], \quad (32)$$

whenever the displayed conditional KL terms are integrable. Fix  $t$ . Conditional on  $(\mathcal{F}_{t-1}, k_t, X_t, F_t)$ , we have  $A_t \sim \text{Bernoulli}(\pi_t)$  and  $A_t$  is independent of  $Y_t$  under [Assumption 3.2](#). Since  $A_t$ 's conditional distribution is the same under  $\nu$  and  $\nu'$ , the conditional KL splits into a proxy part and an audited outcome part revealed only when  $A_t = 1$ :

$$\begin{aligned} & \text{KL}\left(P_\nu(O_t \mid \mathcal{F}_{t-1}, k_t) \parallel P_{\nu'}(O_t \mid \mathcal{F}_{t-1}, k_t)\right) \\ &= \mathbb{E}_\nu \left[ \text{KL}(P_\nu(F_t \mid X_t, k_t) \parallel P_{\nu'}(F_t \mid X_t, k_t)) + \pi_t \text{KL}(P_\nu(Y_t \mid X_t, F_t, k_t) \parallel P_{\nu'}(Y_t \mid X_t, F_t, k_t)) \mid \mathcal{F}_{t-1}, k_t \right]. \end{aligned} \quad (33)$$

The algorithm may choose  $\pi_t$  adaptively as a function of the full history. For the lower bound, we summarize its effect by an averaged auditing kernel that depends only on the current observables  $(X, F)$ . Fix arm  $k$ . Define two finite measures on  $\mathcal{X} \times [0, 1]$ : for any measurable set  $B \subseteq \mathcal{X} \times [0, 1]$ ,

$$\begin{aligned} \Lambda_k(B) &:= \mathbb{E}_\nu \left[ \sum_{t=1}^{\tau} \mathbf{1}\{k_t = k\} \mathbf{1}\{(X_t, F_t) \in B\} \right], \\ \Gamma_k(B) &:= \mathbb{E}_\nu \left[ \sum_{t=1}^{\tau} \mathbf{1}\{k_t = k\} \pi_t \mathbf{1}\{(X_t, F_t) \in B\} \right]. \end{aligned}$$

Since  $0 \leq \pi_t \leq 1$ , we have  $0 \leq \Gamma_k(B) \leq \Lambda_k(B)$ , so  $\Gamma_k \ll \Lambda_k$ . By the Radon-Nikodym Theorem, there exists a measurable  $\bar{\pi}_k : \mathcal{X} \times [0, 1] \rightarrow [0, 1]$  such that for all measurable  $B$ ,

$$\Gamma_k(B) = \int_B \bar{\pi}_k(x, f) d\Lambda_k(x, f).$$

Equivalently, for any integrable measurable  $h(x, f)$ ,

$$\mathbb{E}_\nu \left[ \sum_{t=1}^{\tau} \mathbf{1}\{k_t = k\} \pi_t h(X_t, F_t) \right] = \mathbb{E}_\nu \left[ \sum_{t=1}^{\tau} \mathbf{1}\{k_t = k\} \bar{\pi}_k(X_t, F_t) h(X_t, F_t) \right]. \quad (34)$$

Moreover, by [Assumption 3.3](#) and the fact that  $\pi_t \geq \pi_{\min}$  whenever auditing is eligible, the averaged kernel satisfies  $\bar{\pi}_k(x, f) \in [\pi_{\min}, 1]$  on the support of  $(X, F) \mid k$ .

Combining (32) and (33) and using (34), we have

$$\mathbb{E}_\nu[L_\tau(\nu, \nu')] = \sum_{k=1}^K \mathbb{E}_\nu[N_k(\tau)] \cdot I_k(\nu, \nu'; \bar{\pi}_k), \quad (35)$$

where  $N_k(\tau) := \sum_{t=1}^{\tau} \mathbf{1}\{k_t = k\}$  and

$$I_k(\nu, \nu'; \pi_k) := \mathbb{E}_\nu \left[ \text{KL}(P_\nu(F \mid X, k) \parallel P_{\nu'}(F \mid X, k)) + \pi_k(X, F) \text{KL}(P_\nu(Y \mid X, F, k) \parallel P_{\nu'}(Y \mid X, F, k)) \mid k \right]. \quad (36)$$

This matches the ‘‘proxy information + audited information’’ structure stated in the main text.

Similarly, for the cost,

$$\mathbb{E}_\nu[\text{Cost}(\tau)] = c_F \mathbb{E}_\nu[\tau] + c_Y \mathbb{E}_\nu \left[ \sum_{t=1}^{\tau} A_t \right].$$

Since  $\mathbb{E}_\nu[A_t \mid \mathcal{F}_{t-1}, k_t, X_t, F_t] = \pi_t$  and by the averaging identity (34),

$$\mathbb{E}_\nu \left[ \sum_{t=1}^{\tau} A_t \right] = \sum_{k=1}^K \mathbb{E}_\nu[N_k(\tau)] \cdot \mathbb{E}_\nu[\bar{\pi}_k(X, F) \mid k].$$

Then

$$\mathbb{E}_\nu[\text{Cost}(\tau)] = \sum_{k=1}^K \mathbb{E}_\nu[N_k(\tau)] \cdot \left( c_F + c_Y \mathbb{E}_\nu[\bar{\pi}_k(X, F) | k] \right). \quad (37)$$

By the standard change-of-measure arguments for BAI [Kaufmann et al., 2016], for any  $\nu' \in \text{Alt}(\nu)$ ,

$$\mathbb{E}_\nu[L_\tau(\nu, \nu')] \geq \text{KL}(1 - \delta, \delta) \geq \log(1/\delta) - \log 2. \quad (38)$$

Combining (35)-(38) and dividing by  $\mathbb{E}_\nu[\text{Cost}(\tau)]$  using (37), we have

$$\frac{\log(1/\delta) - \log 2}{\mathbb{E}_\nu[\text{Cost}(\tau)]} \leq \frac{\sum_{k=1}^K w_k I_k(\nu, \nu'; \bar{\pi}_k)}{c_F + c_Y \sum_{k=1}^K w_k \mathbb{E}_\nu[\bar{\pi}_k(X, F) | k]},$$

where  $w_k := \mathbb{E}_\nu[N_k(\tau)]/\mathbb{E}_\nu[\tau]$  and  $w \in \Delta_K$ . Taking  $\inf_{\nu' \in \text{Alt}(\nu)}$  and then  $\sup_{w \in \Delta_K, \pi}$ , and letting  $\delta \rightarrow 0$ , we obtain

$$\liminf_{\delta \rightarrow 0} \frac{\mathbb{E}_\nu[\text{Cost}(\tau)]}{\log(1/\delta)} \geq C^*(\nu),$$

where  $C^*(\nu)$  is exactly the characteristic cost defined in (17). This proves the theorem.

## F.2 Decomposition of the Characteristic Cost

**Proposition F.1.** *Suppose the admissible auditing policies are restricted to an implementation-relevant compact class  $\Pi_k \subseteq \{\pi_k : \mathcal{X} \times [0, 1] \rightarrow [\pi_{\min}, 1]\}$  for each arm (e.g., piecewise-constant policies on a finite partition of  $(X, F)$ , or a clipped parametric family). Then the optimization in (17) can be viewed in two levels: for each arm, selecting an information-efficient auditing  $\pi_k^* \in \Pi_k$  that trades off audit information and audit cost; and given the induced per-arm information rates, selecting sampling proportions  $w^* \in \Delta_K$  with the usual Track-and-Stop balancing against the worst alternative.*

For any fixed  $\nu'$ , the numerator and denominator in (17) are continuous in  $(w, \pi)$  and additively separable among arms, with each arm's contribution linear in  $(w_k, \pi_k)$ . Under the stated restriction, the feasible set  $\Delta_K \times \prod_{k=1}^K \Pi_k$  is compact, so an optimizer exists.

Moreover, for fixed  $w$ , both  $\sum_k w_k I_k(\nu, \nu'; \pi_k)$  and  $\sum_k w_k \mathbb{E}_\nu[\pi_k(X, F) | k]$  separate across arms, so the choice of each  $\pi_k$  can be interpreted as an arm-wise efficiency design, and the remaining choice of  $w$  balances the resulting arm-wise information rates against the alternatives  $\text{Alt}(\nu)$ , as in classical fixed-confidence BAI [Garivier and Kaufmann, 2016, Kaufmann et al., 2016].

## F.3 PP-Track-and-Audit Algorithm and its Asymptotic Optimality

Based on the lower bound, we introduce PP-Track-and-Audit (Prediction-Powered Track-and-Audit), a tracking variant of PP-LUCB that targets the optimizer  $(w^*, \pi^*)$  of (17) by learning the instance parameters, tracking the implied sampling proportions, and tracking the implied auditing shape.

PP-Track-and-Audit is (informally) described as below. At each pull  $t$ :

1. Update parameter estimates  $\hat{\nu}_t$ .
2. Solve the plug-in characteristic-cost program (a version of (17) with  $\nu$  replaced by  $\hat{\nu}_t$ ) over  $w \in \Delta_K$  and  $\pi \in \Pi$  to obtain  $(\hat{w}_t, \hat{\pi}_t)$ .

3. Select arm  $k_t$  by C-tracking (pick the arm whose current count  $N_k(t)$  is most below its target  $\sum_{s \leq t} \hat{w}_{s,k}$ ; see [Garivier and Kaufmann \[2016\]](#)) so that  $N_k(t)$  tracks  $\sum_{s \leq t} \hat{w}_{s,k}$ , with a vanishing forced-exploration schedule (e.g.,  $\epsilon_t = t^{-1/2}$ ).
4. After observing  $(X_t, F_t)$ , set the audit probability  $\pi_t \leftarrow \hat{\pi}_{t,k_t}(X_t, F_t)$  (clipped to  $[\pi_{\min}, 1]$ ), draw  $A_t \sim \text{Bern}(\pi_t)$ , and if  $A_t = 1$  observe  $Y_t$ .
5. Maintain anytime-valid confidence sequences for each  $\theta_k = \mathbb{E}[Y \mid k]$ : a sequence of intervals  $\text{CS}_k(t) = [L_k(t), U_k(t)]$  such that

$$\mathbb{P}\left(\forall t \geq 1, \forall k \in [K] : \theta_k \in [L_k(t), U_k(t)]\right) \geq 1 - \delta.$$

6. Let  $\hat{k}_t \in \arg \max_k \hat{\theta}_k(t)$  be the leader. Stop at

$$\tau_\delta := \inf \left\{ t \geq 1 : L_{\hat{k}_t}(t) > \max_{j \neq \hat{k}_t} U_j(t) \right\}, \quad (39)$$

and output  $\hat{k} = \hat{k}_{\tau_\delta}$ .

**Theorem F.2.** *Assume [Assumptions 3.1 to 3.3](#) and [6.2](#). Suppose the admissible auditing class  $\Pi$  is compact and that the optimizer  $(w^*, \pi^*)$  of [\(17\)](#) is unique at  $\nu$ . Then PP-Track-and-Audit with stopping rule [\(39\)](#) is  $\delta$ -correct. Moreover, it is asymptotically optimal in expected cost:*

$$\limsup_{\delta \rightarrow 0} \frac{\mathbb{E}_\nu[\text{Cost}(\tau_\delta)]}{C^*(\nu) \log(1/\delta)} \leq 1.$$

Below we prove [Theorem F.2](#).

By the simultaneous coverage of the confidence sequences, the event

$$\mathcal{E} := \left\{ \forall t \geq 1, \forall k \in [K] : \theta_k \in [L_k(t), U_k(t)] \right\}$$

satisfies  $\mathbb{P}(\mathcal{E}) \geq 1 - \delta$ . On  $\mathcal{E}$ , whenever the stopping condition [\(39\)](#) holds, we have  $\theta_{\hat{k}_t} \geq L_{\hat{k}_t}(t) > \max_{j \neq \hat{k}_t} U_j(t) \geq \max_{j \neq \hat{k}_t} \theta_j$ , so  $\hat{k}_t$  is a best arm. Therefore  $\mathbb{P}(\hat{k} = k^*) \geq 1 - \delta$ , i.e., the algorithm is  $\delta$ -correct (same logic as [Theorem 5.1](#)).

Note that the forced exploration implies  $N_k(t) \rightarrow \infty$  almost surely for all arms. Then,  $(\hat{w}_t, \hat{\pi}_t) \rightarrow (w^*, \pi^*)$  almost surely. C-tracking then yields  $N_k(t)/t \rightarrow w_k^*$  almost surely and the realized audit frequency for arm  $k$  converges to its target level induced by  $\pi_k^*$ .

Under [Assumption 6.2](#), the CS-based stopping rule [\(39\)](#) stops once enough cumulative information has been gathered to separate the best arm from all alternatives. With the tracking limits above, the cumulative information rate converges to the optimal rate in [\(17\)](#), hence

$$\limsup_{\delta \rightarrow 0} \frac{\tau_\delta}{\log(1/\delta)} \leq C^*(\nu).$$

Last, the per-pull cost is  $c_F + c_Y A_t$ . By the law of large numbers for bounded martingale differences and the convergence of sampling and auditing frequencies,

$$\frac{\text{Cost}(\tau_\delta)}{\tau_\delta} \rightarrow c_F + c_Y \sum_{k=1}^K w_k^* \mathbb{E}_\nu[\pi_k^*(X, F) \mid k] \quad \text{almost surely.}$$

Then, we have

$$\limsup_{\delta \rightarrow 0} \frac{\mathbb{E}_\nu[\text{Cost}(\tau_\delta)]}{C^*(\nu) \log(1/\delta)} \leq 1,$$

which proves the theorem.

## G Proofs for Delayed Audit Feedback

This section provides proofs for the theorems in [Section 7 \(Theorem 7.3-Theorem 7.5\)](#) on delayed audit feedback.

### G.1 Proof of Confidence Sequences under Delayed Returns ([Theorem 7.3](#))

Let  $A_s \in \{0, 1\}$  denote the audit indicator at round  $s$ , let  $D_s \in \{0, 1, 2, \dots\}$  be the delay, let  $B_s(t) = \mathbf{1}\{A_s = 1, s + D_s \leq t\}$  indicate whether the audit from round  $s$  has returned by time  $t$ , and let  $\mathcal{G}_t = \sigma(\{(k_s, X_s, F_s)\}_{s \leq t}, \{Y_s : B_s(t) = 1\}, \{\pi_s\}_{s \leq t})$  be the returned-outcome filtration. Define the enlarged filtration

$$\mathcal{H}_t := \sigma(\mathcal{F}_t, D_1, \dots, D_t),$$

where  $\mathcal{F}_t = \sigma(\{(k_s, X_s, F_s, A_s, Y_s \cdot A_s, \pi_s)\}_{s \leq t})$  is the filtration at request time. This enlarged filtration contains all outcomes and all delays through round  $t$ , and satisfies  $\mathcal{G}_t \subset \mathcal{H}_t$  and  $\mathcal{F}_t \subset \mathcal{H}_t$ .

Fix arm  $k$  and let  $t_1 < t_2 < \dots$  denote the successive pull times of arm  $k$ . Define the centered IPW increments

$$\xi_i := \frac{A_{t_i}}{\pi_{t_i}}(Y_{t_i} - F_{t_i}) - \mu_{R,k}, \quad i = 1, 2, \dots,$$

exactly as in the proof of [Proposition 4.2](#). We verify that  $\mathbb{E}[\xi_i \mid \mathcal{H}_{t_{i-1}}] = 0$  via a two-stage argument that parallels the tower property already used implicitly in the no-delay proof.

First, we show  $\mathbb{E}[\xi_i \mid \mathcal{H}_{t_{i-1}}] = 0$ , where  $t_i - 1$  denotes one step before the current pull (as opposed to  $t_{i-1}$ , which is the time of the previous pull of arm  $k$ ). The arm choice  $k_{t_i}$  is  $\mathcal{G}_{t_{i-1}}$ -measurable (the delayed algorithm selects arms based on returned outcomes), and  $\mathcal{G}_{t_{i-1}} \subset \mathcal{H}_{t_{i-1}}$  at the same time. The data  $(X_{t_i}, F_{t_i}, Y_{t_i})$  at round  $t_i$  are drawn from the arm distribution independently of  $\mathcal{H}_{t_{i-1}}$ . Therefore, the computation in the proof of [Proposition 4.2](#) gives

$$\mathbb{E}[\xi_i \mid \mathcal{H}_{t_{i-1}}] = \mathbb{E}_{(X,F)} \left[ \mathbb{E} \left[ \frac{A_{t_i}}{\pi_{t_i}}(Y_{t_i} - F_{t_i}) \mid \mathcal{H}_{t_{i-1}}, X_{t_i}, F_{t_i} \right] - \mu_{R,k} \right] = \mathbb{E}_{(X,F)} [\mu_{R,k}(X_{t_i}, F_{t_i})] - \mu_{R,k} = 0.$$

The second equality uses [Assumption 3.2](#) to cancel the IPW weight, exactly as in the no-delay proof. The delay information  $\{D_s\}_{s < t_i}$  in  $\mathcal{H}_{t_{i-1}}$  does not affect this calculation, because  $(X_{t_i}, F_{t_i}, Y_{t_i})$  at round  $t_i$  are drawn independently of past delays.

Then, since  $t_{i-1} \leq t_i - 1$  (at least one step elapses between consecutive pulls of arm  $k$ ), the filtration inclusion  $\mathcal{H}_{t_{i-1}} \subset \mathcal{H}_{t_{i-1}}$  holds. By the tower property of conditional expectation:

$$\mathbb{E}[\xi_i \mid \mathcal{H}_{t_{i-1}}] = \underbrace{\mathbb{E}[\mathbb{E}[\xi_i \mid \mathcal{H}_{t_{i-1}}] \mid \mathcal{H}_{t_{i-1}}]}_{=0} = 0.$$

Since  $|\xi_i| \leq M := 2/\pi_{\min}$  (same bound as in [Proposition 4.2](#)), the process  $S_{R,k}(n) = \sum_{i=1}^n \xi_i$  is a sub-Gaussian martingale with variance process  $V_{R,k}(n) = n \cdot M^2/4$ . By [Theorem C.1](#), with probability at least  $1 - \delta_k$ , simultaneously for all  $n \geq 1$ :

$$|S_{R,k}(n)| \leq \psi \left( \frac{nM^2}{4}; \frac{\delta_k}{2} \right). \quad (40)$$

In particular, (40) holds at  $n = N_k(t)$  for every calendar time  $t$ .

The oracle estimator  $\widehat{\mu}_{R,k}(t) = \frac{1}{N_k(t)} \sum_{s \leq t: k_s = k} \frac{A_s}{\pi_s} (Y_s - F_s)$  uses all outcomes, while the delayed estimator  $\widehat{\mu}_{R,k}^{\text{del}}(t)$  uses only returned outcomes. Their relationship gives the decomposition

$$\begin{aligned} S_{R,k}(N_k(t)) &= \underbrace{N_k(t) (\widehat{\mu}_{R,k}^{\text{del}}(t) - \mu_{R,k})}_{\text{computable from returned outcomes}} + \underbrace{\sum_{\substack{s \leq t: k_s = k, \\ A_s = 1, B_s(t) = 0}} \frac{1}{\pi_s} (Y_s - F_s)}_{=: Q_k(t) \text{ (pending sum)}} \\ &=: Q_k(t) \text{ (pending sum)} \end{aligned}$$

where  $Q_k(t)$  aggregates the IPW residuals of audits that have been requested but not yet returned.

Each pending term satisfies  $|\frac{1}{\pi_s} (Y_s - F_s)| \leq 1/\pi_{\min}$  (since  $|Y_s - F_s| \leq 1$  and  $\pi_s \geq \pi_{\min}$ ), so

$$|Q_k(t)| \leq \frac{P_k(t)}{\pi_{\min}},$$

where  $P_k(t) = |\{s \leq t : k_s = k, A_s = 1, B_s(t) = 0\}|$  counts the pending audits for arm  $k$  at time  $t$ . By the triangle inequality and (40), on the event that the submission-time CS holds:

$$\begin{aligned} |N_k(t) (\widehat{\mu}_{R,k}^{\text{del}}(t) - \mu_{R,k})| &= |S_{R,k}(N_k(t)) - Q_k(t)| \\ &\leq |S_{R,k}(N_k(t))| + |Q_k(t)| \\ &\leq \psi\left(\frac{N_k(t) M^2}{4}; \frac{\delta_k}{2}\right) + \frac{P_k(t)}{\pi_{\min}}. \end{aligned}$$

Dividing both sides by  $N_k(t)$ :

$$|\widehat{\mu}_{R,k}^{\text{del}}(t) - \mu_{R,k}| \leq \underbrace{\frac{\psi(N_k(t) M^2/4; \delta_k/2)}{N_k(t)}}_{= w_{R,k}(N_k(t))} + \frac{P_k(t)}{\pi_{\min} N_k(t)} = w_{R,k}^{\text{del}}(t).$$

This holds simultaneously for all  $t \geq 1$  with probability at least  $1 - \delta_k$ , because the result of (40) is uniform in  $n$ .

The delayed estimator  $\widehat{\mu}_{R,k}^{\text{del}}(t)$  is computed from returned outcomes, and the pending count  $P_k(t)$  is determined by which audits have been requested and which have returned. Both are  $\mathcal{G}_t$ -measurable quantities. When there are no delays ( $D_s = 0$  for all  $s$ ), every audit returns immediately, so  $P_k(t) = 0$  and  $\widehat{\mu}_{R,k}^{\text{del}}(t) = \widehat{\mu}_{R,k}(t)$ . This recovers [Proposition 4.2](#).

## G.2 Proof of $\delta$ -Correctness with Delayed Returns ([Theorem 7.4](#))

Define the delayed confidence bounds

$$\begin{aligned} \underline{\mu}_k(t) &:= \widehat{\theta}_k^{\text{del}}(t) - w_{F,k}(N_k(t)) - w_{R,k}^{\text{del}}(t), \\ \bar{\mu}_k(t) &:= \widehat{\theta}_k^{\text{del}}(t) + w_{F,k}(N_k(t)) + w_{R,k}^{\text{del}}(t), \end{aligned}$$

where  $\widehat{\theta}_k^{\text{del}}(t) = \widehat{\mu}_{F,k}(t) + \widehat{\mu}_{R,k}^{\text{del}}(t)$ . Both  $\widehat{\theta}_k^{\text{del}}(t)$  and  $w_{R,k}^{\text{del}}(t)$  are  $\mathcal{G}_t$ -measurable, so  $\tau = \inf\{t \geq 1 : \exists \hat{k} \text{ s.t. } \underline{\mu}_{\hat{k}}(t) > \max_{j \neq \hat{k}} \bar{\mu}_j(t)\}$  is a  $\{\mathcal{G}_t\}$ -stopping time.

Let  $E = \{\forall t, \forall k : \theta_k \in [\underline{\mu}_k(t), \bar{\mu}_k(t)]\}$ . By [Theorem 7.3](#) (applied to the residual CS) and [Proposition 4.1](#) (applied to the proxy CS), together with a union bound over  $K$  arms,  $\mathbb{P}(E) \geq 1 - \delta$ .

On  $E$ , if the algorithm stops at  $\tau$  with empirically best arm  $\hat{k}$ :

$$\theta_{\hat{k}} \geq \underline{\mu}_{\hat{k}}(\tau) > \max_{j \neq \hat{k}} \bar{\mu}_j(\tau) \geq \max_{j \neq \hat{k}} \theta_j.$$

Thus  $\hat{k} = k^*$ , and  $\mathbb{P}(\hat{k} = k^*) \geq \mathbb{P}(E) \geq 1 - \delta$ .

### G.3 Proof of High-Probability Completion Bound (Theorem 7.5)

Let  $D_s$  denote the (integer-valued) feedback delay of the audit requested at time  $s$  (when  $A_s = 1$ ), so that audit  $s$  has returned by time  $\tau_0 + d$  if and only if  $D_s \leq d$ . Equivalently,  $B_s(\tau_0 + d) = 1$  if and only if  $D_s \leq d$ .

Consider the bad event that at least one audit requested no later than  $\tau_0$  has not yet returned by time  $\tau_0 + d^*$ :

$$\mathcal{E}_{\text{bad}} \triangleq \left\{ \exists s \leq \tau_0 \text{ such that } A_s = 1 \text{ and } D_s > d^* \right\}.$$

Using  $\tau_0 \leq T_{\max}$  almost surely, we have the set inclusion

$$\mathcal{E}_{\text{bad}} \subseteq \left\{ \exists s \leq T_{\max} \text{ such that } A_s = 1 \text{ and } D_s > d^* \right\},$$

and therefore, by the union bound,

$$\begin{aligned} \mathbb{P}(\mathcal{E}_{\text{bad}}) &\leq \sum_{s=1}^{T_{\max}} \mathbb{P}(A_s = 1, D_s > d^*) \\ &\leq \sum_{s=1}^{T_{\max}} \mathbb{P}(D_s > d^* \mid A_s = 1) \\ &= \sum_{s=1}^{T_{\max}} \mathbb{E} \left[ \mathbb{P}(D_s > d^* \mid \sigma(\mathcal{G}_{s-1}, k_s, X_s, F_s, A_s = 1, \pi_s)) \right] \\ &\leq \sum_{s=1}^{T_{\max}} h(d^*) = T_{\max} h(d^*). \end{aligned}$$

By the definition of  $d^* = d_{\eta/T_{\max}}$ , we have  $h(d^*) \leq \eta/T_{\max}$ . Then

$$\mathbb{P}(\mathcal{E}_{\text{bad}}) \leq \eta.$$

Equivalently, with probability at least  $1 - \eta$ , every audit requested up to (and including)  $\tau_0$  has returned by time  $\tau_0 + d^*$ :

$$\mathbb{P} \left\{ \forall s \leq \tau_0 \text{ with } A_s = 1 : B_s(\tau_0 + d^*) = 1 \right\} \geq 1 - \eta.$$

On the event  $\{\forall s \leq \tau_0 \text{ with } A_s = 1 : B_s(\tau_0 + d^*) = 1\}$ , by time  $\tau_0 + d^*$  the delayed-feedback procedure has received the outcomes of all audits that were requested up to  $\tau_0$ . Therefore, by time  $\tau_0 + d^*$  it has sufficient information to verify the same stopping condition that triggered at  $\tau_0$  in the no-delay setting, and therefore must have stopped by (at latest)  $\tau_0 + d^*$ . In other words,

$$\left\{ \forall s \leq \tau_0, A_s = 1 \implies B_s(\tau_0 + d^*) = 1 \right\} \subseteq \{\tau_D \leq \tau_0 + d^*\}.$$

Then,

$$\mathbb{P}(\tau_D \leq \tau_0 + d^*) \geq 1 - \eta.$$

## H Additional Experimental Results

This section reports additional experiments mentioned in [Section 8](#).

## H.1 Adaptive vs. Fixed Auditing

This experiment tests the two failure modes described in [Theorem 3.5](#). In particular, [Theorem 3.5](#) shows that proxy-only procedures can fail under arm-dependent proxy bias, and under selective auditing, naive use of selectively audited outcomes can remain biased. Here we focus on the first argument (proxy-only failure) and on the benefit of adaptive audit allocation (compared to fixed allocation), while keeping the arm-sampling rule the same.

We use the same synthetic fixed-confidence BAI setup as in [Section 8.1](#), where there are  $K = 4$  arms, with audited outcomes  $Y \sim \text{Bernoulli}(\theta_k)$  and means  $\theta_k \in \{0.7, 0.6, 0.5, 0.4\}$ . The proxy score  $F \in [0, 1]$  is generated to mimic an informative but biased LLM judge  $F = \text{clip}(Y + b + \epsilon, 0, 1)$ , where  $b > 0$  is a systematic bias term and  $\epsilon$  is proxy noise. As discussed in the main text, the key difficulty is that the best arm under  $\mathbb{E}[F | k]$  may differ from the best arm under  $\mathbb{E}[Y | k]$  when the bias is arm dependent, so proxy-only selection can be confidently wrong.

We compare the following degenerate strategies designed to isolate the role of auditing.

- **No-Judge (audit-only)**. Always audit ( $\pi_t \equiv 1$ ). This yields an unbiased estimate of  $\theta_k$  using audited outcomes alone, but it is expensive because every pull incurs audit cost  $c_Y$ .
- **No-Audit (proxy-only)**. Never audit ( $A_t \equiv 0$ ). The procedure selects the arm using proxy scores  $F$  only. This is exactly the setting ruled out by [Theorem 3.5](#) (Part 1) when proxy bias is not controlled.
- **Fixed and Adaptive Auditing**. Both strategies use the same debiased estimator  $\hat{\theta}_k = \hat{\mu}_{F,k} + \hat{\mu}_{R,k}$  with the IPW residual correction from [Section 4](#), but differ in how audits are requested:
  - *Fixed Auditing*:  $\pi_t \equiv \rho$  for a constant audit rate (e.g.,  $\rho = 0.1$ ), clipped to satisfy  $\pi_t \in [\pi_{\min}, 1]$ .
  - *Adaptive Auditing*:  $\pi_t$  depends on observables available at decision time, again clipped to  $[\pi_{\min}, 1]$ . This is the setting of selective auditing, where validity requires IPW rather than naive averaging.

[Figure 6](#) summarizes the results. The *No-Audit* strategy achieves 0% identification accuracy in this setting. This matches the message of [Theorem 3.5](#) (Part 1) that without any verified outcomes, the algorithm cannot distinguish between a truly better arm and an arm that is systematically over-scored by the proxy. The *No-Judge* strategy is correct but incurs high cost (10,500 in our normalized units), because every pull requires a human audit. Compared with *Fixed Auditing* at the same audit rate level, *Adaptive Auditing* reduces cost by about 10% while maintaining the same identification accuracy. The gain comes from spending audits where they reduce the uncertainty in the residual correction  $\mathbb{E}[Y - F | k]$  more quickly, rather than auditing uniformly. That is, even under a simple synthetic setup, selective (adaptive) auditing can reduce total cost relative to a fixed-rate policy, provided that estimation correctly accounts for selection via IPW.

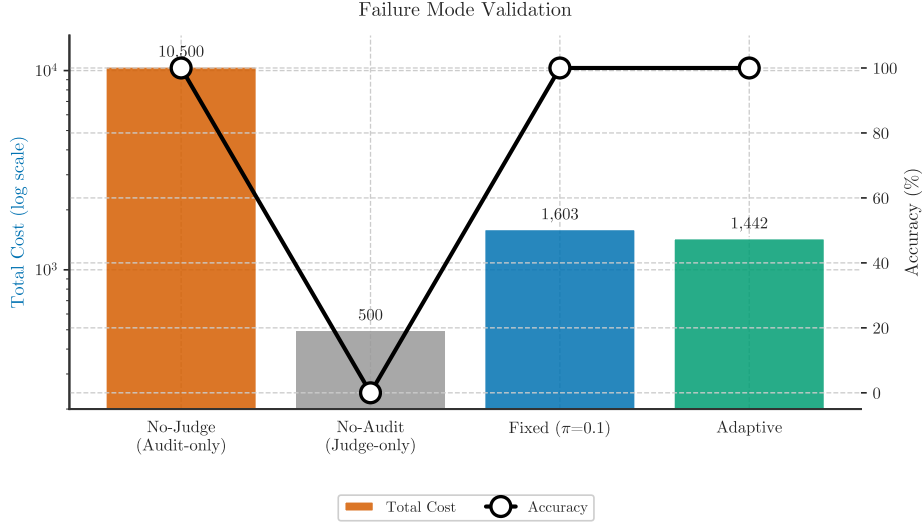


Figure 6: Failure mode validation. No-Audit fails completely (0% accuracy), while Adaptive auditing achieves 10% cost reduction over Fixed auditing. Cost bars use log scale.

## H.2 Detailed Result under Delayed Audit Feedbacks

This section reports additional results for the delayed-audit experiments summarized in [Section 8.4](#). We describe the delay models used to represent common operational review processes, and measure how delay and audit strategies affect the number of pulls required to certify stopping and the realized audit fraction.

### H.2.1 Audit Usage

We use the real LLM environment described in [Section 8.1](#) and test three delay distributions that capture different audit operations. In all cases,  $D$  denotes the number of pulls between audit request and outcome return.

- **Bounded:**  $D \sim \text{Uniform}\{0, 1, \dots, D_{\max}\}$  with  $D_{\max} = 10$ . This approximates settings with a managed review service-level agreement (SLA) in which audits are returned within a known window, with some variability due to batching or reviewer availability.
- **Geometric:**  $D \sim \text{Geometric}(p)$  with  $p = 0.3$  (mean delay  $\approx 2.3$ ). This represents a memoryless queue in which each audit has a constant probability of being completed at each step. This is a common approximation when completion times are driven by a large pool of independent reviews.
- **Heavy-tailed:**  $D \sim \text{Pareto}(\alpha, x_m)$  with  $\alpha = 2.5$ ,  $x_m = 1$ , truncated at  $D_{\max} = 50$ . This captures the presence of occasional long backlogs (for example, audits that require specialized reviewers, additional context gathering, or follow-up).

We compare three audit strategies that determine the audit probability  $\pi_t$  (and then sample  $A_t \sim \text{Bern}(\pi_t)$ ) after observing  $(k_t, X_t, F_t)$ , subject to the same positivity constraint  $\pi_t \in [\pi_{\min}, 1]$  as in the main paper.

- **Fixed-10:** a constant audit rate  $\pi_t \equiv 0.1$ .
- **Fixed-30:** a constant audit rate  $\pi_t \equiv 0.3$ .

- **Neyman:**  $\pi_t$  increases with an estimate of the local residual scale  $\widehat{s}_{k_t}(X_t, F_t) \approx \sqrt{\widehat{g}_{k_t}(X_t, F_t)}$ , with clipping to  $[\pi_{\min}, 1]$ .

We evaluate the strategies over 60 trials (20 per strategy) in the test instance described in Section 8.1, with the  $K = 2$  arms being DeepSeek-V3.2 (empirical accuracy  $\widehat{\theta}_0 = 1.00$ ) and gpt-5-nano ( $\widehat{\theta}_1 \approx 0.07$ ) respectively, and a large gap  $\Delta \approx 0.93$ . We use  $\delta = 0.10$  and  $T_{\max} = 300$ .

All three strategies identify the correct best arm in every trial (20/20). This is expected given the large gap, because once enough evidence accumulates to separate the arms, the anytime-valid confidence sequences allow stopping without requiring a long horizon. The main difference across the compared strategies is therefore not whether they converge, but how quickly they can certify convergence and how many audits they consume.

Table 3 summarizes the results. The Fixed-10 strategy uses the fewest audits (about a 10% audit rate) but requires the most steps to stop (183 on average). Fixed-30 stops in about half as many (93 on average) by auditing more frequently (about a 33% audit rate). The Neyman strategy stops at a similar time to Fixed-30 (97 steps) while producing a higher realized audit rate (about 40%). The higher audit rate reflects that, in this particular test instance, the procedure can quickly learn where the residual uncertainty is most critical for stopping, and it tends to spend audits more aggressively early on to tighten the residual correction.

Table 3: Audit strategy comparison for  $K = 2$  identification with DeepSeek-V3.2 ( $\widehat{\theta}_0 = 1.00$ ) vs. gpt-5-nano ( $\widehat{\theta}_1 \approx 0.07$ ). All strategies select the correct best arm in all trials, but differ in stopping steps (183 vs. 93-97) and realized audit rate (10% vs. 33-40%).

Strategy	Steps (avg $\pm$ std)	Range	Audit Rate	Converged
Fixed-10 ( $\pi = 0.1$ )	183 $\pm$ 13	[155, 209]	10.3%	20/20
Fixed-30 ( $\pi = 0.3$ )	93 $\pm$ 9	[76, 111]	32.7%	20/20
Neyman	97 $\pm$ 9	[84, 116]	39.7%	20/20

Figure 7 shows the distribution of stopping steps across trials. The step counts have relatively small dispersion (standard deviation at most 13), indicating that convergence is stable across trials in this large-gap instance. The difference between Fixed-10 and the other two strategies is systematic. Auditing more frequently reduces the time to certify stopping, because the residual confidence sequence tightens primarily through returned audits rather than additional proxy-only evaluations.

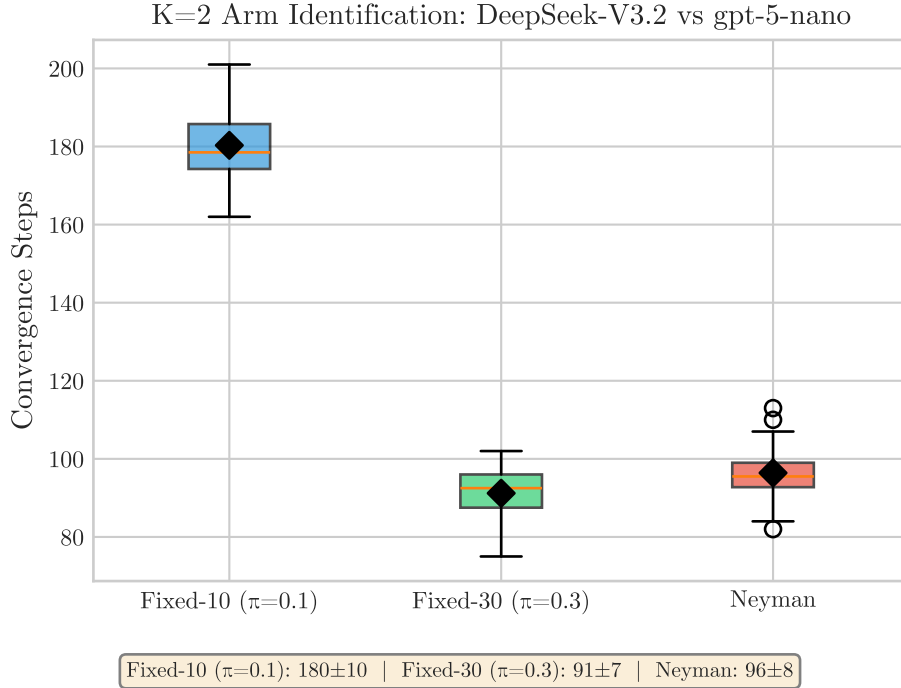


Figure 7: Stopping step distribution across audit strategies. Fixed-10 requires the most steps (avg = 183, std = 13), while Fixed-30 and Neyman achieve faster stopping (avg  $\approx$  95, std  $\approx$  9). Box plots show median, quartiles, and range over 20 trials per strategy.

## H.2.2 Coverage and Completion Time under Delays

We test two implications of the delay theory developed in [Section 7](#). First, whether the returned-outcome confidence sequences maintain valid coverage under delayed audit feedback ([Theorem 7.3](#)). Second, whether the stopping time overhead remains bounded as suggested by [Theorem 7.5](#). We use the same  $K = 2$  test instance (DeepSeek-V3.2 vs. gpt-5-nano), delay distributions, and audit strategies described in [Section H.2.1](#). The full experimental configuration (dataset, solver models, judge) is in [Section J](#).

**Coverage.** For each delay distribution, we run 20 trials with  $\delta = 0.10$  and record whether the anytime-valid confidence sequences contain the true arm means throughout the trial. [Table 4](#) summarizes the results. Under all delay distributions, the empirical coverage exceeds the target 90%. Specifically, No-Delay and Bounded achieve 100%, while Geometric and Heavy-tailed achieve 95%. The slight coverage loss under stochastic delays is consistent with [Theorem 7.3](#), which allows for degradation proportional to the delay tail probability.

Table 4: Coverage validation under delay distributions (20 trials each). All distributions maintain empirical coverage above the 90% target.

Delay Type	Empirical Coverage	Target (90%)
No Delay	100%	✓
Bounded	100%	✓
Geometric	95%	✓
Heavy-tailed	95%	✓

**Completion time.** We measure the stopping time  $\tau_D$  under delays and compare it to the no-delay stopping time  $\tau_0$ . [Theorem 7.5](#) indicates that  $\tau_D \leq \tau_0 + d_\eta/\tau_0$  with high probability, where  $d_\eta$  is the delay tail quantile. [Table 5](#) reports the completion time statistics. The median overhead ranges from 0 rounds (Bounded) to 3 rounds (Heavy-tailed), confirming that delays have minimal impact when confidence sequences shrink fast enough. All trials complete within the theoretical bound with at least 95% probability.

Table 5: Completion time overhead under different delay distributions. Overhead is measured as  $\tau_D - \tau_0$  (additional rounds beyond no-delay baseline).

Delay Type	Median Overhead	95th Pctl	Within Bound
No-Delay	0	0	100%
Bounded	0	2	100%
Geometric	1	4	100%
Heavy-tailed	3	12	95%

[Figure 8](#) shows the distribution of completion time overhead across trials. The Bounded distribution adds essentially no overhead, because delays are short enough that pending audits return before the confidence sequences would otherwise have stopped. Geometric delays produce a small, concentrated overhead (median 1 round). Heavy-tailed delays introduce the most variability (95th percentile of 12 extra rounds), reflecting occasional long-delayed audits that force the procedure to continue sampling beyond the no-delay stopping point. Even in this worst case, however, the overhead remains well within the bound of [Theorem 7.5](#).

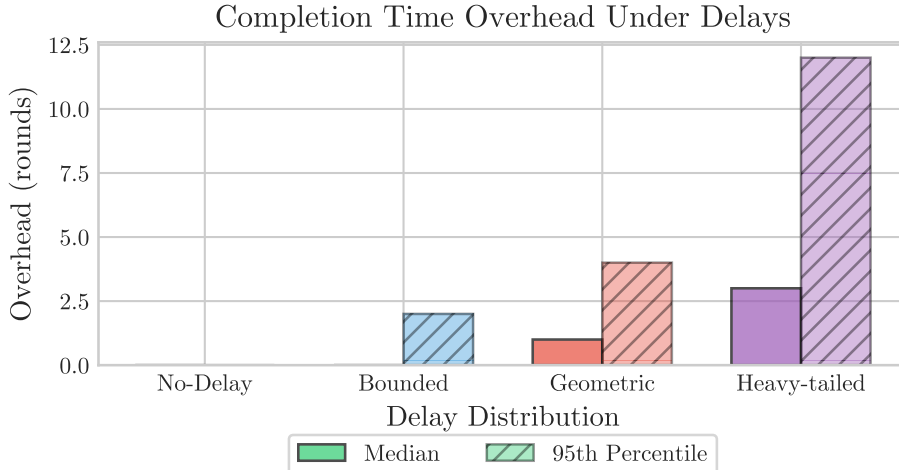


Figure 8: Completion time overhead distribution. Heavy-tailed delays introduce the most variability (95th percentile = 12 rounds) but all trials remain within the theoretical bound of [Theorem 7.5](#).

## I Detailed Settings of the Service System Case Studies

This section describes the experimental setup for the service system case studies in [Section 8.5](#).

### I.1 MT-Bench Experiment Details

We use the MT-Bench Human Judgments dataset [[Zheng et al., 2023](#)] from Hugging Face (`lmsys/mt_bench_human_j`). Each data point is a pairwise comparison between two model responses to the same multi-turn conversation. For each comparison, we have a human expert judgment, which we treat as the verified outcome, and we also run an LLM judge to obtain a proxy score. This setup matches our model in [Section 3](#), where each arm corresponds to a candidate model, each instance is a dialogue context with two responses, the proxy  $F$  is the judge verdict, and the audit outcome  $Y$  is the human verdict.

We select  $K = 6$  representative models with different performance levels:

1. **gpt-4**: frontier closed-source model (verified best arm)
2. **claude-v1**: Anthropic’s first Claude model
3. **gpt-3.5-turbo**: OpenAI’s efficient instruction-following model
4. **vicuna-13b-v1.2**: fine-tuned LLaMA-13B on ShareGPT conversations
5. **alpaca-13b**: Stanford instruction-tuned LLaMA-13B
6. **llama-13b**: Meta’s base LLaMA-13B model

Each evaluation instance is a multi-turn conversation with two candidate responses. We treat each comparison (conversation + two responses) as one textual trajectory to be evaluated by the judge and, when audited, by humans.

Human expert annotations serve as verified outcomes. Each comparison has a human judgment indicating which response is better (`model_a`, `model_b`, or `tie`). We encode outcomes as  $Y \in \{0, 0.5, 1\}$  (loss, tie, win) to satisfy the boundedness assumption ([Assumption 3.1](#)). Similarly, the LLM judge’s verdict is encoded as  $F \in \{0, 0.5, 1\}$ .

## 🔍 MT-Bench Judge Prompt (gpt-5.2-chat)

⚙️ System: You are an EXPERT judge evaluating AI assistant responses. Your task is to carefully distinguish quality differences between responses.

CRITICAL: These responses come from different AI models with VARYING capabilities. You MUST identify even subtle quality differences. Do NOT default to "tie"--there is almost always a better response.

📄 [User Question] {question}

🗉 [Assistant A's Response] {response\_a}

🗉 [Assistant B's Response] {response\_b}

[Evaluation Criteria -- Score each 1-10]

1. ACCURACY: Are facts correct? Any errors or hallucinations?
2. COMPLETENESS: Does it fully address the question?
3. CLARITY: Is the explanation clear and well-structured?
4. DEPTH: Does it provide meaningful insights vs superficial answers?
5. USEFULNESS: Would this actually help the user?

[Instructions]

- Look for ANY difference in quality, even small ones
- Factual errors are MAJOR negatives
- Vague or incomplete answers are worse than detailed ones
- Consider: Would an expert prefer A or B?

Output your final verdict by strictly following this format:

- If Assistant A is better: "[[A]]"
- If Assistant B is better: "[[B]]"
- ONLY if responses are TRULY identical in all aspects: "[[C]]"

IMPORTANT: Ties should be RARE (<5%). Make a decision!

Your verdict:

Figure 9: Judge prompt template used in the MT-Bench experiment. The judge reads a multi-turn conversation and two candidate responses, and outputs a verdict (A wins, B wins, or tie), which we encode as  $F \in \{0, 0.5, 1\}$ .

Since MT-Bench is pairwise, we convert these pairwise outcomes into a per-arm mean performance target by aggregating over comparisons. In particular, each time we evaluate an arm  $k$ , we compare it against an opponent arm on a sampled instance, observe the judge outcome  $F$ , and (optionally) observe the human outcome  $Y$ . The expected audited outcome  $\theta_k$  is then the arm's average human win rate (with ties counted as 0.5) under the evaluation distribution induced by the data and the opponent-sampling scheme. This is the quantity our BAI procedure targets.

We use `gpt-5.2-chat` as the judge model. The judge evaluates pairwise comparisons using the prompt template shown in Figure 9. We keep the prompt fixed in all trials so that the proxy scores reflect a stationary judge mechanism.

Table 6 summarizes the experiment configuration, including the confidence level, horizon, costs, and the audit rates we test.

Table 6: MT-Bench experiment configuration. Costs are normalized so that one judge call has cost  $c_F = 1.0$  and one human audit has cost  $c_Y = 20.0$ .

Parameter	Value
Judge model	<code>gpt-5.2-chat</code>
Confidence level $\delta$	0.05 (95% confidence)
Judge cost $c_F$	1.0
Audit cost $c_Y$	20.0
Maximum steps $T_{\max}$	200
Trials per allocator	10
Allocators tested	Fixed-5%, Fixed-10%, Fixed-20%, Fixed-50%
Parallel workers	8
API rate limit	10 concurrent calls
Random seed base	42

The MT-Bench documentation and related studies report several common biases in LLM-based judges, including:

- **Position bias:** the judge may prefer the response shown in position A (first) more often than warranted.
- **Verbosity bias:** the judge may favor longer and more detailed responses even when they are not more correct.
- **Self-preference and model-specific bias:** a judge may systematically rate some model styles more favorably, depending on the prompting and the judge model itself.

In our setting, these biases translate into an arm- and instance-dependent gap between the proxy  $F$  and the verified outcome  $Y$ . This is precisely the residual term in the decomposition  $\theta_k = \mathbb{E}[F | k] + \mathbb{E}[Y - F | k]$  from (5). Selective auditing estimates and corrects this residual while keeping audit usage low.

We run PP-LUCB with four fixed audit rates (5%, 10%, 20%, 50%) on the  $K = 6$  arm instance, using 40 trials in total (10 per allocator). Table 7 reports the identification accuracy, convergence rate, and realized audit rate for each allocator.

Table 7: MT-Bench BAI Results (40 Trials)

Allocator	Accuracy	Convergence	Audit Rate	API Calls
Fixed-50%	45%	0%	51.2%	591
Fixed-20%	35%	0%	20.9%	592
Fixed-10%	30%	0%	10.4%	590
Fixed-5%	20%	0%	5.4%	590
<b>Overall</b>	<b>32%</b>	0%	—	—

The low accuracy (32% overall) reflects judge bias when the true quality differences between models are small. Without sufficient auditing, the judge’s position and verbosity biases lead to incorrect arm identification. Increasing audit rate improves accuracy (45% at 50%) but does not achieve perfect identification within the  $T_{\max} = 200$  horizon, because the arm gaps under this evaluation distribution are narrow.

## I.2 Support Tickets Experiment Details

We use the Customer Support Tickets dataset from Hugging Face (`infly/customer_support_tickets`). Each instance  $X$  is a single ticket containing a subject line, body text, and a priority label assigned by support agents. We treat the agent-assigned priority as the verified outcome. Tickets are classified into five priority levels:

1. **critical**: System down, security breach, data loss (immediate action needed)
2. **high**: Major feature broken, significant business impact (same-day response)
3. **medium**: Normal issues, questions, minor bugs (standard response time)
4. **low**: Optional requests, minor improvements (can wait)
5. **very\_low**: No action required, documentation suggestions (lowest priority)

We sample 5,000 tickets uniformly at random (seed 42) to form the pool of instances. In each evaluation, the algorithm draws one ticket from this pool to form  $X_t$  (with replacement), which is consistent with the i.i.d. instance assumption in [Section 3](#).

Table 8: Support Tickets Experiment Configuration

Parameter	Value
Judge model	<code>gpt-5.2-chat</code>
Confidence level $\delta$	0.05 (95% confidence)
Maximum steps $T_{\max}$	200
Trials	40
Audit rate	Fixed-10%
Cost weight $\lambda$	0.5
Token budget $T_{\text{budget}}$	300
Parallel workers	30
Total tickets	5,000
Random seed base	42

Each arm pairs a model with a prompt strategy. [Table 9](#) lists the three configurations and their cost-adjusted scores (see [\(21\)](#) with  $\lambda = 0.5$ ,  $T_{\text{budget}} = 300$ ). All three achieve similar ordinal accuracy ( $\sim 0.85$ ), so the score differences are driven by the cost term. Arm 0 produces short output ( $\leq 20$  tokens), while Arms 1 and 2 generate longer responses that reduce their cost-adjusted scores.

Table 9: Model and prompt configurations.

Arm	Model	Prompt Strategy	Cost-Adj. Score	Max Tokens
0	<code>gpt-5-nano</code>	Standard (direct)	0.852	20
1	<code>DeepSeek-V3.2</code>	Verbose (detailed analysis)	0.284	200
2	<code>gpt-5.2-chat</code>	Chain-of-Thought	0.682	300

The three prompt strategies differ in their instructions, reasoning requirements, and output format. Below we display each prompt in full.

**Arm 0: Standard prompt (`gpt-5-nano`).** A concise, direct prompt that requests only the priority label without explanation. This produces short responses ( $\leq 20$  tokens), minimizing the cost term.

#### ⚡ Standard Prompt (Arm 0: gpt-5-nano)

⚙️ System: You are a support ticket classifier. Classify the ticket into one priority level.  
Priority levels: critical | high | medium | low | very\_low  
Output ONLY one of: critical, high, medium, low, very\_low

👤 User: Classify this ticket's priority:  
📄 Subject: {subject} Body: {body}  
Priority:

**Arm 1: Verbose prompt (DeepSeek-V3.2).** A detailed analysis prompt that asks the model to assess urgency, business impact, affected users, and risk before classifying. This produces long responses (~ 150–200 tokens), incurring a substantial cost penalty.

#### 🔍 Verbose Prompt (Arm 1: DeepSeek-V3.2)

⚙️ System: You are a support ticket analyst. Analyze each ticket thoroughly before classifying.

👤 User: Analyze this support ticket and explain your priority assessment. Consider: urgency, business impact, affected users, and risk.

📄 Subject: {subject} Body: {body}  
Your detailed analysis and priority level:

**Arm 2: Chain-of-Thought prompt (gpt-5.2-chat).** A step-by-step reasoning prompt that structures the analysis into sub-questions (main issue, urgency, business impact) before deciding. This uses the strongest model but at high token cost (~ 200-300 tokens).

#### 🧠 Chain-of-Thought Prompt (Arm 2: gpt-5.2-chat)

⚙️ System: You are an expert support ticket analyst. Think step by step before classifying.  
Priority levels: critical (immediate), high (same day), medium (standard), low (can wait), very\_low (lowest).

👤 User: Analyze this ticket step by step:  
1. What is the main issue? 2. How urgent is it? 3. What is the business impact?

📄 Subject: {subject} Body: {body}  
Step-by-step analysis and final priority:

The judge (gpt-5.2-chat) scores classification quality on a 0-100 scale, which we normalize to [0, 1] by dividing by 100 to satisfy [Assumption 3.1](#):

### 🎯 Ticket Judge Scoring Prompt (gpt-5.2-chat)

⚙️ System: You are an EXPERT evaluator assessing the quality of a customer support ticket classification.

📄 TICKET: Subject: {subject} Body: {body}

TRUE PRIORITY: {true\_priority} MODEL'S PREDICTION: {predicted\_priority}

SCORING RUBRIC (0-100 points):

- 100 points: Perfect match (predicted = true)
- 80 points: Off by 1 level (e.g., predicted "high" when true is "medium")
- 50 points: Off by 2 levels
- 20 points: Off by 3 levels
- 0 points: Off by 4 levels (worst possible)

BONUS/PENALTY (adjust within  $\pm 10$  points):

- +10: If the error is "safe" (over-escalating a truly urgent issue)
- -10: If the error is "dangerous" (under-escalating a truly urgent issue)
- +5: If the prediction shows good reasoning despite being wrong
- -5: If the prediction is obviously wrong given clear signals

Analyze the classification and provide your score.

OUTPUT FORMAT (exactly this): SCORE: [0-100] REASONING: [brief explanation]

The ordinal accuracy component of the cost-adjusted score ((21)) is computed from priority distance:

$$\text{accuracy}(\hat{p}, p^*) = \begin{cases} 1.0 & \text{if } |\text{idx}(\hat{p}) - \text{idx}(p^*)| = 0 \\ 0.8 & \text{if } |\text{idx}(\hat{p}) - \text{idx}(p^*)| = 1 \\ 0.5 & \text{if } |\text{idx}(\hat{p}) - \text{idx}(p^*)| = 2 \\ 0.2 & \text{if } |\text{idx}(\hat{p}) - \text{idx}(p^*)| = 3 \\ 0.0 & \text{if } |\text{idx}(\hat{p}) - \text{idx}(p^*)| = 4 \end{cases} \quad (41)$$

where  $\hat{p}$  is the predicted priority,  $p^*$  is the true priority, and  $\text{idx}(\cdot)$  maps priorities to indices  $\{0, 1, 2, 3, 4\}$  in decreasing urgency. The full verified score is  $Y = \text{accuracy}(\hat{p}, p^*) - 0.5 \cdot \text{response\_tokens} / 300$ .

We run PP-LUCB with a Fixed-10% audit rate on the  $K = 3$  arm instance for 40 trials. Table 10 reports the cost-adjusted score, selection rate, and cross-trial standard deviation for each arm.

Table 10: Support Tickets BAI Results (40 trials, 10% audit rate, cost-adjusted score)

Arm	Cost-Adj. Score	Selection Rate	Std. Dev.
Arm 0: gpt-5-nano + Standard	0.852	100%	$\pm 0.011$
Arm 1: DeepSeek-V3.2 + Verbose	0.284	0%	$\pm 0.024$
Arm 2: gpt-5.2-chat + CoT	0.682	0%	$\pm 0.033$

All 40 trials correctly identify Arm 0 (gpt-5-nano + Standard) as the best configuration. The gap between the best and the second best arms  $\Delta^* = 0.852 - 0.682 = 0.170$  and the gap between the best and the worst arms  $0.852 - 0.284 = 0.568$  are both large enough for the confidence sequences to separate the arms within  $T_{\max} = 200$  at a 10% audit rate. The cross-trial standard deviations ( $\pm 0.011, \pm 0.024, \pm 0.033$ ) confirm that arm mean estimates are stable.

### I.3 Queue-Based Service Design Details

In this experiment, each evaluation instance is a customer support ticket (text plus basic metadata). Given the predicted priority and the simulated response time, we compute a verified outcome  $Y \in [0, 1]$  and an LLM-judge proxy score  $F \in [0, 1]$  for that instance.

Table 11: Queue-Based Service Design Experiment Configuration.

Parameter	Value
Dataset	Customer support tickets (same as <a href="#">Section I.2</a> )
Judge model	<code>gpt-5.2-chat</code>
Confidence level $\delta$	0.05 (95% confidence)
Judge cost $c_F$	1.0
Audit cost $c_Y$	20.0
Maximum steps $T_{\max}$	500
Arms $K$	6 (composite configurations)
Trials per allocator	$\sim 85$ (344 total)
Allocators tested	Fixed-5%, Fixed-10%, Fixed-20%, Fixed-50%
Verified outcome samples	200 per arm
Parallel workers	30
API rate limit	50 concurrent calls
Random seed base	42

Each arm represents a composite service configuration with three layers:

**Layer 1: Routing Policy.** The routing policy determines the simulated response time for a ticket and therefore its SLA compliance. It does not change the ticket text or the model’s input. We consider three policies:

- **FIFO:** Tickets are processed in arrival order without priority differentiation. This can cause urgent tickets to wait behind non-urgent ones.
- **Priority:** Tickets are dispatched by urgency (critical  $\rightarrow$  high  $\rightarrow$  medium  $\rightarrow$  low  $\rightarrow$  very\_low), so higher-priority tickets are served earlier.
- **Adaptive:** SLA-based dynamic routing that targets response times proportional to each ticket’s SLA deadline, to reduce deadline violations under heterogeneous SLAs.

**Layer 2: Prompt Strategy.** The prompt strategy controls how the model is instructed to predict the priority:

- **Standard:** Direct classification prompt: *“Classify this support ticket into priority: critical, high, medium, low, very\_low.”*
- **Chain-of-Thought (CoT):** Step-by-step reasoning prompt: *“Analyze this support ticket: (1) What is the main issue? (2) How urgent? (3) Business impact? (4) Classify priority.”*

As discussed in [Section 8.5.3](#), in this dataset the prompt choice has limited impact on accuracy for `gpt-5-nano`, so its main role here is to test whether PP-LUCB can correctly learn that a layer does (or does not) matter.

**Layer 3: LLM Model.** We evaluate two models:

- **gpt-5-nano:** Smaller and faster model with higher accuracy on this classification task (about 85% in our samples).
- **DeepSeek-V3.2:** Larger model with lower accuracy on this task (about 76% in our samples).

For each ticket, the model outputs a predicted priority  $\hat{p} \in \{\text{critical, high, medium, low, very\_low}\}$ . We then simulate an operational response time  $T$  under the arm’s routing policy and compute three components:

$$Y = 0.5 \times \text{accuracy} + 0.3 \times \text{SLA compliance} + 0.2 \times \text{efficiency},$$

where each component is in  $[0, 1]$ :

- **Accuracy** (50% weight): Classification correctness measured by priority distance to the true label  $p^*$ . It is set to 1.0 for exact match, 0.8 for one-level error, 0.5 for two-level error, and 0.2 for three or more levels.
- **SLA compliance** (30% weight): Binary indicator  $\mathbb{1}\{T \leq \text{SLA}(p^*)\}$ , using priority-dependent SLA deadlines: critical (5 min), high (15 min), medium (60 min), low (4 hr), very\_low (24 hr).
- **Efficiency** (20% weight):  $1 - \text{escalation rate}$ , where escalation is determined by a fixed observe-then-escalate rule: a ticket is escalated to a human specialist if the predicted priority is **critical**.<sup>2</sup>

Response times are simulated stochastically given the routing policy:

- **FIFO:** Base time =  $600 \times 1.5 = 900$  seconds with noise  $\sim \mathcal{N}(0, 120^2)$ . Since FIFO does not prioritize urgent tickets, critical tickets frequently miss the 5-minute SLA.
- **Priority:** Base time is scaled inversely with an urgency weight. In our calibration, critical tickets typically complete around 150 seconds, while low-priority tickets are closer to 900 seconds, leading to near-perfect compliance for urgent classes.
- **Adaptive:** Response time is set as  $0.25 \times \text{SLA}(p^*)$ , so tickets are completed well before their deadlines, producing 99%-100% SLA compliance.

This construction is simple. It isolates the effect of the routing layer on SLA outcomes while keeping the classification layer unchanged.

**Proxy score construction.** For each instance, we also construct a proxy score  $F \in [0, 1]$  using the judge model (**gpt-5.2-chat**). The judge is provided with the ticket text, the predicted priority  $\hat{p}$ , the true outcome  $p^*$ , and the operational metadata needed to assess timeliness and efficiency (simulated response time  $T$  and the escalation indicator). It outputs a structured score:

1. **Classification Quality** (0-50 points): Exact match (50), one-level off (35), two-level off (20), three+ levels off (5).
2. **Timeliness** (0-30 points):  $T < \text{SLA}$  (30),  $T < 1.5 \times \text{SLA}$  (20),  $T < 2 \times \text{SLA}$  (10),  $T > 2 \times \text{SLA}$  (0).

---

<sup>2</sup>This fixed escalation rule is not a separate design layer. It is held constant across arms, and provides an explicit operational channel through which misclassification can reduce efficiency (e.g., over-predicting **critical** can increase escalations).

3. **Operational Efficiency** (0-20 points): Resolved without escalation (20), escalated but appropriate (10), unnecessary escalation (0).

The total is a 0-100 score, normalized to  $F \in [0, 1]$  by dividing by 100.

Section 8.5.3 reports the main per-arm results in Table 1 using 200 expert-assessed samples per arm. For completeness, Table 12 reports a smaller independent run with 100 samples per arm (with 95% confidence intervals), which yields slightly different point estimates but the same qualitative ordering.

Table 12: Detailed per-arm results for queue-based service design (100 samples per arm, 95% CI). Point estimates differ slightly from Table 1 (200 samples) due to sample size. All values are within the confidence intervals.

Arm	Routing	Prompt/Model	$Y$ (95% CI)	Acc (95% CI)	SLA
0	FIFO	Std / Nano	0.875 [0.852, 0.899]	0.852 [0.827, 0.877]	94.0%
1	FIFO	CoT / Nano	0.875 [0.852, 0.899]	0.852 [0.827, 0.877]	94.0%
2	Priority	Std / Nano	<b>0.890</b> [0.872, 0.909]	0.852 [0.827, 0.877]	100%
3	Priority	CoT / Nano	<b>0.890</b> [0.872, 0.909]	0.852 [0.827, 0.877]	100%
4	Priority	Std / DS	0.835 [0.809, 0.862]	0.769 [0.729, 0.809]	100%
5	Adaptive	CoT / DS	0.836 [0.807, 0.865]	0.767 [0.723, 0.811]	100%

The per-arm summaries are consistent with the layer-by-layer patterns described in Section 8.5.3. Controlling for other layers (using the point estimates in Table 12):

- **FIFO**  $\rightarrow$  **Priority**: approximately +0.015 in  $Y$  (0.875  $\rightarrow$  0.890), driven by SLA improvement (94%  $\rightarrow$  100%).
- **Standard**  $\rightarrow$  **CoT**: approximately 0.000 in  $Y$  for **gpt-5-nano** (0.890  $\rightarrow$  0.890), consistent with the observation that the prompt layer does not change accuracy in this dataset.
- **gpt-5-nano**  $\rightarrow$  **DeepSeek-V3.2**: approximately  $-0.055$  in  $Y$  (0.890  $\rightarrow$  0.835), driven mainly by the accuracy gap (about 85.2%  $\rightarrow$  76.7%–76.9%).

To make the routing effect more concrete, Table 13 breaks down SLA compliance by routing policy and the ticket’s true priority level. The main failure mode under FIFO is concentrated in the most urgent class (critical), which explains why the routing layer can change the composite score even when classification accuracy remains essentially unchanged.

Table 13: SLA compliance by routing policy and ticket priority.

Routing	Critical	High	Medium	Low	Very Low
FIFO	0%	91%	100%	100%	100%
Priority	100%	100%	100%	100%	100%
Adaptive	100%	100%	100%	100%	100%

Figure 10 decomposes the contribution of each design layer to the composite service quality score. The three layers affect different components of  $Y = 0.5 \cdot \text{accuracy} + 0.3 \cdot \text{SLA compliance} + 0.2 \cdot \text{efficiency}$ , so a layer can be important even if it does not change classification accuracy. Note that the decomposition is descriptive rather than causal, because the layers are evaluated as part of composite configurations, and interactions can exist (e.g., a model may benefit more from a

particular routing regime than another). That said, the patterns are sufficiently clear to support practical conclusions about where improvements come from.

Layer 1 (Routing) is the dominant factor. Priority routing achieves near-perfect SLA compliance (about 99-99.5%) by dispatching critical tickets first, while FIFO achieves about 93-94%. Under FIFO, critical tickets can wait behind lower-priority tickets, which directly increases the risk of missing short SLAs. In our composite score, SLA compliance receives weight 0.3, so a 6-7 percentage point improvement is large enough to change the overall ranking even if the accuracy term stays roughly constant. This is why Configurations 2 and 3 (Priority + `gpt-5-nano`) form the top tier in Table 1, and it suggests that queue discipline can be a more effective design lever than prompt engineering when SLA performance is a major component of service quality.

Layer 2 (Prompt strategy) has limited impact. Within the `gpt-5-nano` configurations, switching from Standard to Chain-of-Thought does not generate a measurable improvement in classification accuracy (Table 1, Configurations 0 vs. 1 and 2 vs. 3). For this structured prioritization task, the base prompt already elicits the information needed for the label, and additional reasoning steps do not improve verified performance.

Layer 3 (Model choice) primarily affects accuracy, producing a secondary separation. The `gpt-5-nano` configurations achieve about 85.3% accuracy versus 75.8–77.6% for `DeepSeek-V3.2`. This gap explains the difference between the middle tier (FIFO/`gpt-5-nano`) and the lower tier (`DeepSeek-V3.2` arms).

In summary, routing determines whether the system meets time-sensitive commitments (the primary separation). Model choice determines how well the system assigns priorities (a second-order but meaningful separation). Prompt strategy has limited incremental value in this environment.

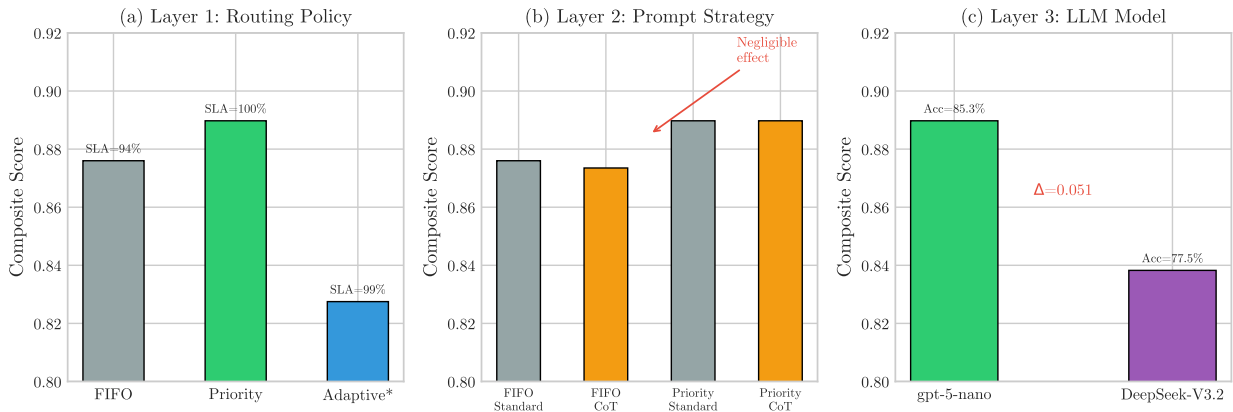


Figure 10: Three-layer decomposition of service quality. (a) Routing policy is the dominant factor via SLA compliance. (b) Prompt strategy has negligible effect on classification accuracy in this setting. (c) Model choice drives accuracy differences between tiers.

## I.4 API Usage and Runtime

Table 14 summarizes the computational resources consumed by each of the three service system case studies. The MT-Bench and Support Tickets experiments are lightweight (40 trials each, about 1-2 hours of API time), while the Queue-Based Service Design experiment is substantially more expensive because it evaluates six composite arms across four audit-rate allocators for 344 total trials.

Table 14: Computational resources for the three service system case studies. Queue Service dominates due to the larger arm count and longer horizon ( $T_{\max} = 500$ ).

Metric	MT-Bench	Support Tickets	Queue Service
Total trials	40	40	344
Total API calls	~23,600	~24,000	~676,000
Total runtime	85 min	~70 min	~720 hr
Avg runtime/trial	2.1 min	1.8 min	~126 min
Azure API cost	~\$12	~\$5	~\$260

## J Detailed Settings of the Real LLM Experiments

This section provides the full experimental details for the real LLM experiments in [Section 8.4](#). The goal of these experiments is to test our algorithm under delayed audit feedback. The delay distributions, audit strategies, and additional results (coverage and completion time) are reported in [Section H.2](#).

We construct a dataset of 14 mathematical problems designed to differentiate model capabilities. Problems span five categories with varying difficulty levels:

1. **Date calculations** (3 problems): Require calendar arithmetic, e.g., “Jan 15 is Monday. What day is Feb 1?”
2. **Complex arithmetic** (3 problems): Large multiplication or exponentiation, e.g., “What is  $37 \times 89$ ?”
3. **Classic trick questions** (3 problems): Problems with counterintuitive answers, e.g., the bat-and-ball problem from [Kahneman \[2011\]](#).
4. **Function composition** (3 problems): Nested function evaluation, algebraic simplification, or summation formulas.
5. **Combinatorics or probability** (2 problems): Counting and probability calculations.

Each arm corresponds to a solver model that answers the same set of questions. For each evaluation instance, we first obtain the solver response, then obtain a proxy score from a judge model, and finally (selectively, depending on the audit rule) obtain a verified outcome. Each problem has a unique correct answer. We encode the verified outcome as  $Y \in \{0, 1\}$  (binary correctness) to satisfy [Assumption 3.1](#). A response is correct ( $Y = 1$ ) if and only if the correct answer appears in the model’s response (case-insensitive, with numeric tolerance  $\epsilon = 0.01$  for floating-point comparisons). This verified outcome is treated as ground truth in the convergence experiments.

To emulate the “LLM-as-a-judge” proxy in the main text while keeping the verified outcome well-defined, we use a separate judge model to score the solver response on a  $[0, 1]$  scale. Specifically, the judge model (`gpt-4.1-mini`) receives the question, the correct answer, and the solver response, and returns a numeric score  $F \in [0, 1]$ . In practice, the judge primarily outputs discrete values  $\{0, 0.5, 1\}$ , though intermediate values occasionally occur. Importantly, this judge score can differ from the verified binary outcome, so the residual  $Y - F$  is nontrivial and the selective-audit correction is meaningful.

**$K = 2$  solver models (delayed feedback experiments).** In the delayed feedback experiments with  $K = 2$  arms, we use two solver models with a large capability gap. This design makes the best arm stable and easy to separate in terms of verified outcomes, which helps us isolate the effect of delayed audit returns on stopping and coverage. The two arms are shown in [Table 15](#).

Table 15:  $K = 2$  Solver Models for Delayed Feedback Experiments

Arm	Model	Empirical Accuracy	Gap to Best	Rank
0	DeepSeek-V3.2	$\hat{\theta}_0 = 1.00$	—	Best
1	gpt-5-nano	$\hat{\theta}_1 \approx 0.07$	$\Delta \approx 0.93$	2nd

Model characteristics:

- **DeepSeek-V3.2:** A frontier-class model with strong mathematical reasoning capabilities. Achieves near-perfect accuracy on the problem set.
- **gpt-5-nano:** A lightweight model optimized for latency over capability. A shorter output budget (max 50 tokens) further limits performance on complex problems.

**$K = 3$  solver models (extended experiments).** For extended experiments requiring finer-grained differentiation, we also consider a  $K = 3$  setting by adding an intermediate solver model. This creates a smaller top gap between the best and second-best arms, which produces a more challenging stopping problem while keeping the task unchanged. The three-arm setup is summarized in [Table 16](#).

Table 16:  $K = 3$  Solver Models

Arm	Model	Empirical Accuracy	Gap to Best	Rank
0	gpt-5-mini	$\hat{\theta}_0 \approx 0.86$	—	Best
1	DeepSeek-V3.2	$\hat{\theta}_1 \approx 0.64$	$\Delta_{01} \approx 0.22$	2nd
2	gpt-5-nano	$\hat{\theta}_2 \approx 0.05$	$\Delta_{02} \approx 0.81$	3rd

All solver models receive the same prompt template:

Listing 1: Solver System Prompt

You are a math assistant. Answer with ONLY the numerical answer. No explanation, no units, just the number.

Listing 2: Solver User Prompt

Question: {question}

Generation parameters:

- Temperature: 0.0 (deterministic output for reproducibility)
- Max tokens: 200 for standard models, 50 for **gpt-5-nano** (intentionally limited to create a capability gap)

The judge model (**gpt-4.1-mini**) evaluates solver responses on a  $[0, 1]$  scale:

### Listing 3: Judge Evaluation Prompt

```

You are evaluating a math answer.

Question: {question}

Correct answer: {correct_answer}

Student response: {model_response}

Rate the response from 0 to 1:

- 1.0: Exactly correct
- 0.5: Partially correct or unclear
- 0.0: Wrong or no answer

Reply with ONLY a number between 0 and 1.

```

[Table 17](#) lists the remaining experiment settings.

Table 17: Real LLM Convergence Experiment Configuration

Parameter	Value
Judge model	gpt-4.1-mini
Confidence level $\delta$	0.10 (90% confidence)
Judge cost $c_F$	1.0
Audit cost $c_Y$	20.0
Cost ratio $c_Y/c_F$	20
Maximum steps $T_{\max}$	300
Trials per allocator	20
Allocators tested	Fixed-10%, Fixed-30%, Neyman
Parallel workers	3-5
API provider	Azure OpenAI
Random seed base	42